

# AUS Repository

## Bond Stress-Slip Models and Behavior of Aluminum Alloys-Concrete Interface

Item Type	Thesis
Authors	Mirghani, Ahmed
Download date	2026-03-07 06:55:40
Link to Item	<a href="http://hdl.handle.net/11073/8712">http://hdl.handle.net/11073/8712</a>

# BOND STRESS-SLIP MODELS AND BEHAVIOR OF ALUMINUM ALLOYS- CONCRETE INTERFACE

by

Ahmed Mirghani

A Thesis Presented to the Faculty of the

American University of Sharjah

College of Engineering

in Partial Fulfillment

of the Requirements

for the Degree of

Master of Science in

Civil Engineering

Sharjah, United Arab Emirates

January 2017

© 2017 Ahmed Mirghani. All rights reserved.

Approval Signature

We, the undersigned, approve the Master's Thesis of Ahmed Mirghani. Thesis Title: Bond Stress-Slip Models and Behavior of Aluminum Alloys-Concrete Interface Signature Date of Signature (dd/mm/yyyy)

\_\_\_\_\_

Dr. Jamal Abdalla Professor, Department of Civil Engineering Thesis Advisor

\_\_\_\_\_

Dr. Rami Hawileh

Professor, Department of Civil Engineering Thesis Co-Advisor \_\_\_\_\_

\_\_\_\_\_

Dr. Farid Abid Professor, Department of Civil Engineering Thesis Committee Member

\_\_\_\_\_

Dr. Wael Abuzaid Assistant Professor, Department of Mechanical Engineering Thesis Committee Member \_\_\_\_\_

Dr. Robert Houghtalen Head, Department of Civil Engineering \_\_\_\_\_

\_\_\_\_\_

Dr. Mohamed El-Tarhuni Associate Dean, College of Engineering \_\_\_\_\_

\_\_\_\_\_

Dr. Richard T. Schoephoerster Dean, College of Engineering \_\_\_\_\_

\_\_\_\_\_

Dr. Khaled Assaleh Interim Vice Provost for Research and Graduate Studies

## Acknowledgment

I would like to express my sincere gratitude to my supervisors, Dr. Jamal A. Abdalla and Dr. Rami Hawileh, not only for their guidance and extreme patience, but for their motivation and encouragement. Moreover, special thanks to the lab instructor Mr. Arshi Faridi for helping in conducting the experimental program. In addition, I'd like to acknowledge my colleague and friend Hassan Umari for his great help with the results part of this thesis. I would also like to thank the College of Engineering, Department of Civil Engineering at the American University of Sharjah for providing me with teaching assistantship throughout my graduate studies.

Dedication

This thesis is dedicated to my family for their endless love and encouragement. They provided me with great moral support throughout my graduate studies.

## Abstract

In the last few decades, different techniques have been used for strengthening reinforced concrete (RC) structures to increase their strength and stiffness. One of these techniques involves the use of steel and fiber reinforced polymers (FRP) as externally bonded reinforcing (EBR) materials. The use of FRP and steel as EBR materials has many advantages and disadvantages. Recently developed aluminum alloys (AA) have many desirable characteristics that may overcome some of these disadvantages making them an attractive candidate as EBR materials. This research aims to examine and evaluate the use of AA as a new EBR material. Achieving a strong bond between AA and concrete is crucial to the success of AA as an EBR material. Several parameters affect the bond strength and behavior. Such parameters include concrete compressive strength, effective bond length, stiffness and surface of the EBR material, concrete surface, thickness and width of the EBR material and adhesive type. In this study the bond strength, effective bond length and bond-slip models for AA-concrete interface were determined. A comprehensive experimental investigation including 96 specimens was conducted to evaluate the bond strength and behavior using adhesive as bonding material. Concrete strength, bond length and plate type were used as variables while other parameters were kept constant. It was observed that the bond stress, loading capacity, and failure modes vary with AA surface roughness and bonded length. The load capacity and maximum bond stress increased by 254.7% and 253.7%, respectively for randomly grinded AA surface compared with those of normal AA surface indicating that AA plates with scratched surface could be used in practical applications. Moreover, AA scratched plates exhibits higher ultimate loads compared with CFRP plates. The load capacity for AA scratched plates increases by 5.6% for the short bonded length up to 22.5% for the long bonded length when compared to the CFRP plates. In addition, the bond-slip models of the AA plates were developed, with reasonable level of accuracy. Moreover, finite element (FE) models were developed for a number of tested specimens. The results of the FE modeling showed a great agreement with the corresponding experimental results.

Search Terms: Aluminum Alloy (AA), Carbon Fiber Reinforced Polymers (CFRP), bond Stress-Slip, Externally-Bonded Material, Interfacial Strength.

7

### Table of Contents

Abstract .....	6
List of Figures .....	11
List of Tables .....	15
Chapter 1: Introduction .....	18
1.1 Overview .....	18
1.2 Problem Statement .....	20
1.3 Research Significance .....	21
1.4 Research Objectives .....	22
1.5 Thesis Organization .....	22

Chapter 2: Background .....	23
2.1 Strengthening of Structures .....	23
2.2 Steel as Externally Bonded Reinforcement .....	24
2.3 FRP as Externally Bonded Reinforcement .....	24
2.4 Shear Tests and Failure Modes .....	26
2.5 Effective Bond Length .....	28
2.6 Composite Action .....	30
2.7 Factors Affecting Bond Stress-Slip Relationship .....	30
2.7.1 Concrete compressive strength.....	30
2.7.2 Concrete surface treatment. ....	31
2.7.3 Bond length .....	31
2.7.4 Adhesive and plate elastic modulus. ....	32
2.8 Bond Strength Models .....	33
2.8.1 Empirical bond strength models. ....	33
2.8.2 Fracture mechanics based bond strength models. ....	34
2.8.3 Proposed design bond strength models. ....	35
2.9 Aluminum .....	36
8	
2.9.1 Wrought alloys. ....	36
2.9.2 Cast alloys. ....	36
2.9.3 Aluminum versus steel .....	40
2.9.4 Aluminum versus FRP .....	40
Chapter 3: Experimental Program .....	41
3.1 Test Specimens .....	41
3.2 Materials and Properties .....	42
3.2.1 Concrete. ....	42
3.2.2 Aluminum alloy plates. ....	44
3.2.3 CFRP plates. ....	49
3.2.4 Epoxy adhesive. ....	50

3.2.5 Strain gauges. ....	51
3.3 Specimen Details and Instrumentation .....	52
3.4 Test Setup .....	55
3.5 Test Matrix .....	56
Chapter 4: Experimental Results and Discussion .....	57
4.1 Group One: Concrete Strength of 20 MPa .....	58
4.1.1 CFRP plate failure. ....	71
4.1.2 AA scratched plate failure. ....	71
4.1.3 AA plain plate failure .....	71
4.2 Group Two: Concrete Strength of 30 MPa .....	72
4.2.1 CFRP plate failure.....	85
4.2.2 AA scratched plate failure. ....	85
4.2.3 AA plain plate failure. ....	85
4.3 Group Three: Concrete Strength of 40 MPa .....	86
4.3.1 CFRP plate failure.....	99
4.3.2 AA scratched plate failure. ....	99
9	
4.3.3 AA plain plate failure. ....	99
4.4 Group Four: Concrete Strength of 60 MPa .....	100
4.4.1 CFRP plate failure.....	113
4.4.2 AA scratched plate failure. ....	113
4.4.3 AA plain plate failure. ....	113
4.5 Results Discussion .....	114
4.5.1 Concrete strength - prisms with CFRP plates. ....	114
4.5.2 Bond length- prisms with CFRP plates. ....	116
4.5.3 Concrete strength - prisms with AA scratched plates. ....	118
4.5.4 Bond length- prisms with AA scratched plates. ....	120
4.5.5 Comparison between AA scratched and CFRP plates. ....	122
4.5.6 Concrete strength - prisms with AA natural plates. ....	126

4.5.7 Bond length- prisms with AA natural plates. ....	127
Chapter 5: Development of Aluminum Alloys and CFRP Plate Models .....	128
5.1 Fitting for Popovic’s Equation .....	128
5.2 Analysis of Factors Affecting the Bond Stress–Slip Model .....	129
5.2.1 Bond length. ....	129
5.2.2 Concrete Strength. ....	129
5.3 Development of Bond-Slip Models .....	133
5.3.1 AA and CFRP model expressions .....	136
5.4 Analytical Predictions.....	139
5.4.1 CFRP statistical measures .....	140
5.4.2 AA scratched statistical measures .....	144
5.4.3 Summary and discussion of the predicted results .....	148
Chapter 6: Finite Element Model Development .....	149
6.1 Geometry .....	149
6.2 Element Types and Material Models .....	151
10	
6.2.1 Concrete. ....	151
6.2.2 AA plates. ....	153
6.2.3 AA- concrete interface element. ....	154
6.2.4 Boundary conditions and mesh generation. ....	157
6.2.6 Analysis settings and nonlinear solution. ....	158
6.3 FE Modeling Results of AA Plate-Concrete Interface .....	159
6.3.1 FE model validation. ....	160
6.3.2 3D failure modes .....	172
Chapter 7: Summary and Conclusion .....	173
References .....	175
Vita .....	180
6.2.5 Construction geometry and path generation. ....	

11

## List of Figures

Figure 1-1: Failure modes of RC beams strengthened with an FRP plate [7] .....	19
Figure 1-2: Problem Statement .....	20
Figure 2-1: Cross-section of an externally bonded RC structure [2] .....	23

Figure 2-2: Use of steel plates as EBR systems [9] .....	24
Figure 2-3: Application of FRP [3] .....	25
Figure 2-4: Types of bond tests [1] .....	26
Figure 2-5: Typical failure modes and failure locations for EBR systems .....	27
Figure 2-6: Effective bond length calculated using existing design codes [9] .....	29
Figure 2-7: Aluminum alloy designation system [32] .....	37
Figure 3-1: Apparatus used to hold the specimen .....	41
Figure 3-2: Single shear test specimen .....	41
Figure 3-3: Prepared cubes, cylinders and prisms .....	42
Figure 3-4: Compressive strength test and tested cubes and cylinders .....	43
Figure 3-5: Dimensions of a typical AA coupon specimen .....	45
Figure 3-6: Tensile coupon test setup and tested AA coupon samples .....	46
Figure 3-7: Stress-strain diagram for the four AA 5083-H111 .....	47
Figure 3-8: Grinding process for different AA surfaces .....	48
Figure 3-9: Carboplate: (a) Strip roll. (b) Plate with plastic film shown .....	49
Figure 3-10: Sikadur-30 LP epoxy components and mixture .....	50
Figure 3-11: Strain gauges and its adhesive .....	51
Figure 3-12: Plan and Elevation of instrumented specimen .....	52
Figure 3-13: Four sets of concrete prisms with the EBR attached. ....	53
Figure 3-14: Specimens with different bond length .....	53
Figure 3-15: Specimen preparation steps .....	54
Figure 3-16: Specimen dimensions and loading configuration .....	55
Figure 3-17: Universal Testing Machine and test setup .....	55
Figure 4-1: Pull test setup with strain gauges .....	57
Figure 4-2: Twenty four Prisms with $f_c'$ of 20MPa. ....	58
Figure 4-3: Three different EBR materials used. ....	58
Figure 4-4: Variation of stress, strain, slip and load of 20-CF-L1 specimen .....	59
Figure 4-5: Variation of stress, strain, slip and load of 20-CF-L2 specimen .....	60

Figure 4-6: Variation of stress, strain, slip and load of 20-CF-L3 specimen .....	61
Figure 4-7: Variation of stress, strain, slip and load of 20-CF-L4 specimen .....	62
Figure 4-8: Variation of stress, strain, slip and load of 20-R-L1 specimen .....	63
Figure 4-9: Variation of stress, strain, slip and load of 20-R-L2 specimen .....	64
Figure 4-10: Variation of stress, strain, slip and load of 20-R-L3 specimen .....	65
Figure 4-11: Variation of stress, strain, slip and load of 20-R-L4 specimen .....	66
Figure 4-12: Variation of stress, strain, slip and load of 20-P-L1 specimen .....	67
Figure 4-13: Variation of stress, strain, slip and load of 20-P-L2 specimen .....	68
Figure 4-14: Variation of stress, strain, slip and load of 20-P-L3 specimen .....	69
Figure 4-15: Variation of stress, strain, slip and load of 20-P-L4 specimen .....	70
Figure 4-16: Twenty four specimens with $f_c'$ of 30 MPa. ....	72
Figure 4-17: Three different EBR materials used. ....	72
Figure 4-18: Variation of stress, strain, slip and load of 30-CF-L1 specimen .....	73
Figure 4-19: Variation of stress, strain, slip and load of 30-CF-L2 specimen .....	74
Figure 4-20: Variation of stress, strain, slip and load of 30-CF-L3 specimen .....	75
Figure 4-21: Variation of stress, strain, slip and load of 30-CF-L4 specimen .....	76
Figure 4-22: Variation of stress, strain, slip and load of 30-R-L1 specimen .....	77
Figure 4-23: Variation of stress, strain, slip and load of 30-R-L2 specimen .....	78
Figure 4-24: Variation of stress, strain, slip and load of 30-R-L3 specimen .....	79
Figure 4-25: Variation of stress, strain, slip and load of 30-R-L4 specimen .....	80
Figure 4-26: Variation of stress, strain, slip and load of 30-P-L1 specimen .....	81
Figure 4-27: Variation of stress, strain, slip and load of 30-P-L2 specimen .....	82
Figure 4-28: Variation of stress, strain, slip and load of 30-P-L3 specimen .....	83
Figure 4-29: Variation of stress, strain, slip and load of 30-P-L4 specimen .....	84
Figure 4-30: Twenty four specimens with $f_c$ of 40 MPa. ....	86
Figure 4-31: Three different EBR materials used. ....	86
Figure 4-32: Variation of stress, strain, slip and load of 40-CF-L1 specimen .....	87
Figure 4-33: Variation of stress, strain, slip and load of 40-CF-L2 specimen .....	88
Figure 4-34: Variation of stress, strain, slip and load of 40-CF-L3 specimen .....	89

Figure 4-35: Variation of stress, strain, slip and load of 40-CF-L4 specimen .....	90
Figure 4-36: Variation of stress, strain, slip and load of 40-R-L1 specimen .....	91
Figure 4-37: Variation of stress, strain, slip and load of 40-R-L2 specimen .....	92
Figure 4-38: Variation of stress, strain, slip and load of 40-R-L3 specimen .....	93
13	
Figure 4-39: Variation of stress, strain, slip and load of 40-R-L4 specimen .....	94
Figure 4-40: Variation of stress, strain, slip and load of 40-P-L1 specimen .....	95
Figure 4-41: Variation of stress, strain, slip and load of 40-P-L2 specimen .....	96
Figure 4-42: Variation of stress, strain, slip and load of 40-P-L3 specimen .....	97
Figure 4-43: Variation of stress, strain, slip and load of 40-P-L4 specimen .....	98
Figure 4-44: Twenty four specimens with fcu of 60 MPa .....	100
Figure 4-45: Three different EBR materials used .....	100
Figure 4-46: Variation of stress, strain, slip and load of 60-CF-L1 specimen .....	101
Figure 4-47: Variation of stress, strain, slip and load of 60-CF-L2 specimen .....	102
Figure 4-48: Variation of stress, strain, slip and load of 60-CF-L3 specimen .....	103
Figure 4-49: Variation of stress, strain, slip and load of 60-CF-L4 specimen .....	104
Figure 4-50: Variation of stress, strain, slip and load of 60-R-L1 specimen .....	105
Figure 4-51: Variation of stress, strain, slip and load of 60-R-L2 specimen .....	106
Figure 4-52: Variation of stress, strain, slip and load of 60-R-L3 specimen .....	107
Figure 4-53: Variation of stress, strain, slip and load of 60-R-L4 specimen .....	108
Figure 4-54: Variation of stress, strain, slip and load of 60-P-L1 specimen .....	109
Figure 4-55: Variation of stress, strain, slip and load of 60-P-L2 specimen .....	110
Figure 4-56: Variation of stress, strain, slip and load of 60-P-L3 specimen .....	111
Figure 4-57: Variation of stress, strain, slip and load of 60-P-L4 specimen .....	112
Figure 4-58: Effect of BL and fcu on load-extension relationship for CFRP .....	114
Figure 4-59: Variation of load, bond stress and slip with BL and fcu for CFRP ....	115
Figure 4-60: Effect of BL and fcu on load-extension relationship for CFRP .....	116
Figure 4-61: Variation of load, bond stress and slip with BL and fcu for CFRP ....	117
Figure 4-62: Effect of BL and fcu on load-extension relationship for AA-R .....	118

Figure 4-63: Variation of load, bond stress and slip with BL and $f_{cu}$ for AA-R ....	119
Figure 4-64: Effect of BL and $f_{cu}$ on load-extension relationship for AA-R .....	120
Figure 4-65: Variation of load, bond stress and slip with BL and $f_{cu}$ for AA-R ....	121
Figure 4-66: Variation of bond slip parameters with BL for CFRP and AA-R .....	122
Figure 4-67: Variation of bond slip parameters with bond length .....	124
Figure 4-68: Effect of BL and $f_{cu}$ on load-extension relationship for AA-P .....	126
Figure 4-69: Effect of BL and $f_{cu}$ on load-extension relationship for AA-P .....	127
Figure 5-1: Fitting results by Popovic's equation .....	129
Figure 5-2: Linear relation between max bond stress and concrete strength .....	130
14	
Figure 5-3: Linear regression between max bond stress and concrete strength .....	131
Figure 5-4: Average max bond stress based on $f_{cu}$ and $f_c'$ .....	132
Figure 5-5: Bond-slip curves for CFRP for different concrete strength .....	134
Figure 5-6: Bond-slip curves for AA-R plates for different concrete strength .....	135
Figure 5-7: Developed bond slip models for AA-R and CFRP plates .....	135
Figure 6-1: FE models .....	150
Figure 6-2: ANSYS SOLID65 reinforced concrete element [42] .....	151
Figure 6-3: ANSYS SOLID185 3D structural element [42] .....	153
Figure 6-4: Three modes of shear crack [48] .....	154
Figure 6-5: Bilinear model for traction and separation [43] .....	155
Figure 6-6: ANSYS CONTA174 and TARGE170 [43] .....	156
Figure 6-7: Contact and target bodies and surfaces .....	156
Figure 6-8: Generated mesh, loading and boundary conditions .....	157
Figure 6-9: Path generation for different bonded lengths .....	158
Figure 6-10: Solution process .....	159
Figure 6-11: Contact Bond stress along the bonded length .....	160
Figure 6-12: Contact sliding distance along the bonded length .....	161
Figure 6-13: Stress strain curve for 30-R-L4 specimen .....	162
Figure 6-14: Strain gauge readings along the bonded length .....	162

Figure 6-15: Contact Bond stress along the bonded length .....	163
Figure 6-16: Contact sliding distance along the bonded length .....	164
Figure 6-17: Stress strain curve for 40-R-L3 specimen .....	165
Figure 6-18: Strain gauge readings along the bonded length .....	165
Figure 6-19: Contact bond stress along the bonded length .....	166
Figure 6-20: Contact sliding distance along the bonded length .....	167
Figure 6-21: Stress strain curve for 40-R-L2 specimen .....	168
Figure 6-22: Strain gauges readings along the bonded length .....	168
Figure 6-23: Contact bond stress along the bonded length .....	169
Figure 6-24: Contact sliding distance along the bonded length .....	170
Figure 6-25: Stress strain curve for 60-R-L1 specimen .....	171
Figure 6-26: Strain gauges readings along the bonded length .....	171
Figure 6-27: 3D FE failure modes for four different samples .....	172

15

## List of Tables

Table 2-1: Effective bond length as stated by different FRP design codes [15] .....	29
Table 2-2: Factors affecting the bond-slip behavior .....	32
Table 2-3: Empirical bond strength models [5, 13] .....	33
Table 2-4: Fracture mechanics based bond strength models [5, 13] .....	34
Table 2-5: Proposed Design bond strength models [5, 13] .....	35
Table 2-6: Wrought and cast aluminum designation system [30, 32] .....	37
Table 2-7: Wrought aluminum designation system and properties [30, 32] .....	38
Table 3-1: Specimens dimensions details .....	42
Table 3-2: Materials and mix proportions .....	43
Table 3-3: Compressive strength for the four mixes .....	44
Table 3-4: Mechanical properties of AA 5083- H111 .....	44
Table 3-5: Chemical properties of AA 5083- H111 .....	45
Table 3-6: AA 5083-H111 properties obtained from the coupon test .....	47
Table 3-7: Carboplate mechanical properties .....	49

Table 3-8: Sikadure-30 LP mechanical properties .....	50
Table 3-9: Plate length, bond length and strain gauges locations .....	52
Table 3-10: Test matrix .....	56
Table 4-1: Summary of results for specimens with $f_c'$ of 20 MPa .....	71
Table 4-2: Summary of results for specimens with $f_c'$ of 30 MPa .....	85
Table 4-3: Summary of results for specimens with $f_c'$ of 40 MPa .....	99
Table 4-4: Summary of results for specimens with $f_c'$ of 60 MPa .....	113
Table 4-5: Variation of failure load and bond slip parameters with BL .....	123
Table 4-6: Variation of failure load and bond slip parameters with BL .....	123
Table 4-7: Variation of failure load and bond slip parameters with BL .....	123
Table 4-8: Variation of failure load and bond slip parameters with $f_{cu}$ .....	125
Table 4-9: Variation of failure load and bond slip parameters with $f_{cu}$ .....	125
Table 4-10: Variation of failure load and bond slip parameters with $f_{cu}$ .....	125
Table 5-1: Bond- Slip parameters for CFRP plates. ....	133
Table 5-2: Bond-Slip parameters for AA scratched plates .....	134
Table 5-3: developed CFRP and AA scratched models based on $f_{cu}$ and $f_c'$ .....	136
Table 5-4: CFRP bond-slip Parameters for different concrete strength .....	137
16	
Table 5-5: AA scratched bond-slip Parameters for different concrete strength .....	138
Table 5-6: Statistical measures for 20 MPa CFRP plates .....	140
Table 5-7: Statistical measures for 30 MPa CFRP plates .....	141
Table 5-8: Statistical measures for 40 MPa CFRP plates .....	142
Table 5-9: Statistical measures for 60 MPa CFRP plates. ....	143
Table 5-10: Statistical measures for 20 MPa AA scratched plates. ....	144
Table 5-11: Statistical measures for 30 MPa AA scratched plates. ....	145
Table 5-12: Statistical measures for 40 MPa AA scratched plates. ....	146
Table 5-13: Statistical measures for 60 MPa AA scratched plates. ....	147
Table 5-14: Summary of the statistical measures for CFRP and AA-R plates .....	148
Table 6-1: four specimens considered for the FE simulation .....	149

Table 6-2: Properties assigned to concrete. ....	151
Table 6-3: Properties assigned to AA plate .....	153
Table 6-4: CZM parameters for the modeled specimens .....	155
Table 6-5: Strain gauge locations for the Exp. samples Modeled .....	158

17

## List of Abbreviations

CFRP

Carbon fiber reinforced polymer.

EBR

EBL

Externally bonded reinforcement.

Effective bond length.

AA

Aluminum Alloy.

Lb

Bond length (mm).

bp

Plate width (mm).

tp

Plate thickness(mm).

Ep

Plate elasticity modulus.

$\tau_u$

Ultimate shear stress (MPa).

Le

Effective bond length (mm).

fctm

Concrete surface tensile strength (MPa).

Gf

Fracture energy (N.mm/mm<sup>2</sup>).

$E_c$

Concrete elasticity modulus.

$t_c$

Concrete prism thickness(mm).

$f_c'$

Concrete compressive strength.

$b_a$

Adhesive width.

$\beta_l$

Geometric bond length coefficient.

$\beta_p$

Geometric width coefficient.

$E_a$

Adhesive elasticity modulus.

18

## 1 Chapter 1: Introduction

### 1.1 Overview

In recent years, the steel plates and Fiber Reinforced Polymers (FRP) sheets and plates have been used as Externally Bonded Reinforcing (EBR) materials for the Reinforced Concrete (RC) structures. Using these materials as EBR has become a key element in extending the services live of RC structures. This is especially apparent with the development of more advanced and new FRP materials. An extensive research work has been conducted in the last two decades to evaluate and monitor the performance of the strengthening materials in order to validate their use in terms of safety, reliability, and durability. As predicted and experimentally proved, the EBR materials can significantly improve the overall strength of the structure [1].

Steel plates were the dominant and the most widely used EBR material for deficient reinforced concrete structures in the 1960's. However, they lost their appeal after a period of time due to steel susceptibility to corrosion, creep deformation and other shortcomings. As a result, the need of a new material to replace steel plates is becoming of a vital importance for the purpose of stronger and more durable structures. Recently FRP have been developed and used as a replacement to steel due to their superior properties regarding corrosion resistance, high tensile strength, low density, high durability and ease of installation. Nevertheless, the use of FRP as EBR material has some shortcomings such as low-temperature resistance, debonding and degradation due to other environmental factors [2-4].

FRP materials are manufactured in various forms such as bars, sheets, and plates. Usually FRP materials are bonded to the treated tensile surfaces using adhesive or epoxy resin. The adhesive acts as a transfer layer for the tensile stresses in the concrete to the FRP plate or sheet. In general, the bonding material has a lower ultimate tensile strength and lower modulus of elasticity than the bonded material. Therefore, failure is likely to occur at the interface if it is not prepared appropriately or if a very weak adhesive is used. Nevertheless, many research studies suggested that the main failure mode of FRP-concrete interface in shear tests is concrete cracking due to shear.

19

The concrete shear cracking occurs mostly at a few millimeters from the adhesive-concrete interface within the concrete. This means the system will fail before the FRP reaches its full capacity due to debonding [5, 6]. Generally, an important issue must be taken into consideration when using EBR materials, which is to design against a number of debonding failure modes. When testing full scale beams, the following failure modes could be encountered as shown in Figure 1-1. Namely, concrete cover separation, interfacial debonding at the plate end, intermediate (flexural or flexural-shear) crack induced interfacial debonding, and critical diagonal crack induced interfacial debonding [1, 5, 6]. Interfacial debonding, bond strength and bond behavior of interface between concrete and EBR material are the major topics to be addressed in this investigation. Figure 1-1: Failure modes of RC beams flexurally-strengthened with an FRP plate [7]

20

related to strengthening and retrofitting of reinforced concrete structures. Figure 1-2 illustrates the problem statement of this research. Figure 1-2: Problem Statement Steel CFRP Shortcomings Enhancing Structural Performance Introducing AA 5083-H111

1.2 Problem Statement The method of using EBR materials to strengthen aging and deteriorating RC structures has proven its feasibility and effectiveness. As previously stated, the use of

steel, FRP and other materials as EBR already had great impact on strengthening and repairing of deficient structures. Nevertheless, due to some shortcoming associated with

these conventional materials used in this technique, new materials need to be introduced. These new materials should have the ability to overcome some of the old

materials shortcomings in order to work as a supplement or a substitute for existing ones. The introduction of Aluminum Alloy AA plates as an EBR material will represent

a valuable addition. The AA plates with their desirable characteristics has the potential

of overcoming the shortcomings of the current and prevailing strengthening materials.

Introduction of the AA plates as EBR material will be advantageous to engineers and researchers locally, regionally and internationally. Therefore, the importance of this research is evident and its outcome will address regional and perhaps global concerns

21

1.3 Research Significance

A variety of materials have been used as EBR materials with the purpose of strengthen reinforced concrete structures. This approach is a viable and more economical solution compared to the alternative which is totally demolishing and replacing the structure. The need for strengthening reinforced concrete structural members and components originates from deficiencies resulting from aging of these structures. Such deficiencies may be due to a number of factors including functional changes such as increase in dead loads or live loads due to changes in structure usage. Furthermore, modifications in the codes of design could necessitate the use of strengthening. In these cases, the carrying capacity of the structure is maintained but it needs to be increased to account for the additional loads. Furthermore, strengthening is needed when the structure starts to deteriorate due to internal problems with in the structure itself such problems include corrosion and carbonation of reinforcement steel, design errors and hazardous factors (earth quakes or fire) leading to a decrease in carrying capacities. In this case the strengthening is needed to regain the lost capacity. Among others Steel and FRP plates have been used effectively in increasing the shear and flexural capacities of RC beams. However, both materials have some shortcomings as stated above. The exploration of an innovative material that has the ability to overcome these shortcomings and to provide comparable performance will contribute significantly to the advancement in the strengthening material industry. The recently developed aluminum alloys AA have desirable characteristics and great potential to be used as externally bonded strengthening materials while overcoming some of the shortcomings of steel and FRP. The desirable characteristics of AA include their light weight, their high resistance to corrosion and their relatively high thermal resistance. Furthermore, AA have the ability to be easily formed and externally bonded to concrete using the epoxy adhesive. In addition, unlike the FRP plates, the AA plates have an important property which is ductility. The ductile failure mode is the most desirable in practical applications. Therefore, the significance of this research stems from exploring the suitability and adaptation of a new EBR material that overcomes the shortcomings of the prevailing steel and FRP and provides new advantages. These significant and novel contributions will advance the knowledge in this field and will positively impact the construction industry locally, regionally and globally

22

#### 1.4 Research Objectives

Bearing in mind the research significance, the objective of this research study is to examine the validity of using aluminum alloy plates in strengthening deficient RC structures. In details the research objectives can be formulated as follows:

- ☒ To propose a bond stress-slip model that can provide the effective bond length and the bond strength for externally bonded aluminum alloy plates to concrete.
- ☒ To study the behavior of reinforced concrete beams strengthened with aluminum alloy plates experimentally using single shear test.
- ☒ To investigate the system modes of failure and how they are affected by the changes in bond length, concrete strength, geometry and other properties of the concrete prism, aluminum alloy plate and adhesive material.
- ☒ To develop a finite element model that predicts and captures the response behavior of bond stress and bond slip between aluminum alloy plates and concrete of a number of tested specimens.

## 1.5 Thesis Organization

The thesis consists of the following chapters:

- ☐ Chapter 1: Introduction. Provides an overview of the EBR techniques and sets out the primary objectives of the research.
- ☐ Chapter 2: Background. Presents a comprehensive literature review on the factors affecting the bond stress-slip relationship and the models produced.
- ☐ Chapter 3: Experimental Program. Provides details of the experimental program including preparation of specimens, instrumentation and testing.
- ☐ Chapter 4: Results and Discussion. Presents the experimental results and discusses the effect of several parameters on the bond stress- slip relation.
- ☐ Chapter 5: Development of AA and CFRP Models. Shows the development of AA & CFRP bond-slip models based on existing models and relations.
- ☐ Chapter 6: Finite element model Development. Presents the development of the FEM for a selected number of tested samples.
- ☐ Chapter 7: Conclusions and Recommendations. Summarizes the key findings and provides suggestions for future research.

23

## 2 Chapter 2: Background

### 2.1 Strengthening of Structures

Although reinforced concrete structures are durable, they deteriorate over the years due to many reasons. In addition, functional changes in the use of RC structures design and construction errors may necessitate the reason for strengthening after years of service. Different strengthening techniques have been developed and used in order to restore and maintain the strength and stiffness of the structure. External reinforcement is one of the most effective techniques for strengthening RC structures as the external reinforcement improves the original tensile strength provided by the steel rebar inside the concrete members resulting in enhancing their strength and stiffness [8, 9].

Reinforced concrete structures that are reinforced with externally bonded material consist of the following components as demonstrated in Figure 2-1 below.

Figure 2-1: Cross-section of an externally bonded RC structure [2]

24

### 2.2 Steel as Externally Bonded Reinforcement

Steel plates have been used as externally bonded strengthening material for deficient reinforced concrete structures since 1960's. This technique is used to increase both strength and stiffness of aging structures. In applying such technique an adhesive is used as a bonding material between the steel and the surface of the reinforced concrete member. Shear forces needs to be transferred between the

concrete and the steel plate, this is done through the adhesive layer between the two materials. Due to steel deficiencies in terms of corrosion resistance, creep deformation and other considerations, development of a new externally bonded strengthening material is of vital importance in the structures strengthening technology [4, 8]. Figure 2-2 illustrates the use of steel plates as an EBR material.

### 2.3 FRP as Externally Bonded Reinforcement

The use of externally bonded FRP as a new material to replace the traditional use of steel plates has increased drastically in the last two decades. This is due to its superior properties regarding corrosion resistance, high tensile strength, low density, high durability and ease of installation. The Swiss federal laboratory for material testing and research (EMPA) was the first facility to examine the FRP plate bonding technology in 1984, when they conducted a number of tests on reinforced concrete beams strengthened with (CFRP) [4, 10].

Figure 2-2: Use of steel plates as EBR systems [9]

25

Recently the FRP material has been used for various application in a number of countries. The majority of the early uses of FRP were in Japan, followed by Europe, North America, and the gulf Region. The FRP material is used in several applications, including strengthening of walls, bridge parking structures, among others. Figure 2-3 shows some of the FRP applications in strengthening reinforced concrete structures [3].

The bond strength between the FRP and concrete represents the key element in understanding the behavior of FRP strengthened reinforced concrete structures. Typically, the FRP material cannot attain its ultimate strength when debonding occurs at or near FRP-concrete interface. A complete understanding of this behavior is not reached. As a result, an extensive research has been conducted and still underway to study the interfacial debonding between the FRP and reinforced concrete using several shear testing techniques. A summary of the commonly used shear test techniques and their corresponding failure mode is given in the following section [5, 6, 8, 10].

Figure 2-3: Application of FRP [3]

26

### 2.4 Shear Tests and Failure Modes

From the time when the steel plates were first used until they recently replaced by the advantageous FRP plates, different experimental setups have been performed to define the interfacial bond strength between the FRP and concrete. Namely, single shear tests, double shear tests, and modified beam tests where used. Figure 2-4 shows the types of bond tests. There is no agreement on a standard shear test layout and therefore a standard methodology has yet to be generally acknowledged [1, 11]. However far end support double shear pull test and near end support single shear pull tests are the most used methods so far due to their simplicity and accuracy. Studies have shown that test results can significantly change due to difference in test setups leading to a wide range of results. Also based on a recent stress analysis, small variation in the test setup within each method such as the support block height in a single or double shear test may also have a significant effect [1, 12].

Figure 2-4: Types of bond tests [1]

27

Generally, two main failure modes take place after testing an EBR bonded material using single shear test including, cohesion failure and adhesion failure. The cohesion failure is a material failure possibly taking place within one of the EBR system materials i.e. concrete, adhesive or the bonded plate. The adhesion failure typically takes place in the interfaces between the EBR system materials. One of the rare failure modes is the concrete prism failure which is a cohesion failure, this failure mode takes place when the FRP plate has the same width as the concrete prism and the FRP plate is relatively short [1, 5, 6, 10]. Figure 2-5 shows the typical failure modes and locations for EBR systems.

☒ Concrete failure (Few millimeters depth).

☒ Concrete prism failure.

☒ Adhesive failure.

☒ Plate delamination.

☒ Plate rupture/yielding.

☒ Concrete/Adhesive interface de-bonding.

☒ Adhesive/Plate interface de-bonding.

Cohesion Failure. (Failure within the material)

Adhesion Failure. (Failure in interface)

1

2

3

6

7

4

5

2

Concrete substrate

Concrete/Adhesive interface

Adhesive/Plate interface

Plate Delamination

Adhesive Layer

1  
3  
4  
6  
7  
5

Figure 2-5: Typical failure modes and failure locations for EBR systems

28

### 2.5 Effective Bond Length

Due to pull force applied on the EBR plates, the material induced force is transferred to concrete primarily through shear stress in the adhesive in a short length near the applied load which is called effective bond length EBL. Beyond this length an extension of the bond length will not increase the ultimate capacity of the joint. In other words, the bond length of the adhesively bonded EBR plate cannot be increased with the intention of assuring that the maximum capacity is achieved through rupture in FRP plate/sheets or yield in steel or aluminum plates. This is considered as a fundamental difference between EBR and internal reinforcement in which a sufficiently long anchored length can be determined in order to develop the full tensile strength of the reinforcement. In addition, increasing the bond length beyond the EBL will not lead to any increase in failure load. Therefore determination of the EBL is of a vital importance in calculating the maximum bond capacity of the EBR [1, 13, 14]. The EBL concept can also be defined by stress or strain distribution through the bond length. Hence, the EBL is the distance required for the bond stresses to fade. With the initiation of debonding taking place in the vicinity due to concrete fracture, the bond stresses will move to a new unfractured region. This shifting in stresses and strains is repeated until the crack propagates throughout the full bonded length. the EBL at any loading phase is considered as the length at which the EBR material can resist the entire load at that phase through the bond stresses [15]. Most theoretical bond strength models tend to model the FRP maximum capacity based on predicting the effective bond length. On the other hand many analytical models have been introduced with the aim to predict the ultimate bond strength and the effective bond length of (EBR) FRP plates [14]. The EBL location has been determined by several studies as the distance at which the bond stresses reach 10% of the maximum bond stress. Table 2-1 shows the effective bond length predictions based on different FRP design codes. The variation of the predicted EBL by a number of design codes versus the axial stiffness (EA) for available laminates in the market is illustrated in Figure 2-6. As shown, in some design codes the EBL increases with the axial stiffness (EA) while in others the EBL decreases. This major difference in these codes predictions indicates that a full understanding of FRP-concrete bond behavior is not yet reached and a further research is required [16, 17].

29

Table 2-1: Effective bond length as stated by different FRP design codes [15]

Code

Year

Expression

ACI 440.2R-02 (USA)

2002

$$L_e = 23300(nEftf)0.58$$

ISIS CSA S806-02(Canada)

2002

$$L_e = 25350(Eftf)0.58$$

FIB B14–Appendix A1 (Europe)

2001

$$L_e = \sqrt{Eftfc^2fctm} \quad c^2=2$$

FIB B14–Appendix A2 (Europe)

2001

$$L_e = c\sqrt{Eftffc}fctm \quad c^2=1.44$$

CS TR55 (UK)

2004

$$L_e = 0.7\sqrt{Eftffc}fctm$$

CNR-DT 200/04 (Italy)

2005

$$L_e = \sqrt{Eftf^2fctm}$$

Euro code 8-3 (Europe)

2004

$$L_e = \sqrt{Eftf^4fctm}$$

CIDAR (Australia)

2006

$$L_e = \sqrt{Eftf\sqrt{fc}}$$

$L_e$  = Effective bond length,  $Ef$  = elastic modulus of FRP,  $fc'$  = concrete strength,  $fc$  = characteristic strength of concrete,  $fctm$  = mean tensile strength of concrete,  $tf$  = thickness of FRP,  $n$  = number of FRP bonded plates.

Figure 2-6: Effective bond length calculated using existing design codes [9]

30

## 2.6 Composite Action

Generally, a perfect bond is assumed between the concrete and the reinforcing steel in conventional reinforced concrete elements, whereas this is not the case for the externally bonded reinforcement. In EBR strain compatibility is the degree to which strain can be transferred to the EBR or the adhesive slip occurrence, these will determine the overall system resistance and the forces of each material [18].

The composite action between EBR and concrete is mainly attained by a chemical connection using a polymeric adhesive, mainly epoxy resin. Since epoxy resin is a brittle material after hardening, failure due to debonding of the reinforcement from concrete is very sudden which takes place at the interface and it occurs without ample warning [19].

## 2.7 Factors Affecting Bond Stress-Slip Relationship

The prediction of the bond stress-slip relationship is mainly achieved by analyzing the factors that affect the relationship. These factors include the following [11, 18]

- ☒ Concrete compressive strength ( $f_c'$ ).
- ☒ The bond length (L) up to an effective bond length ( $L_e$ ).
- ☒ Axial stiffness of (EBR)  $E_{ptp}$ .
- ☒ Width ratio between (EBR) and concrete  $b/b_c$ .
- ☒ Adhesive axial stiffness  $E_a t_a$ .
- ☒ Concrete surface treatment.
- ☒ Plate surface treatment.

2.7.1 Concrete compressive strength. Numerus studies concluded that higher concrete compressive strength results in a higher failure loads and also higher bond stresses. Nakaba et al [20] examined the effect of concrete compressive strength  $f_c'$  on the bond behavior using double shear test. The  $f_c'$  value used ranges from 23.8 MPa to 57.76 MPa. He concluded that higher concrete strength results in a higher bond stresses and failure loads. Similar results were obtained by Savoia et al [21]. Additionally, other investigators [22] concluded that higher compressive stress of concrete will result in slightly higher interface shear stresses at failure.

31

2.7.2 Concrete surface treatment. Toutanji and Ortiz [23] conducted an experimental analysis on how the concrete surface treatment and the type of the FRP reinforcement affects the bond strength between concrete and FRP sheet. In their study the surface of the specimens was treated using two methods before FRP was bonded to concrete surface. The first method consisted of concrete surface sanding using an ordinary sander. This method is conducted in order to get rid of the weak thin layer of mortar from the specimens. The second method was performed using a water jet from an intensifier

pump machine. In this method, double shear face test was used, and their experimental results showed that the bond between the FRP and concrete was significantly improved resulting in a higher value of load and strain when water jet was used for surface preparation. He concluded that the water jet method exhibits higher bonding loads ranging between 60-75% higher than sander. The results of another experimental study conducted by Yoshizawa et al.[24] shows that surface treatment by water jet produce a better bonding strength than treatment by sander (about 37% higher than the sander). Talbot et al. [25] had studied various concrete surface roughness using chipping, sandblasting, grinding, and water jetting. Their results showed that water jetting provides higher bond stresses particularly when sandblasting is used afterwards. Additionally, Júlio et al. [26] used different techniques for concrete surface preparation including chipping with a light jackhammer, wire-brushing and sandblasting. After adding the new concrete and performing the pull out test, they concluded that sandblasting is the best method for concrete surface preparation for bonding.

2.7.3 Bond length Chajes et al. [27] conducted an experimental investigation using a single shear test to monitor the strain profile and failure loads. They observed that the bond became fully developed when the bond length falls in the range of 75 mm to 100 mm. As a result, specimens having 100 mm, 150 mm and 200 mm bond lengths showed a very similar failure load. Maeda et al. [39] reported that effective bond length increases with increase in stiffness of FRP which is not true by considering the large amount of experimental data available. Yuan et al deduced the effective bond length expression based on the relationship between fracture energy and shear stress-bond slip relationship.

32

2.7.4 Adhesive and plate elastic modulus. An adhesive with a higher elastic modulus will result in a higher interfacial stresses, while a reduction in the adhesive thickness will result in an increase of the interfacial shear and normal stresses. In addition, the location of the peak stresses will be affected. Whereas an increase in both of the plates thickness and elastic modulus will result in an increase in the interfacial shear stresses with no effect on the location of the peak value [3, 28, 29]. Table 2-2 shows a summary of factors that affect the bond stress-slip in the FRP-concrete interface as reported by several researchers.

Table 2-2: Factors affecting the bond-slip behavior

Concrete strength

FRP stiffness

Surface treatment

Bond length

Width ratio

Adhesive properties

Ultimate load

Increase [30]

Increase [20, 31, 32]

Increase [32-34]

Increase [5, 12]

Increase [8]

---

Bond strength

Increase [8]

---

Increase [34]

---

---

Increase with adhesive flexibility[14]

Effective Bond length

Slightly decreased [22]

---

Increase [34]

---

---

Increase with adhesive flexibility [14]

Still the effect of each of the above-mentioned parameters separately on bond-slip behavior is yet to be addressed due to the interaction between these parameters. A large experimental program with a wide range of specimens needs to be developed in order to study the effect of these parameters on the bond-slip behavior individually by changing the properties of one factor and set others as constant.

33

## 2.8 Bond Strength Models

The EBR is considered as one of the most used reinforced concrete strengthening techniques for existing structures with many advantages as previously stated. Nevertheless, the EBR efficiency could be severely affected by premature debonding. Therefore, the EBR-concrete bond strength is the major factor that controls the debonding failure in reinforced concrete members strengthened by EBR. As a result, a wide range of experimental and theoretical investigations have been conducted and various bond-slip models have been suggested in order to predict the bond capacity of EBR-RC composite system [13, 22, 35]. Generally, bond strength models can be classified into three main categories [8, 13, 18].

2.8.1 Empirical bond strength models. These models are directly based on the regression of the test data. An example of that is the simple expression model proposed by Tanaka [36]. Likewise, Hiroyuki and Wu [37] performed a number of double shear tests on reinforced concrete-carbon fiber sheets CFS to generate their empirical model. Similarly Maeda et al. [38] presented a more resilient model taking into account the effective bond length. These relations are illustrated in Table 2-3.

Table 2-3: Empirical bond strength models [5, 13]

Model

Model

Tanaka et al. 1998 [36]

$$\tau u = 6.13 - \ln(L) \quad p u = \tau u \cdot L \cdot b p$$

Hiroyuki and Wu 1997 [37]

$$\tau u = 0.27 \cdot L - 0.669 \quad P u = \tau u \cdot L \cdot b p$$

Maeda et al. 1997 [38]

$$\tau u = (110.2 \times 10^{-6}) E p t p \quad P u = \tau u L e b p \quad L e = e^{2.1235 - 0.580 \cdot \ln(E p t p)}$$

34

2.8.2 Fracture mechanics based bond strength models. These models can be generally classified as a semi-empirical models which are based on fracture mechanics theory with parameters calibrated with experimental data. several fracture mechanics models have been developed by several researchers including Blaschko et al. [39], Täljsten [40], Yuan et al. [41] and Neubauer and Rostásy [42]. Table 2-4 shows a summary of fracture mechanics-based models developed for FRP-concrete interface.

Table 2-4: Fracture mechanics based bond strength models [5, 13]

Model

Model

Täljsten 1994 [40]

$$P u = b p \sqrt{2 E p t p G f} \cdot 1 + a t \quad a t = E p t p E c t c$$

Yuan et al. 1999 [41]

$$P u = b p \sqrt{2 E p t p G f} \cdot 1 + \alpha y \quad \alpha y = b p E p t p b c E c t c$$

Blaschko et al. 1998 [39]

$$0.78 b p \sqrt{2 G f E p t p} \quad \text{if } L \geq L e$$

$$P u = 0.78 b p \sqrt{2 G f E p t p} L L e (2 - L L e) \quad \text{if } L < L e \quad L e = \sqrt{E p t p} \cdot 4 f c t m \quad G f = c f k p 2 f c t m$$

$$K p = \sqrt{1.1252 - b p b c / 1 + b p / 400}$$

Neubauer and Rostásy 1997 [42]

$$0.64 b p k p \sqrt{f_{ctm}} E p t p \text{ if } L \geq L_e$$

$$P_u = 0.64 b p k p \sqrt{f_{ctm}} E p t p L L_e (2 - L L_e) \text{ if } L < L_e \quad L_e = \sqrt{E p t p} 2 \sqrt{f_{ctm}} \quad G_f = c f f_{ctm}$$

35

2.8.3 Proposed design bond strength models. Beside the empirical and fracture mechanics models, several design models have been developed. These models are generally proposed by adopting simple assumptions then verified against test data. Several researchers including Van Ge-mert [43], Challal et al. [44], Khalifa et al. [45], Izumo et al. [46], Dai et al. 2005 [47], Sato et al. [48] and Chen and Teng [8] have developed design models. Table 2-5 shows a summary of practical design models developed for FRP-concrete interface.

Table 2-5: Proposed Design bond strength models [5, 13]

Model Name

Model

Khalifa et al. 1998 [45]

$$\tau_u = (110.2 \times 10^{-6}) (f'c)^{0.42} E p t p \quad P_u = \tau_u L_e b p \quad L_e = e^{2.1235 - 0.580 \ln(E p t p)}$$

Sato et al. 2001 [48]

$$\tau_u = 2.68 \times 10^{-5} E p t p \quad P_u = \tau_u L_e (b p + 7.4) \quad L_e = 1.89 (E p t p)^{0.4} \text{ if } L > L_e: L_e = L$$

Izumo et al. 1999 [46]

$$\text{CFRP: } P_u = (3.8 f'c^{0.67} + 15.2) L E p t p b p$$

$$\text{AFRP: } P_u = (3.4 f'c^{0.67} + 69) L E p t p b p$$

Chen and Teng 2001 [8]

$$P_u = 0.427 \beta p \beta L \sqrt{f'c} \quad L_e = \sqrt{E p t p} \sqrt{f'c} \quad \beta p = [2 - (b p b c / \lambda) + (b p b c / \lambda)^2]^{0.5} \text{ if } L \geq L_e$$

$$\beta L = \sin[\pi L / 2 L_e] \text{ if } L < L_e$$

Van Ge-mert 1980 [43]

$$p_u = 0.5 \cdot L \cdot b p \cdot f_{ctm}$$

Challal et al. 1998 [44]

$$\tau_u = \tau_{max debonding} = 2.7 / (1 + k_1 \tan 33^\circ)$$

$$k_1 = t p (E_a b a 4 E p l p t a)^{0.25}$$

36

## 2.9 Aluminum

During the last few decades a number of materials have been used as externally bonded reinforcement to strengthen reinforced concrete aging structures. FRP and steel were the most widely used materials

in this industry due to their various advantages. However, due to some shortcomings associated with these materials, researchers are continuously exploring the possibility of developing new materials that have all FRP and steel advantages and few or none of their shortcomings. In this research the potential of using AA plates as EBR will be investigated.

Aluminum is one of the most commonly used metals. Due to its formability and other desirable characteristics, it is the second widely used metal after steel. This metal and its alloys offers a variety of desirable characteristics and advantages that make it favorable for many applications. The use of aluminum alloys in engineering design and application is based on many factors related to its physical and mechanical characteristics such as its high strength to weight ratio, corrosion resistance, machinability, fire resistance, good formability and has relatively low cost [49-51].

The alloys of aluminum can be classified into several groups depending on the primary alloying element and other materials properties forming the alloy. In general, there are two main aluminum alloys, mainly wrought alloys and cast alloys. Figure 2-7 and Table 2-6 show the designation system of wrought and cast aluminum alloys.

2.9.1 Wrought alloys. These alloys are cast as ingot or billet and then mechanically worked by some process such as rolling, extrusion, hammering or forgings to final form. Wrought alloys in general have high strength as they have been worked, heated and cooled down [52].

2.9.2 Cast alloys. These alloys are cast to its final or near final form by pouring the molten alloy into a mold to give it the final shape without any mechanical working. In general, cast alloys have a very low strength and they contain higher percentages of alloying elements. The properties of different aluminum alloys are shown in Table 2-7 [52].

37

Figure 2-7: Aluminum alloy designation system [32]

Table 2-6: Wrought and cast aluminum designation system [30, 32]

Wrought aluminum alloy designation system

Cast aluminum alloy designation system

Alloy Series

Principal Alloying Element

Alloy Series

Principal Alloying Element

1xxx

Pure Aluminum (99.00% or greater)

1xx.x

Pure Aluminum (99.00% or greater)

2xxx

Copper

2xx.x

Copper

3xxx

Manganese

3xx.x

Silicon plus copper and/or magnesium

4xxx

Silicon

4xx.x

Silicon

5xxx

Magnesium

5xx.x

Magnesium

6xxx

Magnesium and Silicon

6xx.x

Unused series

7xxx

Zinc

7xx.x

Zinc

8xxx

Other elements

8xx.x

Tin

9xxx

Unused series

9xx.x

Other elements

38

Table 2-7: Wrought aluminum designation system and properties [30, 32]

Wrought aluminum alloy designation system

Alloy Series

Principal Alloying Element

properties

Applications & Remarks

1xxx

Pure aluminum

- ☒ Aluminum (99.00) % or greater.
- ☒ Non-heat treatable but strain hardenable.
- ☒ Representative designations: 1100, 1350.
- ☒ Ultimate tensile strength of 10 to 27 ksi.
- ☒ Weldable (narrow melting range).
- ☒ Superior corrosion resistance.
- ☒ Excellent electrical conductivity
- ☒ Poor mechanical properties.
- ☒ Not considered for general structural applications.
- ☒ Depending on the application they often welded with 4xxx filler alloys or matching filler

2xxx

Copper

- ☒ additions ranges from (0.7 to 6.8) %
- ☒ Heat treatable.
- ☒ Ultimate tensile strength of 27 to 62 ksi.
- ☒ High strength and high performance
- ☒ Superior corrosion resistance.

- ☒ Excellent strength for verity of temperatures.
- ☒ Representative alloys: 2014, 2017, 2024, 2219, 2195.
- ☒ Some are non-wieldable by arc welding.
- ☒ Some are welded successfully with the correct welding procedure.
- ☒ Often welded with high strength 2xxx to match their performance.
- ☒ Also can be welded to 4xxx depending on the application.
- ☒ Used for aerospace aircraft applications 2024 and trucks body 2014.

3xxx

Manganese

- ☒ additions ranges from (0.05 to 1.8) %
- ☒ Non-heat treatable.
- ☒ Ultimate tensile strength of 16 to 41 ksi.
- ☒ Moderate strength, Good corrosion resistance, formable and suitable to use in high temperatures.
- ☒ Welded with 1xxx, 4xxx, 5xxx depending on chemistry and specific application.
- ☒ Firstly, used for pots and pans.
- ☒ Heat exchange in vehicles and power plants
- ☒ Not considered for general structural applications due to their moderate strength.

4xxx

Silicon

- ☒ Silicon additions ranges from (0.6 to 21.5) %
- ☒ Heat treatable / non-heat treatable.
- ☒ Ultimate tensile strength of 25 to 55 ksi.
- ☒ Improved fluidity when molten.
- ☒ Reduced melting point.
- ☒ Pistons, complex-shaped forgings
- ☒ Only series that contains heat and non-heat treatable.
- ☒ Filler materials used for both fusion welding and brazing.
- ☒ 4032 and 4043 are the most used alloys.

39

5xxx

### Magnesium

- ☒ magnesium additions ranges from (0.2 to 6.2) %
- ☒ Non-heat treatable but Strain hardenable.
- ☒ Ultimate tensile strength of 18 to 51 ksi.
- ☒ Excellent corrosion resistance, toughness, moderate strength
- ☒ Easily weldable.
- ☒ Regularly welded with filler alloys.
- ☒ More than 3.0% magnesium alloys are not recommended for elevated temperature above 150° F (stress corrosion cracking possibility).
- ☒ The 5052 alloy has maximum magnesium content that can be welded with a 4xxx series filler alloy.
- ☒ It's not recommended to weld high magnesium alloys with 4xxx series but this is possible for 5xxx series.
- ☒ Highest strength among non-heat-treatable alloys.
- ☒ Used for a wide variety of applications (ship building, transportation, pressure vessels, bridges and buildings).
- ☒ alloys with less than around 2.5% magnesium are often welded successfully with the 5xxx or 4xxx series filler alloys series

6xxx

### Magnesium and Silicon

- ☒ Magnesium and silicon additions about 1.0%
- ☒ Heat treatable.
- ☒ Ultimate tensile strength of 18 to 58 ksi.
- ☒ High corrosion resistance and moderate strength.
- ☒ Magnesium-silicide is produced which provides material ability to become solution heat treated for enhanced strength.
- ☒ Solidification crack sensitive.
- ☒ Most widely used alloy in aluminum extrusion.
- ☒ Found through welding fabrication industry.
- ☒ Mainly used as extrusions and incorporated in many structural components.

☒ Cannot be used as arc welded autogenously (without filler material) the addition of filler material is vital for arc welding.

☒ Welded with 4xxx, 5xxx depending on application.

7xxx

Zinc

☒ Zinc additions ranging from 0.8 to 12.0%)

☒ Heat treatable.

☒ Ultimate tensile strength of 32 to 88 ksi.

☒ Involves some of the highest strength aluminum alloys.

☒ Some are non-weldable by arc welding.

☒ Some are welded successfully with the correct welding procedure.

☒ 7005 are the common welded alloys welded with 5xxx series alloys.

☒ Zinc additions ranges from (0.8 to 12.0) %.

☒ used in high performance applications including aircraft, aerospace, and competitive sporting equipment

8xxx

Other Elements

☒ Heat treatable.

☒ Ultimate tensile strength of 17 to 35 ksi.

☒ High conductivity and strength hardness.

☒ Used in aerospace, electrical and bearing applications.

40

### 2.9.3 Aluminum versus steel

☒ Aluminum alloys weighs about  $27.145\text{KN}/\text{m}^3$ , this is approximately about one third of that's of steel iron  $76.01\text{KN}/\text{m}^3$ . This difference in weight accompanied by aluminum strength makes it more attractive when the dead loads are the main issue. This property of having high strength to weight ratio leads to more use of aluminum in a variety of applications such as crane booms and large clear span roofs. The reduced dead load of aluminum allows for a higher service loads.

☒ Another property that favors aluminum over steel is its high corrosion resistance, which leads to a reduction in maintenance cost. In addition, steel needs coating to prevent or decrease the rate of steel corrosion, which is an imperfect solution due to difficulties in maintaining the coating [50].

☒ A less but effective property is the cost of aluminum compared to steel as the cost of both materials is approximately the same for equivalent volumes of the two materials. Yet the Aluminum overall cost is lower due to its corrosion resistance and light weight compared to steel. In the case of aluminum, corrosion resistance cancels the need for coating which is necessary for steel leading to a decrease in the cost of aluminum.

#### 2.9.4 Aluminum versus FRP

☒ Aluminum has a lower melting point when compared to steel. This will lead to a higher strength loss with increased temperature. However, strength disintegration is not significant until  $200^{\circ}C$  ( $392^{\circ}F$ ). As for the FRP a loss in dimensional stability accumulates due to rise of temperature.

☒ Unlike FRP aluminum is an isotropic material that is able to resist forces in all directions, whereas the FRP material lacks this property which leads to a decrease for the FRP-concrete composite system in resisting forces perpendicular to the FRP direction.

☒ Aluminum ductility is a property that enables it to behave differently. In other words, when the failure occurs the aluminum will fail by yielding rather than FRP brittle failure or sheet/plate rupture. This property of aluminum makes it a better strengthening material when compared to FRP.

41

## 3 Chapter 3: Experimental Program

The experimental program conducted in this research is aimed at studying the AA-concrete and FRP-concrete bond strength and the effective bond length using a flexible epoxy adhesive.

### 3.1 Test Specimens

A total of 96 concrete prisms with average concrete strength of 20, 30, 40 and 60 were prepared and strengthened with AA and CFRP plates using epoxy adhesives as a bonding material. As shown in Figure 3-2 all prisms have a cross section of  $75 \times 75\text{mm}$  and a length of 250mm. The specimens were subjected to a tensile load using near-end supported single shear test technique to evaluate the performance of the AA/CFRP plates as an EBR materials. Figure 3-1 shows the apparatus used to confine the concrete specimens during loading in a Universal Testing Machine (UTM) that has a capacity of 100 KN. The apparatus is made of welded C-steel sections and plates to provide adequate confinement to the concrete prisms. Additionally, a 10 mm space is kept between the concrete prism and the loaded end support to insure that failure will take place due to debonding and not in the prisms. The bonded plates were subjected to a displacement control loading rate of  $2\text{mm}/\text{min}$  and were prevented from movement in the vertical and lateral directions.

Figure 3-2: Single shear test specimen

Figure 3-1: Apparatus used to hold the specimen

42

### 3.2 Materials and Properties

3.2.1 Concrete. Four normal weight concrete mixes with a targeted compressive strength of 20, 30, 40, and 60 MPa were casted. Six concrete cylinders and six cubes were casted for each mix along with the concrete prisms as illustrated in Figure 3-3. An ordinary water curing scheme is conducted after hardening. Six cylinders and six cube were tested during 28 days from which three cubes and three cylinders were tested on the 28th day as shown in Figure 3-4. The dimensions of the cubes, cylinders and the concrete prisms are shown in Table 3-1. The four mixes proportions in (Kg) are shown in Table 3-2 and the crushing test results are illustrated in Table 3-3.

Table 3-1: Specimens dimensions details

(a) Cubes and cylinders to be tested

for each mix

(b) Formwork used for casting the concrete prisms

(c) Four concrete Prism sets with different concrete strength

Figure 3-3: Prepared cubes, cylinders and prisms

43

Table 3-2: Materials and mix proportions

Material (Kg)

Mixes Weight (0.1Kg/m<sup>3</sup>)

(20 MPa)

(30 MPa)

(40 MPa)

(60 MPa)

Water

25.88

24.29

20.33

17.5

Cement

25.88

35.29

40.66

50

Coarse aggregate (10mm)

78.82

76.47

93.77

110

Dune Sand

42.94

47.06

37.25

27.4

Crushed Sand

42.35

38.24

30.59

41.3

Super Plasticizer

-----

-----

-----

600 ml

(a) Cylinder testing

(b) Cube testing

(c) Cubes and cylinders to be tested

(d) Failure modes of cubes and cylinders

Figure 3-4: Compressive strength test and tested cubes and cylinders

44

Table 3-3: Compressive strength for the four mixes Mix No Specimen Compressive Strength (MPa) 3-day  
7-day 14-day 28-day Target Remarks

1

Cube

5.7

9.4

14.2

17.9

20

Ok

Cylinder

3.2

7.6

10.4

14.7

2

Cube

14.09

21.3

28.5

30.3

30

Ok

Cylinder

12.47

18.4

23.6

25.2

3

Cube

21.31

28.3

37.35

40.15

40

Ok

Cylinder

18.84

20.5

22.6

28.5

4

Cube

28.25

48.3

55.8

61.5

60

Ok

Cylinder

20.13

31.19

40.49

43.53

3.2.2 Aluminum alloy plates. One type of aluminum alloy is explored, mainly marine grade Aluminum Alloy AA5083 which is the hardened wrought alloy. This AA type has high tensile strengths that reaches 300 MPa. It is used in wide variety of applications such as ship building, transportation, pressure vessels, bridges and buildings.

3.2.2.1 Mechanical properties. The mechanical properties of the AA 5083 are shown in Table 3-4.

Table 3-4: Mechanical properties of AA 5083- H111

AA type

Tensile strength

Yield  
strength  
Elasticity modulus  
Elongation  
Thickness  
5083-H111  
41 ksi  
288.6 MPa  
21.4ksi  
148.8MPa  
70.3 GPa  
20.9%  
3 mm  
45

3.2.2.2 Chemical properties. The chemical properties of the AA 5083-H111 are illustrated in Table 3-5.

Table 3-5: Chemical properties of AA 5083- H111

Chemical Element
Percentage (%)
Aluminum (Al)
92.4 to 95.6
Manganese (Mn)
0.40 - 1.00
Iron (Fe)
0.0 - 0.40
Copper (Cu)
0.0 - 0.10
Magnesium (Mg)
4.00 - 4.90
Silicon (Si)

0.0 - 0.40

Zinc (Zn)

0.0 - 0.10

Chromium (Cr)

0.05 - 0.25

Titanium (Ti)

0.0 - 0.15

Figure 3-5: Dimensions of a typical AA coupon specimen

Gauge Length = 100 mm

Total Length = 300 mm

Cross section area = 20 mm x 3 mm

3.2.2.3 Coupon test for aluminum plates 5083-H111. Using the INSTRON machine, four specimens of AA plates 5083-H111 were shaped and tested according to ASTM specifications, which states that the tested sample under tension should have minimum values for the total length, grip section length and the radius of fillet of 203.3mm, 50mm and 12.7mm respectively. Figure 3-5 illustrates the dimensions of a typical coupon specimen.

46

Based on ASTM standards, four AA specimens have been prepared and labeled as AA(1), AA(2), AA(3), and AA(4), these are illustrated in Figure 3-6 (b). The tensile coupon test setup using the INSTRON machine is shown in Figure 3-6 (a). The failure mode for all four AA samples is illustrated in Figure 3-6 (c). The stress-strain diagrams for the four AA 5083-H111 samples are shown in Figure 3-7. These values were obtained using the load-extension curve readings provided by the Universal Testing Machine. Through the stress-strain curves it can be seen that the elasticity modulus is almost the same for all the four AA samples measured as the slope of the elastic straight line. The coupon test results are shown in Table 3-6.

(c) Tested AA samples

(a) Tensile coupon test setup with failure mode magnified

(b) Prepared AA samples

Figure 3-6: Tensile coupon test setup and tested AA coupon samples

47

Figure 3-7: Stress-strain diagram for the four AA 5083-H111

Table 3-6: AA 5083-H111 properties obtained from the coupon test

0

0

50

50

100

100

150

150

200

200

250

250

300

300

350

350

0

0

0.05

0.05

0.1

0.1

0.15

0.15

0.2

0.2

0.25

0.25

0.3

0.3

Stress (Mpa)

Stress (Mpa)

Strain

Strain

Stress Strain diagram for AA 5083

Stress Strain diagram for AA 5083--H111 platesH111 plates

AA 1

AA 1

AA 2

AA 2

AA 3

AA 3

AA 4

AA 4

AA ID

Tensile Strength (MPa)

Yield Strength (MPa)

Modulus of Elasticity (GPa)

Elongation (%)

AA #1

308.69

140.02

70

23.10

AA #2

307.67

139.82

70

21.44

AA #3

308.69

139.37

70

21.30

AA #4

309.24

140.36

70

21.96

Average

308.57

139.89

70

21.95

Specifications

288.60

148.00

70.3

20.90

Difference (%)

6.92

-5.48

-0.427

5.02

48

(b) Grinding process

(c) Grinded AA specimen with Smooth surface

(a) Grinding heads used to develop smooth and rough surfaces

(d) Grinded AA specimen with Rough surface

Figure 3-8: Grinding process for different AA surfaces 3.2.2.4 Grinding of AA plates. A grinder is used on the AA plates. Two different

grinding heads were used as shown in Figure 3-8 (a) to deliver different surface textures. The first grinding head is a steel head used for metals. This head is applied on

the adhesively bonded surface of the AA plate in order to develop a rough surface which provides a higher bond strength. The second grinding head is a sand paper head. This head is applied on the opposite upper surface of the AA plate in order to remove dust and other excessive scraps. The result is a smooth surface of the AA plates. A smooth surface is essential for a proper attachment of the strain gauges for more accurate strain results. The grinding process and grinded AA plates with smooth and rough surfaces are shown in Figure 3-8 (b), (c) and (d) respectively.

49

Table 3-7: Carboplate mechanical properties

Material

Carboplate E 170

Color

Black

Weight (gm/m)

113

Density (gm/cm<sup>3</sup>)

1.61

Fiber content (%)

68

Thickness (mm)

1.4

Tensile strength (MPa)

3100

Modulus of elasticity (GPa)

170

Ultimate elongation (%)

2.00

b

a

Figure 3-9: Carboplate: (a) Strip roll. (b) Plate with plastic film shown 3.2.3 CFRP plates . The (CFRP) used in this study is carboplate E170 which is a range of pultruded carbon fiber reinforced polymers. The plate is used as EBR for existing reinforced concrete, masonry and steel structural members. As illustrated in Figure 3-9 the plate is protected by a plastic film on both sides which eliminates the need for cleaning before installing. The mechanical properties are shown in Table 3-7.

50

3.2.4 Epoxy adhesive. In this study, Sikadur-30LP epoxy is used for bonding AA 5083-H111 and CFRP plates to the concrete prisms. It is an adhesive consists of two components A and B with a mixing ratio of 1:3. The two components are mixed together until a light grey color emerges. As soon as the light grey color emerges, the adhesive must be used within 45 minutes, which is the time needed to dry it. It specially designed for use at higher temperatures between +25oC and +55oC. The advantage of using epoxy is that no primer is needed, easy to mix and apply, also it is suitable for dried concrete surfaces. Figure 3-10 shows the epoxy adhesive used in this research. The mechanical properties are shown in Table 3-8

Table 3-8: Sikadure-30 LP mechanical properties

Physical Characteristics

Curing Time

Curing Temperature

25° C

55° C

Compressive Strength (N/mm<sup>2</sup>)

1 day

>75

85-115

3 days

>85

95-120

Tensile Strength (N/mm<sup>2</sup>)

1 day

-

23-28

3 days

12-15

25-30

Bond Strength (N/mm<sup>2</sup>) (on concrete)

1 day

>4

>4

Bond Strength (N/mm<sup>2</sup>) (on steel)

1 day

15

25

3 days

22

28

Shear Strength (N/mm<sup>2</sup>)

7 days

+40°C to +55°C (17-21)

Modulus of elasticity (N/mm<sup>2</sup>)

10000 at 25°C (compressive & tensile)

b

c

a

(c) Mixed epoxy

(b) Components A&B

(a) Sikadur-30 LP

Figure 3-10: Sikadur-30 LP epoxy components and mixture

(Concrete fracture)

(Concrete fracture)

51

10°C. The adhesive, manual and the strain gauge attachment are shown in Figure 3-11 (b), (c) and (d) respectively. (a) Strain gauges used with AA & FRP plates (b) Adhesive used to attach the strain gauge to the plate (c) Adhesive with manual (d) Strain gauge attachment to AA plate Figure 3-11: Strain gauges and its adhesive a b c d

3.2.5 Strain gauges. General purpose 10 mm foil strain gauges and their adhesive were used as shown in Figure 3-11 (a) in order to measure strains at different locations and load increments. From these strains the shear stress and slip are derived to develop the bond-slip curves for the AA and CFRP to concrete specimens. According to the manufacturer, the strain gauge adhesive should be kept in a low temperature below

52

### 3.3 Specimen Details and Instrumentation

Concrete prisms with dimensions of 250 × 75 × 75 mm were casted and used in

Table 3-9: Plate length, bond length and strain gauges locations

Bonded & free lengths (mm)

Strain gauges locations from free end (mm)

AA/CFRP plate length (mm)

S.G 20, 50, 110

210

S.G 50, 100, 160

260

S.G 50, 100, 150, 210

310

S.G 50, 100, 150, 200, 260

360

Figure 3-12: Plan and Elevation of instrumented specimen

160

200

160

100

50

160

160

150

Free end

AA/CFRP Plate

Strain gauge

P

250 mm

75 mm

50

50

50

50

60

P

250 mm

75

mm

Adhesive

AA/CFRP Plate

210 - 360

50 - 200

160

Loaded end

(a) Top view.

(b) Side view. this study along with AA and FRP plates attached as externally bonded reinforcement with different lengths as illustrated in Table 3-9. The AA and CFRP plates has the same width of 50 mm however the thickness differs with 3mm thickness for the AA plate and 1.2 mm for the CFRP. The AA and FRP plates has also the same length varying depending on the bonded length of the plate. The AA/FRP plates are externally bonded to concrete prism using epoxy adhesive with a thickness ranges between 1.0 and 1.3 mm. The surface of the concrete and the AA plates were cleaned before bonding the plates to the concrete prism surface. Several strain gauges were placed at 50 mm spacing along the bonded part and one along the free part of the plates as shown in Figure 3-12. The strain gauges were connected to a data logger (recorder) in order to record the strain development in the plates.

The four concrete prisms sets with the EBR attached are shown in Figure 3-13. The different bond lengths for AA and CFRP plates with the strain gauges attached are illustrated in Figure 3-14 (a) and (b) respectively.

Figure 3-13: Four sets of concrete prisms with the EBR attached.

a

b

c

d

(a) AA

(b) CFRP

Figure 3-14: Specimens with different bond length

a

b

54

d

e

f

j

c

b

a

i

h

g

l

Marked prism

Prism marking

Strain gauge attaching

Mounting

Testing

Excess epoxy removal

Epoxy leveling

Epoxy poring

Plate attaching

Grinding

Plate marking

Cleaning

k

Figure 3-15: Specimen preparation steps Figure 3-15 provides a step by step illustration of specimen preparation starting from cleaning the sample by removing dust and other excessive scraps Figure 3-15(a) until the testing of specimen Figure 3-15(l).

55

### 3.4 Test Setup

All concrete prisms strengthened with AA 5083-H111 and CFRP were mounted in a special apparatus which is used to hold the concrete prisms during loading. The specimens were subjected to a tensile load using near-end supported single shear test technique to evaluate the performance of the AA/FRP plates as an EBR materials. The specimens were subjected to a displacement control loading rate of  $2\text{mm}/\text{min}$  and prevented from movement in vertical and lateral directions. Figure 3-16 and Figure 3-17 show the specimen testing setup.

Figure 3-17: Universal Testing Machine and test setup

65 mm

mm

AA/CFRP

Strain gauge

P

250 mm

75 mm

50mm

Supports

P

75 mm

mm

Lb

Figure 3-16: Specimen dimensions and loading configuration

56

### 3.5 Test Matrix

A total of ninety-six concrete prisms were tested. Sixty-four prisms were strengthened with AA 5083-H111 plates while thirty-two prisms were strengthened using CFRP plates. The test matrix is divided into three groups, the first and second group contains AA plates with plain and rough scratched surfaces respectively. Whilst the third group consists of CFRP plates. One duplicate is made for each sample. Table 3-10 below lists all the concrete prisms tested in this study. The prisms strengthened with CFRP are denoted with CF, on the other hand the prisms strengthened with AA plates are designated by P and R, referring to the AA plate surface as plain (natural) and rough surface.

Table 3-10: Test matrix

Concrete Strength (MPa)

Bonded length (mm)

Specimens & Plate Type (96 Specimens)

CFRP×2

AA (Plain)×2

AA (Rough)×2

20

L1 = 50

20-CF-L1

20-P-L1

20-R-L1

L2 = 100

20-CF-L2

20-P-L2

20-R-L2

CFRP

G1F

AAP

G1P

AAR

G1R

L3 = 150

20-CF-L3

20-P-L3

20-R-L3

L4 = 200

20-CF-L4

20-P-L4

20-R-L4

30

L1 = 50

30-CF-L1

30-P-L1

30-R-L1

L2 = 100

30-CF-L2

30-P-L2

30-R-L2

CFRP

G2F

AAP

G2P

AAR

G2R

L3 = 150

30-CF-L3

30-P-L3

30-R-L3

L4 = 200

30-CF-L4

30-P-L4

30-R-L4

40

L1 = 50

40-CF-L1

40-P-L1

40-R-L1

L2 = 100

40-CF-L2

40-P-L2

40-R-L2

CFRP

G3F

AAP

G3P

AAR

G3R

L3 = 150

40-CF-L3

40-P-L3

40-R-L3

L4 = 200

40-CF-L4

40-P-L4

40-R-L4

60

L1 = 50

60-CF-L1

60-P-L1

60-R-L1

L2 = 100

60-CF-L2

60-P-L2

60-R-L2

CFRP

G4F

AAP

G4P

AAR

G4R

L3 = 150

60-CF-L3

60-P-L3

60-R-L3

L4 = 200

60-CF-L4

60-P-L4

60-R-L4

57

## 4 Chapter 4: Experimental Results and Discussion

This chapter presents the results obtained from the experimental program in which the testing of 96 concrete prisms has been carried out. As stated in the literature, many factors have effects on the bond between the EBR systems and the concrete surface. Three of these factors are considered in this investigation which include concrete strength, bond length and surface treatment of the EBR material

used. The results below have been divided into four groups based on the concrete strength of the prisms. For each specimen the relation between shear stress ( $\tau$ ), slip ( $S$ ) and distance ( $x$ ) is illustrated in charts along with the load strain and load extension curves. Considering

Figure 4-1: Pull test setup with strain gauges

Using the strain gauge readings at their locations, the shear stress  $\tau(x)$  at a location of each strain gauge can be calculated as given by Equation (1).

$$\tau(x_i) = 0.5 n p t_p E_p [(\epsilon_i - \epsilon_{i-1})(x_i - x_{i-1}) + (\epsilon_{i+1} - \epsilon_i)(x_{i+1} - x_i)] \quad (1)$$

where  $\epsilon_i$  is the strain reading from the strain gauge  $i$ ,  $x_i$  is the location of the strain gauge  $i$ ,  $n p$  is the number of plates,  $t_p$  is the thickness of the AA/CFRP plate, and  $E_p$  is the modulus of elasticity of the AA/CFRP plate.

The cumulative slip  $S(x)$  can also be derived using the strain gauges readings and is given by Equation (2).

$$S(x_i) = S(x_{i-1}) + 0.5 \sum_{m=2}^i [(\epsilon_i - \epsilon_{i-1})(x_i - x_{i-1}) + (\epsilon_{i+1} - \epsilon_i)(x_{i+1} - x_i)] \quad (2)$$

where  $m$  is the number of strain gauges attached to the bonded length of the plate.

P

250 mm

75

mm

Adhesive

AA/CFRP Plate

BL

m

i+1

i

i-1

0

x0

x<sub>i-1</sub>

x<sub>i</sub>

xi+1

Figure 4-1, the following equations were used by many researchers [20, 53, 54] to calculate the shear stress ( $\tau$ ) and slip ( $S$ ).

58

#### 4.1 Group One: Concrete Strength of 20 MPa

This group contains 24 specimens as illustrated in Figure 4-2 below. In this group the targeted concrete cube strength of the prisms is 20 MPa. Two different plate types were used as EBR materials that include CFRP and AA plates with rough and plan surfaces as shown in Figure 4-3. Eight prisms were reinforced with CFRP plates and sixteen prisms with AA plates from which eight plates were used with plain (natural) surface and another eight with a randomly scratched rough surface. Four bond lengths were used for each plate type along with a duplicate sample with the same properties for each specimen.

Six charts have been developed for each sample. In these graphs the variation of different parameters along the bonded length of the EBR plate is displayed. Namely, bond stress, strain and slip variations with the bonded length are shown. In addition, other relations including bond stress-slip, load-strain and load-extension relationships are also shown. As previously stated, two identical samples with the same properties were cast and tested, however the results of only one specimen of the two are presented in the charts below. Table 4-1 given in the end of this section shows all the samples results for this group.

Figure 4-3: Three different EBR materials used.

Figure 4-2: Twenty four Prisms with  $f_c'$  of 20MPa.

59

Figure 4-4: Variation of stress, strain, slip and load of 20-CF-L1 specimen

0

0.6

1.2

1.8

2.4

3

0 10 20 30 40 50 60

Shear Stress (MPa)

Distance From Loaded End (mm)

0

0.005

0.01

0.015

0.02

0.025

0 10 20 30 40 50 60

Slip (mm)

Distance from loaded end (mm)

0

0.6

1.2

1.8

2.4

3

0 0.004 0.008 0.012 0.016 0.02 0.024

Shear Stress (MPa)

Slip (mm)

0

150

300

450

600

750

0 10 20 30 40 50 60

Strain ( $\mu\epsilon$ )

Distance from free end (mm)

0

1500

3000

4500

6000

7500  
0 200 400 600 800 1000

Load (N)

Strain ( $\mu\epsilon$ )

SG 1 SG 2 SG 3

0

1500

3000

4500

6000

7500

0 0.4 0.8 1.2 1.6 2

Load (N)

Extension (mm)

(a) Bond stress-distance curves (b) Slip-distance curves

(c) Bond stress-slip curves (d) Strain gauge-distance curves.

(f) Load-strain curves (g) Load-extension curve

(a) Sample failure mode

60

Figure 4-5: Variation of stress, strain, slip and load of 20-CF-L2 specimen

0

0

0.006

0.006

0.012

0.012

0.018

0.018

0.024

0.024

0.03

0.03

0

0

20

20

40

40

60

60

80

80

100

100

120

120

Slip (mm)

Slip (mm)

Distance from loaded end (mm)

Distance from loaded end (mm)

0

0

0.3

0.3

0.6

0.6

0.9

0.9

1.2

1.2

1.5

1.5

0

0

0.006

0.006

0.012

0.012

0.018

0.018

0.024

0.024

0.03

0.03

Shear stress (MPa)

Shear stress MPa)

Slip (mm)

Slip (mm)

0

0

0.2

0.2

0.4

0.4

0.6

0.6

0.8

0.8

1

1

0

0

20

20

40

40

60

60

80

80

100

100

120

120

Shear stress (MPa)

Distance from loaded end (mm)

Distance from loaded end (mm)

0

0

80

80

160

160

240

240

320

320

400

400

0

0

20

20

40

40

60

60

80

80

100

100

120

120

Strain (

Strain  $\mu\epsilon\mu\epsilon$ )

Distance from free end (mm)

Distance from free end (mm)

0

0

2000

2000

4000

4000

6000

6000

8000

8000

10000

10000

0

0

0.3

0.3

0.6

0.6

0.9

0.9

1.2

1.2

1.5

1.5

Load (N)

Load N)

Extension (mm)

Extension (mm)

0

0

2000

2000

4000

4000

6000

6000

8000

8000

10000

10000

0

0

200

200

400

400

600

600

800

800

1000

1000

Load (N)

Strain (

Strain ( $\mu\text{m}\mu\text{m}$ )

SG 1

SG 1

SG 2

SG 2

SG 3

SG 3

(b) Bond stress-distance curves

(c) Slip-distance curves

(d) Bond stress-slip curves

(e) Strain gauge-distance curves.

(f) Load-strain curves

(g) Load-extension curve

(b) Sample failure mode

61

Figure 4-6: Variation of stress, strain, slip and load of 20-CF-L3 specimen

0

0

150

150

300

300

450

450

600

600

0

0

25

25

50

50

75

75

100

100

125

125

150

150

175

175

Strain (

Strain ( $\mu\epsilon$ )

Distance from free end (mm)

Distance from free end (mm)

0

0

0.2

0.2

0.4

0.4

0.6

0.6

0.8

0.8

1

1

0

0

25

25

50

50

75

75

100

100

125

125

150

150

175

175

Shear Stress (MPa)

Shear Stress MPa)

Distance From Loaded End (mm)

Distance From Loaded End (mm)

0

0

0.01

0.01

0.02

0.02

0.03

0.03

0.04

0.04

0.05

0.05

0

0

25

25

50

50

75

75

100

100

125

125

150

150

175

175

SLIP (

SLIP mmmm))

Distance From Loaded End (mm)

Distance From Loaded End (mm)

0

0

0.2

0.2

0.4

0.4

0.6

0.6

0.8

0.8

1

1

0

0

0.01

0.01

0.02

0.02

0.03

0.03

0.04

0.04

0.05

0.05

Shear Stress (MPa)

Slip (mm)

Slip (mm)

0

0

2000

2000

4000

4000

6000

6000

8000

8000

10000

10000

0

0

200

200

400

400

600

600

800

800

1000

1000

Load (N)

Load N)

Strain (

Strain ( $\mu\text{m}\epsilon\epsilon$ )

SG 1

SG 1

SG 2

SG 2

SG 3

SG 3

SG 4

SG 4

0

0

2000

2000

4000

4000

6000

6000

8000

8000

10000

10000

0

0

0.4

0.4

0.8

0.8

1.2

1.2

1.6

1.6

2

2

Load (N)

Extension (mm)

Extension (mm)

20

20--CFCF--L3B L3B

(b) Bond stress-distance curves

(c) Slip-distance curves

(d) Bond stress-slip curves

(e) Strain gauge-distance curves.

(f) Load-strain curves

(g) Load-extension curve

(a) Sample failure mode

62

Figure 4-7: Variation of stress, strain, slip and load of 20-CF-L4 specimen

0

0

0.2

0.2

0.4

0.4

0.6

0.6

0.8

0.8

1

1

0

0

50

50

100

100

150

150

200

200

250

250

Shear Stress (MPa)

Shear Stress (MPa)

Distance from loaded end (mm)

Distance from loaded end (mm)

0

0

0.01

0.01

0.02

0.02

0.03

0.03

0.04

0.04

0.05

0.05

0

0

50

50

100

100

150

150

200

200

250

250

Slip (mm)

Slip mm)

Distance From Loaded End (mm)

Distance From Loaded End (mm)

0

0

0.2

0.2

0.4

0.4

0.6

0.6

0.8

0.8

1

1

0

0

0.01

0.01

0.02

0.02

0.03

0.03

0.04

0.04

0.05

0.05

Shear Stress (MPa)

Slip (mm)

Slip (mm)

0

0

120

120

240

240

360

360

480

480

600

600

0

0

50

50

100

100

150

150

200

200

250

250

Strain (

Strain  $\mu\epsilon\mu\epsilon$ )

Distance from free end (mm)

Distance from free end (mm)

0

0

2000

2000

4000

4000

6000

6000

8000

8000

10000

10000

0

0

170

170

340

340

load (N)

load N)

Strain (

Strain ( $\mu\text{m}\epsilon\epsilon$ )

SG 1

SG 1

SG 2

SG 2

SG 3

SG 3

SG 4

SG 4

0

0

2000

2000

4000

4000

6000

6000

8000

8000

10000

10000

0

0

0.5

0.5

1

1

1.5

1.5

2

2

2.5

2.5

Load (N)

Load Extension (mm)

Extension (mm)

(b) Bond stress-distance curves

(c) Slip-distance curves

(d) Bond stress-slip curves

(e) Strain gauge-distance curves.

(f) Load-strain curves

(g) Load-extension curve

(a) Sample failure mode

63

Figure 4-8: Variation of stress, strain, slip and load of 20-R-L1 specimen

0

0

600

600

1200

1200

1800

1800

2400

2400

3000

3000

0

0

0.8

0.8

1.6

1.6

2.4

2.4

3.2

3.2

4

4

Load (N)

Load (N)

Extension (mm)

Extension (mm)

0

0

0.1

0.1

0.2

0.2

0.3

0.3

0.4

0.4

0.5

0.5

0

0

10

10

20

20

30

30

40

40

50

50

60

60

Shear Stress (MPa)

Shear Stress MPa)

Distance From Loaded End (mm)

Distance From Loaded End (mm)

0

0

0.005

0.005

0.01

0.01

0.015

0.015

0.02

0.02

0.025

0.025

0

0

10

10

20

20

30

30

40

40

50

50

60

60

Slip (mm)

Slip mm)

Distance From Loaded End (mm)

Distance From Loaded End (mm)

0

0

0.1

0.1

0.2

0.2

0.3

0.3

0.4

0.4

0.5

0.5

0

0

0.005

0.005

0.01

0.01

0.015

0.015

0.02

0.02

0.025

0.025

Shear Stress (MPa)

Slip (mm)

Slip (mm)

0

0

300

300

600

600

900

900

1200

1200

1500

1500

0

0

10

10

20

20

30

30

40

40

50

50

60

60

Strain (

Strain  $\mu\epsilon\mu\epsilon$ )

Distance from free end (mm)

Distance from free end (mm)

0

0

600

600

1200

1200

1800

1800

2400

2400

3000

3000

0

0

250

250

500

500

750

750

1000

1000

1250

1250

1500

1500

Load (N)

Strain (

Strain ( $\mu\text{m}$ )m)

SG 1

SG 1

SG 2

SG 2

SG 3

SG 3

(b) Bond stress-distance curves

(c) Slip-distance curves

(d) Bond stress-slip curves

(e) Strain gauge-distance curves.

(f) Load-strain curves

(g) Load-extension curve

(a) Sample failure mode

64

Figure 4-9: Variation of stress, strain, slip and load of 20-R-L2 specimen

0

0

40

40

80

80

120

120

160

160

200

200

0

0

20

20

40

40

60

60

80

80

100

100

120

120

Strain (

Strain ( $\mu\epsilon$ )

Distance from free end (mm)

Distance from free end (mm)

0

0

0.003

0.003

0.006

0.006

0.009

0.009

0.012

0.012

0

0

20

20

40

40

60

60

80

80

100

100

120

120

Slip (mm)

Slip mm)

Distance from loaded end (mm)

Distance from loaded end (mm)

0

0

0.08

0.08

0.16

0.16

0.24

0.24

0.32

0.32

0.4

0.4

0

0

20

20

40

40

60

60

80

80

100

100

120

120

Shear Stress (MPa)

Shear Stress MPa)

Distance from loaded end (mm)

Distance from loaded end (mm)

0

0

0.08

0.08

0.16

0.16

0.24

0.24

0.32

0.32

0.4

0.4

0

0

0.0025

0.0025

0.005

0.005

0.0075

0.0075

0.01

0.01

0.0125

0.0125

Shear Stress (MPa)

Slip (mm)

Slip (mm)

0

0

1000

1000

2000

2000

3000

3000

4000

4000

5000

5000

0

0

60

60

120

120

180

180

240

240

300

300

Load (N)

Load N)

Strain (

Strain ( $\mu\text{m}\epsilon\epsilon$ )

SG 1

SG 1

SG 2

SG 2

SG 3

SG 3

0

0

900

900

1800

1800

2700

2700

3600

3600

4500

4500

0

0

0.2

0.2

0.4

0.4

0.6

0.6

0.8

0.8

1

1

Load (N)

Extension (mm)

Extension (mm)

(b) Bond stress-distance curves

(c) Slip-distance curves

(d) Bond stress-slip curves

(e) Strain gauge-distance curves.

(f) Load-strain curves

(g) Load-extension curve

(a) Sample failure mode

65

Sample failure mode

0

0

0.015

0.015

0.03

0.03

0.045

0.045

0.06

0.06

0

0

25

25

50

50

75

75

100

100

125

125

150

150

175

175

Slip (mm)

Slip (mm)

Distance from loaded end (mm)

Distance from loaded end (mm)

0

0

0.4

0.4

0.8

0.8

1.2

1.2

1.6

1.6

2

2

0

0

25

25

50

50

75

75

100

100

125

125

150

150

175

175

Shear Stress (MPa)

Shear Stress MPa)

Distance from loaded end (mm)

Distance from loaded end (mm)

0

0

0.5

0.5

1

1

1.5

1.5

2

2

0

0

0.015

0.015

0.03

0.03

0.045

0.045

0.06

0.06

Shear Stress (MPa)

Slip (mm)

Slip (mm)

0

0

200

200

400

400

600

600

800

800

1000

1000

1200

1200

0

0

25

25

50

50

75

75

100

100

125

125

150

150

175

175

Strain (

Strain  $\mu\epsilon\mu\epsilon$ )

Distance from free end (mm)

Distance from free end (mm)

0

0

2500

2500

5000

5000

7500

7500

10000

10000

12500

12500

0

0

250

250

500

500

750

750

1000

1000

1250

1250

Load (N)

Load N)

Strain (

Strain (μεμε))

SG 1

SG 1

SG 2

SG 2

SG 3

SG 3

SG 4

SG 4

0

0

2500

2500

5000

5000

7500

7500

10000

10000

12500

12500

0

0

0.4

0.4

0.8

0.8

1.2

1.2

1.6

1.6

2

2

Load (N)

Extension (mm)

Extension (mm)

(b) Bond stress-distance curves

(c) Slip-distance curves

(d) Bond stress-slip curves

(e) Strain gauge-distance curves.

(f) Load-strain curves

(g) Load-extension curve

Figure 4-10: Variation of stress, strain, slip and load of 20-R-L3 specimen

66

Figure 4-11: Variation of stress, strain, slip and load of 20-R-L4 specimen

0

0

0.012

0.012

0.024

0.024

0.036

0.036

0.048

0.048

0.06

0.06

0

0

50

50

100

100

150

150

200

200

250

250

Slip (mm)

Slip (mm)

Distance from loaded end (mm)

Distance from loaded end (mm)

0

0

0.3

0.3

0.6

0.6

0.9

0.9

1.2

1.2

1.5

1.5

0

0

50

50

100

100

150

150

200

200

250

250

Shear Stress (MPa)

Shear Stress MPa)

Distance from loaded end (mm)

Distance from loaded end (mm)

0

0

0.3

0.3

0.6

0.6

0.9

0.9

1.2

1.2

1.5

1.5

0

0

0.012

0.012

0.024

0.024

0.036

0.036

0.048

0.048

0.06

0.06

Shear Stress (MPa)

Slip (mm)

Slip (mm)

0

0

150

150

300

300

450

450

600

600

750

750

0

0

50

50

100

100

150

150

200

200

250

250

Strain (

Strain  $\mu\epsilon\mu\epsilon$ )

Distance from free end (mm)

Distance from free end (mm)

0

0

2500

2500

5000

5000

7500

7500

10000

10000

12500

12500

0

0

250

250

500

500

750

750

1000

1000

1250

1250

Load (N)

Load N)

Strain (

Strain ( $\mu\text{m}\epsilon$ )

SG 1

SG 1

SG 2

SG 2

SG 3

SG 3

SG 4

SG 4

SG 5

SG 5

0

0

2500

2500

5000

5000

7500

7500

10000

10000

12500

12500

0

0

0.6

0.6

1.2

1.2

1.8

1.8

2.4

2.4

3

3

Load (N)

Extension (mm)

Extension (mm)

(b) Bond stress-distance curves

(c) Slip-distance curves

(d) Bond stress-slip curves

(e) Strain gauge-distance curves.

(f) Load-strain curves

(g) Load-extension curve

(a) Sample failure mode

67

Figure 4-12: Variation of stress, strain, slip and load of 20-P-L1 specimen

0

0

120

120

240

240

360

360

480

480

600

600

0

0

12

12

24

24

36

36

48

48

60

60

Strain (

Strain ( $\mu\epsilon$ )

Distance from free end (mm)

Distance from free end (mm)

0

0

0.004

0.004

0.008

0.008

0.012

0.012

0.016

0.016

0.02

0.02

0

0

12

12

24

24

36

36

48

48

60

60

Slip (mm)

Slip mm)

Distance from loaded end (mm)

Distance from loaded end (mm)

0

0

0.5

0.5

1

1

1.5

1.5

2

2

2.5

2.5

0

0

12

12

24

24

36

36

48

48

60

60

Shear Stress (MPa)

Shear Stress MPa)

Distance from loaded end (mm)

Distance from loaded end (mm)

0

0

0.5

0.5

1

1

1.5

1.5

2

2

2.5

2.5

0

0

0.004

0.004

0.008

0.008

0.012

0.012

0.016

0.016

0.02

0.02

Shear Stress (MPa)

Slip (mm)

Slip (mm)

0

0

1200

1200

2400

2400

3600

3600

4800

4800

6000

6000

0

0

150

150

300

300

450

450

600

600

750

750

Load (N)

Load N)

Strain (

Strain (μεμε))

SG 1

SG 1

SG 2

SG 2

SG 3

SG 3

0

0

1200

1200

2400

2400

3600

3600

4800

4800

6000

6000

0

0

0.5

0.5

1

1

1.5

1.5

2

2

2.5

2.5

Load (N)

Extension (mm)

Extension (mm)

(b) Bond stress-distance curves

(c) Slip-distance curves

(d) Bond stress-slip curves

(e) Strain gauge-distance curves.

(f) Load-strain curves

(g) Load-extension curve

(a) Sample failure mode

Figure 4-13: Variation of stress, strain, slip and load of 20-P-L2 specimen

0  
0  
0.005  
0.005  
0.01  
0.01  
0.015  
0.015  
0.02  
0.02  
0.025  
0.025  
0  
0  
20  
20  
40  
40  
60  
60  
80  
80  
100  
100  
120  
120  
Slip (mm)

Slip (mm)

Distance from loaded end (mm)

Distance from loaded end (mm)

0

0

0.3

0.3

0.6

0.6

0.9

0.9

1.2

1.2

1.5

1.5

0

0

20

20

40

40

60

60

80

80

100

100

120

120

Shear Stress (MPa)

Shear Stress MPa)

Distance from loaded end (mm)

Distance from loaded end (mm)

0

0

0.3

0.3

0.6

0.6

0.9

0.9

1.2

1.2

1.5

1.5

0

0

0.005

0.005

0.01

0.01

0.015

0.015

0.02

0.02

0.025

0.025

Shear Stress (MPa)

Slip (mm)

Slip (mm)

0

0

1500

1500

3000

3000

4500

4500

6000

6000

7500

7500

0

0

120

120

240

240

360

360

480

480

600

600

Load (N)

Load N)

Strain (

Strain ( $\mu\text{m}\epsilon\epsilon$ )

SG 1

SG 1

SG 2

SG 2

SG 3

SG 3

SG 4

SG 4

0

0

1500

1500

3000

3000

4500

4500

6000

6000

7500

7500

0

0

0.5

0.5

1

1

1.5

1.5

2

2

2.5

2.5

Load (N)

Extension (mm)

Extension (mm)

0

0

120

120

240

240

360

360

480

480

600

600

0

0

20

20

40

40

60

60

80

80

100

100

120

120

Strain (

Strain  $\mu\mu\epsilon\epsilon$ )

Distance (mm)

Distance (mm)

(b) Bond stress-distance curves

(c) Slip-distance curves

(d) Bond stress-slip curves

(e) Strain gauge-distance curves.

(f) Load-strain curves

(g) Load-extension curve

(a) Sample failure mode

69

(a) Sample failure mode

0

0

0.007

0.007

0.014

0.014

0.021

0.021

0.028

0.028

0.035

0.035

0

0

25

25

50

50

75

75

100

100

125

125

150

150

175

175

Slip (mm)

Slip (mm)

Distance from loaded end (mm)

Distance from loaded end (mm)

0

0

0.25

0.25

0.5

0.5

0.75

0.75

1

1

1.25

1.25

0

0

25

25

50

50

75

75

100

100

125

125

150

150

175

175

Shear Stress (MPa)

Shear Stress MPa)

Distance from loaded end (mm)

Distance from loaded end (mm)

0

0

0.25

0.25

0.5

0.5

0.75

0.75

1

1

1.25

1.25

0

0

0.008

0.008

0.016

0.016

0.024

0.024

0.032

0.032

0.04

0.04

Shear Stress (MPa)

Slip (mm)

Slip (mm)

0

0

150

150

300

300

450

450

600

600

750

750

0

0

25

25

50

50

75

75

100

100

125

125

150

150

175

175

Strain (

Strain  $\mu\epsilon\mu\epsilon$ )

Distance from free end (mm)

Distance from free end (mm)

0

0

1500

1500

3000

3000

4500

4500

6000

6000

7500

7500

0

0

150

150

300

300

450

450

600

600

750

750

Load (N)

Load N)

Strain (

Strain (μεμε))

SG 1

SG 1

SG 2

SG 2

SG 3

SG 3

SG 4

SG 4

0

0

1500

1500

3000

3000

4500

4500

6000

6000

7500

7500

0

0

0.4

0.4

0.8

0.8

1.2

1.2

1.6

1.6

2

2

Load (N)

Extension (mm)

Extension (mm)

- (b) Bond stress-distance curves
- (c) Slip-distance curves
- (d) Bond stress-slip curves
- (e) Strain gauge-distance curves.
- (f) Load-strain curves
- (g) Load-extension curve

Figure 4-14: Variation of stress, strain, slip and load of 20-P-L3 specimen

70

Figure 4-15: Variation of stress, strain, slip and load of 20-P-L4 specimen

0

0

0.006

0.006

0.012

0.012

0.018

0.018

0.024

0.024

0.03

0.03

0

0

50

50

100

100

150

150

200

200

250

250

Slip (mm)

Slip (mm)

Distance from loaded end (mm)

Distance from loaded end (mm)

0

0

0.25

0.25

0.5

0.5

0.75

0.75

1

1

1.25

1.25

0

0

50

50

100

100

150

150

200

200

250

250

Shear Stress (MPa)

Shear Stress MPa)

Distance from loaded end (mm)

Distance from loaded end (mm)

0

0

0.25

0.25

0.5

0.5

0.75

0.75

1

1

1.25

1.25

0

0

0.006

0.006

0.012

0.012

0.018

0.018

0.024

0.024

0.03

0.03

Shear Stress (MPa)

Slip (mm)

Slip (mm)

0

0

120

120

240

240

360

360

480

480

600

600

0

0

50

50

100

100

150

150

200

200

250

250

Strain (

Strain  $\mu\epsilon$ )

Distance from free end (mm)

Distance from free end (mm)

0

0

1500

1500

3000

3000

4500

4500

6000

6000

7500

7500

0

0

120

120

240

240

360

360

480

480

600

600

Load (N)

Load N)

Strain (

Strain (μεμε))

SG 1

SG 1

SG 2

SG 2

SG 3

SG 3

SG 4

SG 4

SG 5

SG 5

0

0

1500

1500

3000

3000

4500

4500

6000

6000

7500

7500

0

0

0.4

0.4

0.8

0.8

1.2

1.2

1.6

1.6

2

2

Load (N)

Extension (mm)

Extension (mm)

(b) Bond stress-distance curves

(c) Slip-distance curves

(d) Bond stress-slip curves

(e) Strain gauge-distance curves.

(f) Load-strain curves

(g) Load-extension curve

(a) Sample failure mode

71

Table 4-1: Summary of results for specimens with  $f_c'$  of 20 MPa

Specimen Identification

AA/CFRP Plate

Cube compressive strength (MPa)

Failure Load (KN)

\*Failure mode

Plate type

Width (mm)

Thickness (mm)

Bonded length (mm)

20-CF-L1

CFRP

50

1.4

50

20

4.75

DB-C

20-CF-L1

CFRP

50

1.4

50

20

6.95

DB-C

20-CF-L2

CFRP

50

1.4

100

20

8.39

DB-C+CS

20-CF-L2

CFRP

50

1.4

100

20

6.78

DB-C+CS

20-CF-L3

CFRP

50

1.4

150

20

8.49

DB-C+CS

20-CF-L3

CFRP

50

1.4

150

20

7.54

DB-C

20-CF-L4

CFRP

50

1.4

200

20

7.89

DB-C

20-CF-L4

CFRP

50

1.4

200

20

7.36

DB-C

20-R-L1

AA-R

50

3.0

50

20

2.39

DB-C+CS

20-R-L1

AA-R

50

3.0

50

20

10.6

DB-C+CS

20-R-L2

AA-R

50

3.0

100

20

3.95

DB-C+CS

20-R-L2

AA-R

50

3.0

100

20

3.42

DB-C+CS

20-R-L3

AA-R

50

3.0

150

20

9.64

DB-C+CS

20-R-L3

AA-R

50

3.0

150

20

5.45

DB-C+CS

20-R-L4

AA-R

50

3.0

200

20

11.0

DB-C+CS

20-R-L4

AA-R

50

3.0

200

20

9.29

DB-C+CS

20-P-L1

AA-P

50

3.0

50

20

4.95

DB-P+DA

20-P-L1

AA-P

50

3.0

50

20

2.6

DB-P

20-P-L2

AA-P

50

3.0

100

20

9.0

DB-C+CS

20-P-L2

AA-P

50

3.0

100

20

7.09

DA+CS

20-P-L3

AA-P

50

3.0

150

20

6.84

DB-P

20-P-L3

AA-P

50

3.0

150

20

6.47

DB-P

20-P-L4

AA-P

50

3.0

200

20

5.75

DB-P

20-P-L4

AA-P

50

3.0

200

20

1.97

DB-P

\*Failure mode: DB-C: Debonding in concrete, DB-P: Plate Debonding (Plate/adhesive interface separation), CS: Concrete spalling, DA: Adhesive debonding (Adhesive/concrete interface separation).

4.1.1 CFRP plate failure. The failure mode for specimens with CFRP plates mainly takes place in the concrete adhesive interface accompanied by concrete spalling in some cases.

4.1.2 AA scratched plate failure. The failure mode for this type of plate is similar to that of the CFRP. However, the concrete spalling in this case takes place in all the specimens due to scratched AA plate rough surface which causes concentration of stresses in the vicinity of the loaded end.

4.1.3 AA plain plate failure The failure mode for AA plates with plain surface usually takes place in the plate adhesive interface due to the weak bond between the plate plain surface and the adhesive, except for some cases when the bond length is short. This is due to stress concentration in the vicinity in addition to the low concrete strength of this group.

72

4.2 Group Two: Concrete Strength of 30 MPa

This group contains 24 specimens as illustrated in Figure 4-16 below. In this group the targeted concrete strength of the prisms is 30 MPa. Two different plate types were used as EBR materials that include CFRP and AA plates with rough and plan surfaces as shown in Figure 4-17. Eight prisms were reinforced with CFRP plates and sixteen prisms with AA plates from which eight plates were used with plain (natural) surface and another eight with a randomly scratched surface. Four bond lengths were used for each plate type along with a duplicate sample with the same properties for each specimen.

Six charts have been developed for each sample. In these graphs the variation of different parameters along the bonded length of the EBR plate is displayed. Namely, bond stress, strain and slip variations with the bonded length are shown. In addition, other relations including bond stress-slip, load-strain and load-extension relationships are also shown. As previously stated, two identical samples with the same properties were cast and tested, however the results of only one specimen of the two are presented in the charts below. Table 4-2 given in the end of this section shows all the samples results for this group.

Figure 4-17: Three different EBR materials used.

Figure 4-16: Twenty four specimens with  $f_c'$  of 30 MPa.

73

Figure 4-18: Variation of stress, strain, slip and load of 30-CF-L1 specimen

0  
0  
0.005  
0.005  
0.01  
0.01  
0.015  
0.015  
0.02  
0.02  
0.025  
0.025  
0  
0  
10  
10

20

20

30

30

40

40

50

50

60

60

Slip (mm)

Slip (mm)

Distance from loaded end (mm)

Distance from loaded end (mm)

0

0

0.4

0.4

0.8

0.8

1.2

1.2

1.6

1.6

2

2

0

0

10

10

20

20

30

30

40

40

50

50

60

60

Shear Stress (MPa)

Shear Stress MPa)

Distance from loaded end (mm)

Distance from loaded end (mm)

0

0

0.4

0.4

0.8

0.8

1.2

1.2

1.6

1.6

2

2

0

0

0.005

0.005

0.01

0.01

0.015

0.015

0.02

0.02

0.025

0.025

Shear Stress (MPa)

Slip (mm)

Slip (mm)

0

0

100

100

200

200

300

300

400

400

500

500

0

0

10

10

20

20

30

30

40

40

50

50

60

60

Strain (

Strain  $\mu\epsilon$ )

Distance from free end (mm)

Distance from free end (mm)

0

0

1500

1500

3000

3000

4500

4500

6000

6000

7500

7500

0

0

200

200

400

400

600

600

800

800

1000

1000

Load (N)

Load N)

Strain (

Strain ( $\mu\text{m}\epsilon\epsilon$ )

SG 1

SG 1

SG 2

SG 2

SG 3

SG 3

0

0

1500

1500

3000

3000

4500

4500

6000

6000

7500

7500

0

0

0.5

0.5

1

1

1.5

1.5

2

2

Load (N)

Extension (mm)

Extension (mm)

(b) Bond stress-distance curves

(c) Slip-distance curves

(d) Bond stress-slip curves

(e) Strain gauge-distance curves.

(f) Load-strain curves

(g) Load-extension curve

(a) Sample failure mode

74

Figure 4-19: Variation of stress, strain, slip and load of 30-CF-L2 specimen

(a) Sample failure mode

0

0

100

100

200

200

300

300

400

400

500

500

0

0

20

20

40

40

60

60

80

80

100

100

120

120

Strain (

Strain ( $\mu\text{m}\epsilon\epsilon$ )

Distance (mm)

Distance (mm)

0

0

0.008

0.008

0.016

0.016

0.024

0.024

0.032

0.032

0.04

0.04

0

0

20

20

40

40

60

60

80

80

100

100

120

120

Slip (mm)

Slip mm)

Distance from loaded end (mm)

Distance from loaded end (mm)

0

0

0.2

0.2

0.4

0.4

0.6

0.6

0.8

0.8

1

1

0

0

20

20

40

40

60

60

80

80

100

100

120

120

Shear Stress (MPa)

Shear Stress MPa)

Distance from loaded end (mm)

Distance from loaded end (mm)

0

0

0.2

0.2

0.4

0.4

0.6

0.6

0.8

0.8

1

1

0

0

0.008

0.008

0.016

0.016

0.024

0.024

0.032

0.032

0.04

0.04

Shear Stress (MPa)

Slip (mm)

Slip (mm)

0

0

2500

2500

5000

5000

7500

7500

10000

10000

12500

12500

0

0

250

250

500

500

750

750

1000

1000

1250

1250

Load (N)

Load N)

Strain (

Strain ( $\mu\text{m}\epsilon\epsilon$ )

SG 1

SG 1

SG 2

SG 2

SG 3

SG 3

0

0

2500

2500

5000

5000

7500

7500

10000

10000

12500

12500

0

0

0.6

0.6

1.2

1.2

1.8

1.8

2.4

2.4

3

3

Load (N)

Extension (mm)

Extension (mm)

- (b) Bond stress-distance curves
- (c) Slip-distance curves
- (d) Bond stress-slip curves
- (e) Strain gauge-distance curves.
- (f) Load-strain curves
- (g) Load-extension curve

75

Figure 4-20: Variation of stress, strain, slip and load of 30-CF-L3 specimen

0

0

3500

3500

7000

7000

10500

10500

14000

14000

17500

17500

0

0

1

1

2

2

3

3

4

4

5

5

Load (N)

Load (N)

Extension (mm)

Extension (mm)

0

0

0.4

0.4

0.8

0.8

1.2

1.2

1.6

1.6

2

2

0

0

25

25

50

50

75

75

100

100

125

125

150

150

175

175

Shear Stress (MPa)

Shear Stress MPa)

Distance from loaded end (mm)

Distance from loaded end (mm)

0

0

0.02

0.02

0.04

0.04

0.06

0.06

0.08

0.08

0.1

0.1

0

0

25

25

50

50

75

75

100

100

125

125

150

150

175

175

Slip (mm)

Slip mm)

Distance from loaded end (mm)

Distance from loaded end (mm)

0

0

0.4

0.4

0.8

0.8

1.2

1.2

1.6

1.6

2

2

0

0

0.02

0.02

0.04

0.04

0.06

0.06

0.08

0.08

0.1

0.1

Shear Stress (MPa)

Slip (mm)

Slip (mm)

0

0

200

200

400

400

600

600

800

800

1000

1000

0

0

25

25

50

50

75

75

100

100

125

125

150

150

175

175

Strain (

Strain  $\mu\mu\epsilon$ )

Distance (mm)

Distance (mm)

0

0

4000

4000

8000

8000

12000

12000

16000

16000

20000

20000

0

0

400

400

800

800

1200

1200

1600

1600

2000

2000

Load (N)

Strain (

Strain ( $\mu\text{m}\epsilon\epsilon$ )

SG 1

SG 1

SG 2

SG 2

SG 3

SG 3

SG 4

SG 4

(b) Bond stress-distance curves

(c) Slip-distance curves

(d) Bond stress-slip curves

(e) Strain gauge-distance curves.

(f) Load-strain curves

(g) Load-extension curve

(a) Sample failure mode

76

0

0

0.02

0.02

0.04

0.04

0.06

0.06

0.08

0.08

0.1

0.1

0

0

50

50

100

100

150

150

200

200

250

250

Slip (mm)

Slip (mm)

Distance from loaded end (mm)

Distance from loaded end (mm)

0

0

0.6

0.6

1.2

1.2

1.8

1.8

2.4

2.4

3

3

0

0

50

50

100

100

150

150

200

200

250

250

Shear Stress (MPa)

Shear Stress MPa)

Distance from loaded end (mm)

Distance from loaded end (mm)

0

0

0.6

0.6

1.2

1.2

1.8

1.8

2.4

2.4

3

3

0

0

0.02

0.02

0.04

0.04

0.06

0.06

0.08

0.08

0.1

0.1

Shear Stress (MPa)

Slip (mm)

Slip (mm)

0

0

300

300

600

600

900

900

1200

1200

1500

1500

0

0

50

50

100

100

150

150

200

200

250

250

Strain (

Strain  $\mu\epsilon\mu\epsilon$ )

Distance from free end (mm)

Distance from free end (mm)

0

0

2500

2500

5000

5000

7500

7500

10000

10000

12500

12500

0

0

300

300

600

600

900

900

1200

1200

1500

1500

Load (N)

Load N)

Strain (

Strain ( $\mu\mu\epsilon\epsilon$ )

SG 1

SG 1

SG 2

SG 2

SG 3

SG 3

SG 4

SG 4

SG 5

SG 5

0

0

2500

2500

5000

5000

7500

7500

10000

10000

12500

12500

0

0

0.6

0.6

1.2

1.2

1.8

1.8

2.4

2.4

3

3

Load (N)

Extension (mm)

Extension (mm)

- (a) Sample failure mode
- (b) Bond stress-distance curves
- (c) Slip-distance curves
- (d) Bond stress-slip curves
- (e) Strain gauge-distance curves.
- (f) Load-strain curves
- (g) Load-extension curve

Figure 4-21: Variation of stress, strain, slip and load of 30-CF-L4 specimen

77

0

0

0.5

0.5

1

1

1.5

1.5

2

2

2.5

2.5

0

0

10

10

20

20

30

30

40

40

50

50

60

60

Shear Stress (MPa)

Shear Stress (MPa)

Distance from loaded end (mm)

Distance from loaded end (mm)

0

0

0.003

0.003

0.006

0.006

0.009

0.009

0.012

0.012

0.015

0.015

0

0

10

10

20

20

30

30

40

40

50

50

60

60

Slip (mm)

Slip mm)

Distance from loaded end (mm)

Distance from loaded end (mm)

0

0

0.5

0.5

1

1

1.5

1.5

2

2

2.5

2.5

0

0

0.003

0.003

0.006

0.006

0.009

0.009

0.012

0.012

0.015

0.015

SHEAR STRESS (MP

SHEAR STRESS MPaa))

SLIP (

SLIP (mmmm))

0

0

150

150

300

300

450

450

600

600

750

750

0

0

10

10

20

20

30

30

40

40

50

50

60

60

Strain (

Strain  $\mu\epsilon\mu\epsilon$ )

Distance from free end (mm)

Distance from free end (mm)

0

0

1250

1250

2500

2500

3750

3750

5000

5000

6250

6250

0

0

150

150

300

300

450

450

600

600

750

750

Load (N)

Load N)

Strain (

Strain ( $\mu\text{m}\epsilon\epsilon$ )

SG 1

SG 1

SG 2

SG 2

SG 3

SG 3

0

0

1400

1400

2800

2800

4200

4200

5600

5600

7000

7000

0

0

0.3

0.3

0.6

0.6

0.9

0.9

1.2

1.2

1.5

1.5

1.8

1.8

Load (N)

Extension (mm)

Extension (mm)

(a) Sample failure mode

(b) Bond stress-distance curves

(c) Slip-distance curves

(d) Bond stress-slip curves

(e) Strain gauge-distance curves.

(f) Load-strain curves

(g) Load-extension curve

Figure 4-22: Variation of stress, strain, slip and load of 30-R-L1 specimen

78

0

0

0.25

0.25

0.5

0.5

0.75

0.75

1

1

1.25

1.25

0

0

20

20

40

40

60

60

80

80

100

100

120

120

Shear Stress (MPa)

Shear Stress (MPa)

Distance from loaded end (mm)

Distance from loaded end (mm)

0

0

100

100

200

200

300

300

400

400

500

500

0

0

20

20

40

40

60

60

80

80

100

100

120

120

Strain (

Strain  $\mu\text{m}\epsilon\epsilon$ )

Distance (mm)

Distance (mm)

0

0

0.01

0.01

0.02

0.02

0.03

0.03

0.04

0.04

0.05

0.05

0

0

20

20

40

40

60

60

80

80

100

100

120

120

Slip (mm)

Slip mm)

Distance from loaded end (mm)

Distance from loaded end (mm)

0

0

0.25

0.25

0.5

0.5

0.75

0.75

1

1

1.25

1.25

0

0

0.01

0.01

0.02

0.02

0.03

0.03

0.04

0.04

0.05

0.05

Shear Stress (MPa)

Slip (mm)

Slip (mm)

0

0

2500

2500

5000

5000

7500

7500

10000

10000

12500

12500

0

0

300

300

600

600

900

900

1200

1200

1500

1500

Load (N)

Load N)

Strain (

Strain ( $\mu\mu\epsilon\epsilon$ )

SG 1

SG 1

SG 2

SG 2

SG 3

SG 3

0

0

2500

2500

5000

5000

7500

7500

10000

10000

12500

12500

0

0

0.6

0.6

1.2

1.2

1.8

1.8

2.4

2.4

3

3

Load (N)

Extension (mm)

Extension (mm)

- (a) Sample failure mode
- (b) Bond stress-distance curves
- (c) Slip-distance curves
- (d) Bond stress-slip curves
- (e) Strain gauge-distance curves.
- (f) Load-strain curves
- (g) Load-extension curve

Figure 4-23: Variation of stress, strain, slip and load of 30-R-L2 specimen

79

0

0

0.015

0.015

0.03

0.03

0.045

0.045

0.06

0.06

0.075

0.075

0

0

25

25

50

50

75

75

100

100

125

125

150

150

175

175

Slip (mm)

Slip (mm)

Distance from loaded end (mm)

Distance from loaded end (mm)

0

0

0.6

0.6

1.2

1.2

1.8

1.8

2.4

2.4

3

3

0

0

25

25

50

50

75

75

100

100

125

125

150

150

175

175

Shear Stress (MPa)

Shear Stress MPa)

Distance from loaded end (mm)

Distance from loaded end (mm)

0

0

0.5

0.5

1

1

1.5

1.5

2

2

2.5

2.5

3

3

0

0

0.015

0.015

0.03

0.03

0.045

0.045

0.06

0.06

0.075

0.075

Shear Stress (MPa)

Slip (mm)

Slip (mm)

0

0

250

250

500

500

750

750

1000

1000

1250

1250

1500

1500

0

0

25

25

50

50

75

75

100

100

125

125

150

150

175

175

Strain (

Strain  $\mu\mu\epsilon\epsilon$ )

Distance (mm)

Distance (mm)

0

0

3000

3000

6000

6000

9000

9000

12000

12000

15000

15000

0

0

0.8

0.8

1.6

1.6

2.4

2.4

3.2

3.2

4

4

Load (N)

Load N)

Extension (mm)

Extension (mm)

0

0

3000

3000

6000

6000

9000

9000

12000

12000

15000

15000

0

0

300

300

600

600

900

900

1200

1200

1500

1500

Load (N)

Strain (

Strain ( $\mu\mu\epsilon\epsilon$ )

SG 1

SG 1

SG 2

SG 2

SG 3

SG 3

SG 4

SG 4

(a) Sample failure mode

(b) Bond stress-distance curves

(c) Slip-distance curves

(d) Bond stress-slip curves

(e) Strain gauge-distance curves.

(f) Load-strain curves

(g) Load-extension curve

Figure 4-24: Variation of stress, strain, slip and load of 30-R-L3 specimen

80

0

0

0.04

0.04

0.08

0.08

0.12

0.12

0.16

0.16

0.2

0.2

0

0

50

50

100

100

150

150

200

200

250

250

Slip (mm)

Slip (mm)

Distance from loaded end (mm)

Distance from loaded end (mm)

0

0

1.2

1.2

2.4

2.4

3.6

3.6

4.8

4.8

6

6

0

0

50

50

100

100

150

150

200

200

250

250

Shear Stress (MPa)

Shear Stress MPa)

Distance from loaded end (mm)

Distance from loaded end (mm)

0

0

1.2

1.2

2.4

2.4

3.6

3.6

4.8

4.8

6

6

0

0

0.04

0.04

0.08

0.08

0.12

0.12

0.16

0.16

0.2

0.2

Shear Stress (MPa)

Slip (mm)

Slip (mm)

0

0

5000

5000

10000

10000

15000

15000

20000

20000

25000

25000

0

0

700

700

1400

1400

2100

2100

2800

2800

3500

3500

Load (N)

Load N)

Strain (

Strain ( $\mu\text{m}\epsilon\epsilon$ )

SG 1

SG 1

SG 2

SG 2

SG 3

SG 3

SG 4

SG 4

SG 5

SG 5

0

0

5000

5000

10000

10000

15000

15000

20000

20000

25000

25000

0

0

1

1

2

2

3

3

4

4

5

5

Load (N)

Extension (mm)

Extension (mm)

0

0

500

500

1000

1000

1500

1500

2000

2000

2500

2500

0

0

50

50

100

100

150

150

200

200

250

250

Strain (

Strain  $\mu\mu\epsilon$ )

Distance (mm)

Distance (mm)

(a) Sample failure mode

(b) Bond stress-distance curves

(c) Slip-distance curves

(d) Bond stress-slip curves

(e) Strain gauge-distance curves.

(f) Load-strain curves

(g) Load-extension curve

Figure 4-25: Variation of stress, strain, slip and load of 30-R-L4 specimen

81

0

0

0.0002

0.0002

0.0004

0.0004

0.0006

0.0006

0.0008

0.0008

0.001

0.001

0

0

10

10

20

20

30

30

40

40

50

50

60

60

Slip (mm)

Slip (mm)

Distance from loaded end (mm)

Distance from loaded end (mm)

0

0

0.12

0.12

0.24

0.24

0.36

0.36

0.48

0.48

0.6

0.6

0

0

10

10

20

20

30

30

40

40

50

50

60

60

Shear Stress (MPa)

Shear Stress MPa)

Distance from loaded end (mm)

Distance from loaded end (mm)

0

0

0.12

0.12

0.24

0.24

0.36

0.36

0.48

0.48

0.6

0.6

0

0

0.0002

0.0002

0.0004

0.0004

0.0006

0.0006

0.0008

0.0008

0.001

0.001

Shear Stress (MPa)

Slip (mm)

Slip (mm)

0

0

50

50

100

100

150

150

200

200

250

250

0

0

10

10

20

20

30

30

40

40

50

50

60

60

Strain (

Strain  $\mu\mu\epsilon\epsilon$ )

Distance from free end (mm)

Distance from free end (mm)

0

0

300

300

600

600

900

900

1200

1200

1500

1500

0

0

50

50

100

100

150

150

200

200

250

250

Load (N)

Load N)

Strain (

Strain ( $\mu\mu\epsilon\epsilon$ )

SG 1

SG 1

SG 2

SG 2

SG 3

SG 3

0

0

300

300

600

600

900

900

1200

1200

1500

1500

0

0

0.1

0.1

0.2

0.2

0.3

0.3

0.4

0.4

0.5

0.5

Load (N)

Extension (mm)

Extension (mm)

(a) Sample failure mode

(b) Bond stress-distance curves

(c) Slip-distance curves

(d) Bond stress-slip curves

(e) Strain gauge-distance curves.

(f) Load-strain curves

(g) Load-extension curve

Figure 4-26: Variation of stress, strain, slip and load of 30-P-L1 specimen

82

0

0

0.003

0.003

0.006

0.006

0.009

0.009

0.012

0.012

0.015

0.015

0

0

20

20

40

40

60

60

80

80

100

100

120

120

Slip (mm)

Slip (mm)

Distance from loaded end (mm)

Distance from loaded end (mm)

0

0

0.2

0.2

0.4

0.4

0.6

0.6

0.8

0.8

1

1

0

0

20

20

40

40

60

60

80

80

100

100

120

120

Shear Stress (MPa)

Shear Stress MPa)

Distance from loaded end (mm)

Distance from loaded end (mm)

0

0

0.2

0.2

0.4

0.4

0.6

0.6

0.8

0.8

1

1

0

0

0.003

0.003

0.006

0.006

0.009

0.009

0.012

0.012

0.015

0.015

Shear Stress (MPa)

Slip (mm)

Slip (mm)

0

0

40

40

80

80

120

120

160

160

200

200

0

0

20

20

40

40

60

60

80

80

100

100

120

120

Strain (

Strain  $\mu\epsilon$ )

Distance from free end (mm)

Distance from free end (mm)

0

0

800

800

1600

1600

2400

2400

3200

3200

4000

4000

0

0

120

120

240

240

360

360

480

480

600

600

Load (N)

Load N)

Strain (

Strain ( $\mu\text{m}$ )m)

SG 1

SG 1

SG 2

SG 2

SG 3

SG 3

SG 4

SG 4

0

0

800

800

1600

1600

2400

2400

3200

3200

4000

4000

0

0

0.25

0.25

0.5

0.5

0.75

0.75

1

1

1.25

1.25

Load (N)

Extension (mm)

Extension (mm)

(a) Sample failure mode

(b) Bond stress-distance curves

(c) Slip-distance curves

(d) Bond stress-slip curves

(e) Strain gauge-distance curves.

(f) Load-strain curves

(g) Load-extension curve

Figure 4-27: Variation of stress, strain, slip and load of 30-P-L2 specimen

83

0

0

0.005

0.005

0.01

0.01

0.015

0.015

0.02

0.02

0.025

0.025

0

0

25

25

50

50

75

75

100

100

125

125

150

150

175

175

Slip (mm)

Slip (mm)

Distance from loaded end (mm)

Distance from loaded end (mm)

0

0

0.12

0.12

0.24

0.24

0.36

0.36

0.48

0.48

0.6

0.6

0

0

25

25

50

50

75

75

100

100

125

125

150

150

175

175

Shear Stress (MPa)

Shear Stress MPa)

Distance from loaded end (mm)

Distance from loaded end (mm)

0

0

0.12

0.12

0.24

0.24

0.36

0.36

0.48

0.48

0.6

0.6

0

0

0.005

0.005

0.01

0.01

0.015

0.015

0.02

0.02

0.025

0.025

Shear Stress (MPa)

Slip (mm)

Slip (mm)

0

0

120

120

240

240

360

360

480

480

0

0

25

25

50

50

75

75

100

100

125

125

150

150

175

175

Strain (

Strain  $\mu\mu\epsilon\epsilon$ )

Distance from free end (mm)

Distance from free end (mm)

0

0

1200

1200

2400

2400

3600

3600

4800

4800

6000

6000

0

0

150

150

300

300

450

450

600

600

750

750

L

Loadoad(N)(N)

Strain (

Strain ( $\mu\text{m}\epsilon\epsilon$ )

SG 1

SG 1

SG 2

SG 2

SG 3

SG 3

SG 4

SG 4

0

0

1200

1200

2400

2400

3600

3600

4800

4800

6000

6000

0

0

0.35

0.35

0.7

0.7

1.05

1.05

1.4

1.4

1.75

1.75

Load (N)

Load Extension (mm)

Extension (mm)

(a) Sample failure mode

(b) Bond stress-distance curves

(c) Slip-distance curves

(d) Bond stress-slip curves

(e) Strain gauge-distance curves.

(f) Load-strain curves

(g) Load-extension curve

Figure 4-28: Variation of stress, strain, slip and load of 30-P-L3 specimen

84

0

0

0.25

0.25

0.5

0.5

0.75

0.75

1

1

1.25

1.25

0

0

50

50

100

100

150

150

200

200

250

250

Shear Stress (MPa)

Shear Stress (MPa)

Distance from loaded end (mm)

Distance from loaded end (mm)

0

0

0.015

0.015

0.03

0.03

0.045

0.045

0.06

0.06

0.075

0.075

0

0

50

50

100

100

150

150

200

200

250

250

Slip (mm)

Slip mm)

Distance from loaded end (mm)

Distance from loaded end (mm)

0

0

0.3

0.3

0.6

0.6

0.9

0.9

1.2

1.2

1.5

1.5

0

0

0.015

0.015

0.03

0.03

0.045

0.045

0.06

0.06

0.075

0.075

Shear Stress (MPa)

Slip (mm)

Slip (mm)

0

0

150

150

300

300

450

450

600

600

750

750

0

0

50

50

100

100

150

150

200

200

250

250

Strain (

Strain  $\mu\epsilon$ )

Distance from free end (mm)

Distance from free end (mm)

0

0

1000

1000

2000

2000

3000

3000

4000

4000

5000

5000

0

0

200

200

400

400

600

600

800

800

Load (N)

Load N)

Strain (

Strain ( $\mu\text{m}\epsilon$ )

SG 1

SG 1

SG 2

SG 2

SG 3

SG 3

SG 4

SG 4

SG 5

SG 5

0

0

1000

1000

2000

2000

3000

3000

4000

4000

5000

5000

0

0

0.25

0.25

0.5

0.5

0.75

0.75

1

1

1.25

1.25

Load (N)

Extension (mm)

Extension (mm)

(a) Sample failure mode

(b) Bond stress-distance curves

(c) Slip-distance curves

(d) Bond stress-slip curves

(e) Strain gauge-distance curves.

(f) Load-strain curves

(g) Load-extension curve

Figure 4-29: Variation of stress, strain, slip and load of 30-P-L4 specimen

85

Table 4-2: Summary of results for specimens with  $f_c'$  of 30 MPa

Specimen Identification

AA/CFRP Plate

Cube compressive strength (MPa)

Failure Load (KN)

\*Failure mode

Plate type

Width (mm)

Thickness (mm)

Bonded length (mm)

30-CF-L1

CFRP

50

1.4

50

30

4.36

DA

30-CF-L1

CFRP

50

1.4

50

30

6.9

DB-C

30-CF-L2

CFRP

50

1.4

100

30

9.64

DA+CS

30-CF-L2

CFRP

50

1.4

100

30

11.77

DB-P+DA

30-CF-L3

CFRP

50

1.4

150

30

11.34

DA+DB-P

30-CF-L3

CFRP

50

1.4

150

30

15.3

DA+CS

30-CF-L4

CFRP

50

1.4

200

30

9.89

DA+DB-P

30-CF-L4

CFRP

50

1.4

200

30

11.34

DA+DB-P

30-R-L1

AA-R

50

3.0

50

30

2.65

DA

30-R-L1

AA-R

50

3.0

50

30

5.85

DB-C

30-R-L2

AA-R

50

3.0

100

30

10.64

DB-C+DB-P

30-R-L2

AA-R

50

3.0

100

30

12.5

DB-C+CS

30-R-L3

AA-R

50

3.0

150

30

13.95

DB-C+CS

30-R-L3

AA-R

50

3.0

150

30

8.64

DB-C

30-R-L4

AA-R

50

3.0

200

30

19.75

DB-C

30-R-L4

AA-R

50

3.0

200

30

15.67

DB-C+CS

30-P-L1

AA-P

50

3.0

50

30

1.25

DB-P

30-P-L1

AA-P

50

3.0

50

30

0.8

DB-P

30-P-L2

AA-P

50

3.0

100

30

10.2#

DB-P

30-P-L2

AA-P

50

3.0

100

30

3.66

DB-P

30-P-L3

AA-P

50

3.0

150

30

3.73

DB-P

30-P-L3

AA-P

50

3.0

150

30

5.6

DB-P

30-P-L4

AA-P

50

3.0

200

30

4.39

DB-P

30-P-L4

AA-P

50

3.0

200

30

3.14

DB-P

\*Failure mode: DB-C: Debonding in concrete, DB-P: Plate Debonding (Plate/adhesive interface separation), CS: Concrete spalling, DA: Adhesive debonding (Adhesive/concrete interface separation).

4.2.1 CFRP plate failure. The failure mode for specimens with CFRP plates mainly takes place in the concrete adhesive interface accompanied by concrete spalling in some cases.

4.2.2 AA scratched plate failure. The failure mode for this type of plate is similar to that of the CFRP. However, the concrete spalling in this case takes place in all the specimens due to scratched AA plate rough surface which causes concentration of stresses in the vicinity of the loaded end.

4.2.3 AA plain plate failure. The failure mode for AA plates with plain surface in all specimens appear to take place in the plate adhesive interface due to the weak bond between the plate plain surface and the adhesive. There is no concrete spalling in this case because the concrete strength in this case is higher than that of the previous group.

86

#### 4.3 Group Three: Concrete Strength of 40 MPa

This group contains 24 specimens as illustrated in Figure 4-30 below. In this group the targeted concrete strength of the prisms is 40 MPa. Two different plate types were used as EBR materials that include CFRP and AA plates with rough and plain surfaces as shown in Figure 4-31 below. Eight prisms were reinforced with CFRP plates and sixteen prisms with AA plates from which eight plates were used with plain (natural) surface and another eight with a randomly scratched surface. Four bond lengths were used for each plate type along with a duplicate sample with the same properties for each specimen.

Six charts have been developed for each sample. In these graphs the variation of different parameters along the bonded length of the EBR plate is displayed. Namely, bond stress, strain and slip variations with the bonded length are shown. In addition, other relations including bond stress-slip, load-strain and load-extension relationships are also shown. As previously stated, two identical samples with the same properties were cast and tested, however the results of only one specimen of the two are presented in the charts below. Table 4-3 given at the end of this section shows all the samples results for this group.

Figure 4-30: Twenty four specimens with  $f_c$  of 40 MPa.

Figure 4-31: Three different EBR materials used.

87

0

0

0.006

0.006

0.012

0.012

0.018

0.018

0.024

0.024

0.03

0.03

0

0

10

10

20

20

30

30

40

40

50

50

60

60

Slip (mm)

Slip (mm)

Distance from loaded end (mm)

Distance from loaded end (mm)

0

0

0.4

0.4

0.8

0.8

1.2

1.2

1.6

1.6

2

2

0

0

10

10

20

20

30

30

40

40

50

50

60

60

Shear Stress (MPa)

Shear Stress MPa)

Distance from loaded end (mm)

Distance from loaded end (mm)

0

0

0.4

0.4

0.8

0.8

1.2

1.2

1.6

1.6

2

2

0

0

0.006

0.006

0.012

0.012

0.018

0.018

0.024

0.024

0.03

0.03

Shear Stress (MPa)

Slip (mm)

Slip (mm)

0

0

100

100

200

200

300

300

400

400

500

500

0

0

10

10

20

20

30

30

40

40

50

50

60

60

Strain (

Strain  $\mu\epsilon\mu\epsilon$ )

Distance from free end (mm)

Distance from free end (mm)

0

0

2500

2500

5000

5000

7500

7500

10000

10000

12500

12500

0

0

250

250

500

500

750

750

1000

1000

1250

1250

Load (N)

Load N)

Strain (

Strain ( $\mu\text{m}\epsilon$ )

SG 1

SG 1

SG 2

SG 2

SG 3

SG 3

0

0

2500

2500

5000

5000

7500

7500

10000

10000

12500

12500

0

0

0.6

0.6

1.2

1.2

1.8

1.8

2.4

2.4

3

3

Load (N)

Extension (mm)

Extension (mm)

(a) Sample failure mode

(b) Bond stress-distance curves

(c) Slip-distance curves

(d) Bond stress-slip curves

(e) Strain gauge-distance curves.

(f) Load-strain curves

(g) Load-extension curve

Figure 4-32: Variation of stress, strain, slip and load of 40-CF-L1 specimen

88

0

0

0.008

0.008

0.016

0.016

0.024

0.024

0.032

0.032

0.04

0.04

0

0

20

20

40

40

60

60

80

80

100

100

120

120

Slip (mm)

Slip (mm)

Distance from loaded end (mm)

Distance from loaded end (mm)

0

0

0.35

0.35

0.7

0.7

1.05

1.05

1.4

1.4

1.75

1.75

0

0

20

20

40

40

60

60

80

80

100

100

120

120

Shear Stress (MPa)

Shear Stress MPa)

Distance from loaded end (mm)

Distance from loaded end (mm)

0

0

0.35

0.35

0.7

0.7

1.05

1.05

1.4

1.4

1.75

1.75

0

0

0.008

0.008

0.016

0.016

0.024

0.024

0.032

0.032

0.04

0.04

Shear Stress (MPa)

Slip (mm)

Slip (mm)

0

0

150

150

300

300

450

450

600

600

750

750

0

0

20

20

40

40

60

60

80

80

100

100

120

120

Strain (

Strain  $\mu\epsilon$ )

Distance from free end (mm)

Distance from free end (mm)

0

0

2500

2500

5000

5000

7500

7500

10000

10000

12500

12500

0

0

250

250

500

500

750

750

1000

1000

1250

1250

Load (N)

Load N)

Strain (

Strain ( $\mu\text{m}\epsilon\epsilon$ )

0

0

2500

2500

5000

5000

7500

7500

10000

10000

12500

12500

0

0

0.5

0.5

1

1

1.5

1.5

2

2

2.5

2.5

Load (N)

Extension (mm)

Extension (mm)

(a) Sample failure mode

(b) Bond stress-distance curves

(c) Slip-distance curves

(d) Bond stress-slip curves

(e) Strain gauge-distance curves.

(f) Load-strain curves

(g) Load-extension curve

Figure 4-33: Variation of stress, strain, slip and load of 40-CF-L2 specimen

89

0

0

0.5

0.5

1

1

1.5

1.5

2

2

2.5

2.5

0

0

0.02

0.02

0.04

0.04

0.06

0.06

0.08

0.08

0.1

0.1

Shear Stress (MPa)

Shear Stress (MPa)

Slip (mm)

Slip (mm)

0

0

0.02

0.02

0.04

0.04

0.06

0.06

0.08

0.08

0.1

0.1

0

0

25

25

50

50

75

75

100

100

125

125

150

150

175

175

Slip (mm)

Slip mm)

Distance from loaded end (mm)

Distance from loaded end (mm)

0

0

2500

2500

5000

5000

7500

7500

10000

10000

12500

12500

0

0

350

350

700

700

1050

1050

1400

1400

1750

1750

Load (N)

Load N)

Strain (

Strain ( $\mu\text{m}\epsilon\epsilon$ )

SG 1

SG 1

SG 2

SG 2

SG 3

SG 3

SG 4

SG 4

0

0

2500

2500

5000

5000

7500

7500

10000

10000

12500

12500

0

0

0.6

0.6

1.2

1.2

1.8

1.8

2.4

2.4

3

3

Load (N)

Extension (mm)

Extension (mm)

0

0

0.5

0.5

1

1

1.5

1.5

2

2

2.5

2.5

0

0

25

25

50

50

75

75

100

100

125

125

150

150

175

175

Shear Stress (MPa)

Distance from loaded end (mm)

Distance from loaded end (mm)

0

0

250

250

500

500

750

750

1000

1000

1250

1250

0

0

25

25

50

50

75

75

100

100

125

125

150

150

175

175

Strain (

Strain  $\mu\mu\epsilon\epsilon$ )

Distance (mm)

Distance (mm)

(a) Sample failure mode

(b) Bond stress-distance curves

(c) Slip-distance curves

(d) Bond stress-slip curves

(e) Strain gauge-distance curves.

(f) Load-strain curves

(g) Load-extension curve

Figure 4-34: Variation of stress, strain, slip and load of 40-CF-L3 specimen

90

(a) Sample failure mode

(b) Bond stress-distance curves

(c) Slip-distance curves

(d) Bond stress-slip curves

(e) Strain gauge-distance curves.

(f) Load-strain curves

(g) Load-extension curve

Figure 4-35: Variation of stress, strain, slip and load of 40-CF-L4 specimen

0

0

0.12

0.12

0.24

0.24

0.36

0.36

0.48

0.48

0.6

0.6

0

0

0.012

0.012

0.024

0.024

0.036

0.036

0.048

0.048

0.06

0.06

Shear Stress (MPa)

Shear Stress (MPa)

Slip (mm)

Slip (mm)

0

0

0.012

0.012

0.024

0.024

0.036

0.036

0.048

0.048

0.06

0.06

0

0

50

50

100

100

150

150

200

200

250

250

Slip (mm)

Slip mm)

Distance from loaded end (mm)

Distance from loaded end (mm)

0

0

0.12

0.12

0.24

0.24

0.36

0.36

0.48

0.48

0.6

0.6

0

0

50

50

100

100

150

150

200

200

250

250

Shear Stress (MPa)

Distance from loaded end (mm)

Distance from loaded end (mm)

0

0

3000

3000

6000

6000

9000

9000

12000

12000

15000

15000

0

0

400

400

800

800

1200

1200

1600

1600

Load (N)

Load N)

Strain (

Strain ( $\mu\text{m}\epsilon\epsilon$ )

SG 1

SG 1

SG 2

SG 2

SG 3

SG 3

SG 4

SG 4

SG 5

SG 5

0

0

3000

3000

6000

6000

9000

9000

12000

12000

15000

15000

0

0

0.6

0.6

1.2

1.2

1.8

1.8

2.4

2.4

3

3

Load (N)

Extension (mm)

Extension (mm)

0

0

80

80

160

160

240

240

320

320

400

400

0

0

50

50

100

100

150

150

200

200

250

250

Strain (

Strain  $\mu\mu\epsilon\epsilon$ )

Distance (mm)

Distance (mm)

91

0

0

0.001

0.001

0.002

0.002

0.003

0.003

0.004

0.004

0.005

0.005

0

0

10

10

20

20

30

30

40

40

50

50

60

60

Slip (mm)

Slip (mm)

Distance from loaded end (mm)

Distance from loaded end (mm)

0

0

0.1

0.1

0.2

0.2

0.3

0.3

0.4

0.4

0.5

0.5

0

0

10

10

20

20

30

30

40

40

50

50

60

60

Shear stress (MPa)

Shear stress MPa)

Distance from loaded end (mm)

Distance from loaded end (mm)

0

0

0.1

0.1

0.2

0.2

0.3

0.3

0.4

0.4

0.5

0.5

0

0

0.001

0.001

0.002

0.002

0.003

0.003

0.004

0.004

0.005

0.005

Shear Stress (MPa)

Stress Slip (mm)

Slip (mm)

0

0

20

20

40

40

60

60

80

80

100

100

0

0

10

10

20

20

30

30

40

40

50

50

60

60

Strain (

Strain  $\mu\epsilon$ )

Distance from free end (mm)

Distance from free end (mm)

0

0

1600

1600

3200

3200

4800

4800

6400

6400

8000

8000

0

0

50

50

100

100

150

150

200

200

Load (N)

Load N)

Strain (

Strain ( $\mu\text{m}$ )m)

SG 1

SG 1

SG 2

SG 2

SG 3

SG 3

0

0

1800

1800

3600

3600

5400

5400

7200

7200

9000

9000

0

0

0.35

0.35

0.7

0.7

1.05

1.05

1.4

1.4

1.75

1.75

Load (N)

Extension (mm)

Extension (mm)

(a) Sample failure mode

(b) Bond stress-distance curves

(c) Slip-distance curves

(d) Bond stress-slip curves

(e) Strain gauge-distance curves.

(f) Load-strain curves

(g) Load-extension curve

Figure 4-36: Variation of stress, strain, slip and load of 40-R-L1 specimen

92

0

0

3000

3000

6000

6000

9000

9000

12000

12000

15000

15000

0

0

300

300

600

600

900

900

1200

1200

Load (N)

Load (N)

Strain (

Strain ( $\mu\text{m}\epsilon$ )

SG 1

SG 1

Series2

Series2

SG 3

SG 3

SG 4

SG 4

0

0

3000

3000

6000

6000

9000

9000

12000

12000

15000

15000

0

0

0.8

0.8

1.6

1.6

2.4

2.4

3.2

3.2

Load (N)

Extension (mm)

Extension (mm)

0

0

0.6

0.6

1.2

1.2

1.8

1.8

2.4

2.4

3

3

0

0

20

20

40

40

60

60

80

80

100

100

120

120

Shear Stress (MPa)

Shear Stress MPa)

Distance from loaded end (mm)

Distance from loaded end (mm)

0

0

0.012

0.012

0.024

0.024

0.036

0.036

0.048

0.048

0.06

0.06

0

0

20

20

40

40

60

60

80

80

100

100

120

120

Slip (mm)

Slip mm)

Distance from loaded end (mm)

Distance from loaded end (mm)

0

0

0.6

0.6

1.2

1.2

1.8

1.8

2.4

2.4

3

3

0

0

0.012

0.012

0.024

0.024

0.036

0.036

0.048

0.048

0.06

0.06

Shear Stress (MPa)

Slip (mm)

Slip (mm)

0

0

250

250

500

500

750

750

1000

1000

1250

1250

0

0

20

20

40

40

60

60

80

80

100

100

120

120

Strain (

Strain  $\mu\epsilon\mu\epsilon$ )

Distance from free end (mm)

Distance from free end (mm)

(a) Sample failure mode

(b) Bond stress-distance curves

(c) Slip-distance curves

(d) Bond stress-slip curves

(e) Strain gauge-distance curves.

(f) Load-strain curves

(g) Load-extension curve

Figure 4-37: Variation of stress, strain, slip and load of 40-R-L2 specimen

93

0

0

0.025

0.025

0.05

0.05

0.075

0.075

0.1

0.1

0.125

0.125

0

0

25

25

50

50

75

75

100

100

125

125

150

150

175

175

Slip (mm)

Slip (mm)

Distance from loaded end (mm)

Distance from loaded end (mm)

0

0

0.6

0.6

1.2

1.2

1.8

1.8

2.4

2.4

3

3

0

0

25

25

50

50

75

75

100

100

125

125

150

150

175

175

Shear Stress (MPa)

Shear Stress MPa)

Distance from loaded end (mm)

Distance from loaded end (mm)

0

0

0.6

0.6

1.2

1.2

1.8

1.8

2.4

2.4

3

3

0

0

0.025

0.025

0.05

0.05

0.075

0.075

0.1

0.1

0.125

0.125

Shear Stress (MPa)

Slip (mm)

Slip (mm)

0

0

350

350

700

700

1050

1050

1400

1400

1750

1750

0

0

25

25

50

50

75

75

100

100

125

125

150

150

175

175

Strain (

Strain  $\mu\epsilon\mu\epsilon$ )

Distance from free end (mm)

Distance from free end (mm)

0

0

5000

5000

10000

10000

15000

15000

20000

20000

25000

25000

0

0

500

500

1000

1000

1500

1500

2000

2000

2500

2500

Load (N)

Load (N)

Strain (

Strain ( $\mu\text{m}\epsilon\epsilon$ )

SG 1

SG 1

SG 2

SG 2

SG 3

SG 3

SG 4

SG 4

0

0

5000

5000

10000

10000

15000

15000

20000

20000

25000

25000

0

0

1

1

2

2

3

3

4

4

5

5

Load (N)

Extension (mm)

Extension (mm)

(a) Sample failure mode

(b) Bond stress-distance curves

(c) Slip-distance curves

(d) Bond stress-slip curves

(e) Strain gauge-distance curves.

(f) Load-strain curves

(g) Load-extension curve

Figure 4-38: Variation of stress, strain, slip and load of 40-R-L3 specimen

94

(a) Sample failure mode

(b) Bond stress-distance curves

(c) Slip-distance curves

(d) Bond stress-slip curves

(e) Strain gauge-distance curves.

(f) Load-strain curves

(g) Load-extension curve

0

0

0.5

0.5

1

1

1.5

1.5

2

2

2.5

2.5

0

0

50

50

100

100

150

150

200

200

250

250

Shear Stress (MPa)

Shear Stress (MPa)

Distance from loaded end (mm)

Distance from loaded end (mm)

0

0

0.015

0.015

0.03

0.03

0.045

0.045

0.06

0.06

0.075

0.075

0

0

50

50

100

100

150

150

200

200

250

250

Slip (mm)

Slip mm)

Distance from loaded end (mm)

Distance from loaded end (mm)

0

0

0.5

0.5

1

1

1.5

1.5

2

2

2.5

2.5

0

0

0.015

0.015

0.03

0.03

0.045

0.045

0.06

0.06

0.075

0.075

Shear Stress (MPa)

Slip (mm)

Slip (mm)

0

0

250

250

500

500

750

750

1000

1000

1250

1250

0

0

50

50

100

100

150

150

200

200

250

250

Strain (

Strain  $\mu\epsilon\mu\epsilon$ )

Distance from free end (mm)

Distance from free end (mm)

0

0

3500

3500

7000

7000

10500

10500

14000

14000

17500

17500

0

0

0.8

0.8

1.6

1.6

2.4

2.4

3.2

3.2

4

4

Load (N)

Load N)

Extension (mm)

Extension (mm)

0

0

3500

3500

7000

7000

10500

10500

14000

14000

17500

17500

0

0

300

300

600

600

900

900

1200

1200

1500

1500

Load (N)

Strain (

Strain ( $\mu\mu\epsilon\epsilon$ )

SG 1

SG 1

SG 2

SG 2

SG 3

SG 3

SG 4

SG 4

SG 5

SG 5

Figure 4-39: Variation of stress, strain, slip and load of 40-R-L4 specimen

95

0

0

0.04

0.04

0.08

0.08

0.12

0.12

0.16

0.16

0.2

0.2

0

0

10

10

20

20

30

30

40

40

50

50

60

60

Shear Stress (MPa)

Shear Stress (MPa)

Distance from loaded end (mm)

Distance from loaded end (mm)

0

0

0.0007

0.0007

0.0014

0.0014

0.0021

0.0021

0.0028

0.0028

0.0035

0.0035

0

0

10

10

20

20

30

30

40

40

50

50

60

60

Slip (mm)

Slip mm)

Distance from loaded end (mm)

Distance from loaded end (mm)

0

0

0.04

0.04

0.08

0.08

0.12

0.12

0.16

0.16

0.2

0.2

0

0

0.0007

0.0007

0.0014

0.0014

0.0021

0.0021

0.0028

0.0028

0.0035

0.0035

Shear Stress (MPa)

Slip (mm)

Slip (mm)

0

0

7

7

14

14

21

21

28

28

35

35

0

0

10

10

20

20

30

30

40

40

50

50

60

60

Strain (

Strain  $\mu\epsilon\mu\epsilon$ )

Distance from free end (mm)

Distance from free end (mm)

0

0

700

700

1400

1400

2100

2100

2800

2800

3500

3500

0

0

25

25

50

50

75

75

100

100

125

125

150

150

Load (N)

Load N)

Strain (

Strain ( $\mu\text{m}\epsilon\epsilon$ )

SG 1

SG 1

SG 2

SG 2

SG 3

SG 3

0

0

700

700

1400

1400

2100

2100

2800

2800

3500

3500

0

0

0.12

0.12

0.24

0.24

0.36

0.36

0.48

0.48

Load (N)

Extension (mm)

Extension (mm)

- (a) Sample failure mode
- (b) Bond stress-distance curves
- (c) Slip-distance curves
- (d) Bond stress-slip curves
- (e) Strain gauge-distance curves.
- (f) Load-strain curves
- (g) Load-extension curve

Figure 4-40: Variation of stress, strain, slip and load of 40-P-L1 specimen

96

0

0

0.35

0.35

0.7

0.7

1.05

1.05

1.4

1.4

1.75

1.75

0

0

0.006

0.006

0.012

0.012

0.018

0.018

0.024

0.024

0.03

0.03

Shear Stress (MPa)

Shear Stress (MPa)

Slip (mm)

Slip (mm)

0

0

0.35

0.35

0.7

0.7

1.05

1.05

1.4

1.4

1.75

1.75

0

0

25

25

50

50

75

75

100

100

125

125

Shear Stress (MPa)

Distance from loaded end (mm)

Distance from loaded end (mm)

0

0

0.006

0.006

0.012

0.012

0.018

0.018

0.024

0.024

0.03

0.03

0

0

20

20

40

40

60

60

80

80

100

100

120

120

Slip (mm)

Slip mm)

Distance from loaded end (mm)

Distance from loaded end (mm)

0

0

150

150

300

300

450

450

600

600

750

750

0

0

20

20

40

40

60

60

80

80

100

100

120

120

Strain (

Strain  $\mu\epsilon\mu\epsilon$ )

Distance from free end (mm)

Distance from free end (mm)

0

0

1000

1000

2000

2000

3000

3000

4000

4000

5000

5000

0

0

150

150

300

300

450

450

600

600

750

750

Load (N)

Load N)

Strain (

Strain ( $\mu\mu\epsilon\epsilon$ )

SG 1

SG 1

SG 2

SG 2

SG 3

SG 3

SG 4

SG 4

0

0

1000

1000

2000

2000

3000

3000

4000

4000

5000

5000

0

0

0.25

0.25

0.5

0.5

0.75

0.75

1

1

1.25

1.25

Load (N)

Extension (mm)

Extension (mm)

(a) Sample failure mode

(b) Bond stress-distance curves

(c) Slip-distance curves

(d) Bond stress-slip curves

(e) Strain gauge-distance curves.

(f) Load-strain curves

(g) Load-extension curve

Figure 4-41: Variation of stress, strain, slip and load of 40-P-L2 specimen

97

(a) Sample failure mode

(b) Bond stress-distance curves

(c) Slip-distance curves

(d) Bond stress-slip curves

(e) Strain gauge-distance curves.

(f) Load-strain curves

(g) Load-extension curve

0

0

0.006

0.006

0.012

0.012

0.018

0.018

0.024

0.024

0.03

0.03

0

0

25

25

50

50

75

75

100

100

125

125

150

150

175

175

Slip (mm)

Slip (mm)

Distance from loaded end (mm)

Distance from loaded end (mm)

0

0

0.16

0.16

0.32

0.32

0.48

0.48

0.64

0.64

0.8

0.8

0

0

25

25

50

50

75

75

100

100

125

125

150

150

175

175

Shear Stress (MPa)

Shear Stress MPa)

Distance from loaded end (mm)

Distance from loaded end (mm)

0

0

0.16

0.16

0.32

0.32

0.48

0.48

0.64

0.64

0.8

0.8

0

0

0.005

0.005

0.01

0.01

0.015

0.015

0.02

0.02

0.025

0.025

Shear Stress (MPa)

Slip (mm)

Slip (mm)

0

0

80

80

160

160

240

240

320

320

400

400

0

0

25

25

50

50

75

75

100

100

125

125

150

150

175

175

Strain (

Strain  $\mu\epsilon$ )

Distance from free end (mm)

Distance from free end (mm)

0

0

800

800

1600

1600

2400

2400

3200

3200

4000

4000

0

0

120

120

240

240

360

360

480

480

600

600

Load (N)

Load N)

Strain (

Strain ( $\mu\text{m}$ )m)

SG 1

SG 1

SG 2

SG 2

SG 3

SG 3

SG 4

SG 4

0

0

700

700

1400

1400

2100

2100

2800

2800

3500

3500

0

0

0.5

0.5

1

1

1.5

1.5

2

2

Load (N)

Extension (mm)

Extension (mm)

Figure 4-42: Variation of stress, strain, slip and load of 40-P-L3 specimen

98

0

0

0.3

0.3

0.6

0.6

0.9

0.9

1.2

1.2

1.5

1.5

0

0

50

50

100

100

150

150

200

200

250

250

Shear Stress (MPa)

Shear Stress (MPa)

Distance from loaded end (mm)

Distance from loaded end (mm)

0

0

0.01

0.01

0.02

0.02

0.03

0.03

0.04

0.04

0.05

0.05

0

0

50

50

100

100

150

150

200

200

250

250

Slip (mm)

Slip mm)

Distance from loaded end (mm)

Distance from loaded end (mm)

0

0

0.3

0.3

0.6

0.6

0.9

0.9

1.2

1.2

1.5

1.5

0

0

0.01

0.01

0.02

0.02

0.03

0.03

0.04

0.04

0.05

0.05

Shear Stress (MPa)

Slip (mm)

Slip (mm)

0

0

120

120

240

240

360

360

480

480

600

600

0

0

50

50

100

100

150

150

200

200

250

250

Strain (

Strain  $\mu\epsilon$ )

Distance from free end (mm)

Distance from free end (mm)

0

0

1500

1500

3000

3000

4500

4500

6000

6000

7500

7500

0

0

160

160

320

320

480

480

640

640

800

800

Load (N)

Load N)

Strain (

Strain ( $\mu\mu\epsilon\epsilon$ )

SG 1

SG 1

SG 2

SG 2

SG 3

SG 3

SG 4

SG 4

SG 5

SG 5

0

0

1500

1500

3000

3000

4500

4500

6000

6000

7500

7500

0

0

0.3

0.3

0.6

0.6

0.9

0.9

1.2

1.2

1.5

1.5

Load (N)

Extension (mm)

Extension (mm)

(a) Sample failure mode

(b) Bond stress-distance curves

(c) Slip-distance curves

(d) Bond stress-slip curves

(e) Strain gauge-distance curves.

(f) Load-strain curves

(g) Load-extension curve

Figure 4-43: Variation of stress, strain, slip and load of 40-P-L4 specimen

99

Table 4-3: Summary of results for specimens with  $f_c'$  of 40 MPa

Specimen Identification

AA/CFRP Plate

Cube compressive strength (MPa)

Failure Load (KN)

\*Failure mode

Plate type

Width (mm)

Thickness (mm)

Bonded length (mm)

40-CF-L1

CFRP

50

1.4

50

40

4.4

DB-C

40-CF-L1

CFRP

50

1.4

50

40

10.0

DA

40-CF-L2

CFRP

50

1.4

100

40

12.4

DB-C+CS

40-CF-L2

CFRP

50

1.4

100

40

10.5

DB-P+DA

40-CF-L3

CFRP

50

1.4

150

40

7.58

DA

40-CF-L3

CFRP

50

1.4

150

40

11.4

DB-C+CS

40-CF-L4

CFRP

50

1.4

200

40

12.23

DB-C

40-CF-L4

CFRP

50

1.4

200

40

9.95

DB-P

40-R-L1

AA-R

50

3.0

50

40

7.8

DA

40-R-L1

AA-R

50

3.0

50

40

5.0

DA

40-R-L2

AA-R

50

3.0

100

40

14.0

DB-C+DB-P

40-R-L2

AA-R

50

3.0

100

40

10.2

DB-C+CS

40-R-L3

AA-R

50

3.0

150

40

16.45

DB-C+CS

40-R-L3

AA-R

50

3.0

150

40

20.07

DB-C

40-R-L4

AA-R

50

3.0

200

40

14.51

DB-C+CS

40-R-L4

AA-R

50

3.0

200

40

9.59

DB-C+CS

40-P-L1

AA-P

50

3.0

50

40

4.19

DB-P

40-P-L1

AA-P

50

3.0

50

40

2.88

DB-P

40-P-L2

AA-P

50

3.0

100

40

4.67

DB-P

40-P-L2

AA-P

50

3.0

100

40

4.78

DB-P+DA

40-P-L3

AA-P

50

3.0

150

40

3.47

DB-P

40-P-L3

AA-P

50

3.0

150

40

9.25

DB-P

40-P-L4

AA-P

50

3.0

200

40

3.46

DB-P

40-P-L4

AA-P

50

3.0

200

40

5.71

DB-P

\*Failure mode: DB-C: Debonding in concrete, DB-P: Plate Debonding (Plate/adhesive interface separation), CS: Concrete spalling, DA: Adhesive debonding (Adhesive/concrete interface separation).

4.3.1 CFRP plate failure. The failure mode for specimens with CFRP plates mainly takes place in the concrete adhesive interface accompanied by concrete spalling in some cases.

4.3.2 AA scratched plate failure. The failure mode for this type of plate is similar to that of the CFRP. However, the concrete spalling in this case takes place in all the specimens due to scratched AA plate rough surface which causes concentration of stresses in the vicinity of the loaded end.

4.3.3 AA plain plate failure. The failure mode for AA plates with plain surface in all specimens takes place in the plate adhesive interface due to the weak bond between the plate plain surface and the adhesive. There is no concrete spalling in this case due to relatively high concrete strength of this group.

100

#### 4.4 Group Four: Concrete Strength of 60 MPa

This group contains 24 specimens as illustrated in Figure 4-44 below. In this group the concrete strength of the prisms is 60 MPa. Two different plate types were used as EBR materials which include CFRP and AA plates with rough and plain surfaces as shown in Figure 4-45. Eight prisms were reinforced with CFRP plates and sixteen prisms with AA plates from which eight plates were used with plain (natural) surface and another eight with a randomly scratched surface as shown below. Four bond lengths were used for each plate type along with a duplicate sample with the same properties for each specimen.

Six charts have been developed for each sample. In these graphs the variation of different parameters along the bonded length of the EBR plate is displayed. Namely, bond stress, strain and slip variations with the bonded length are shown. In addition, other relations including bond stress-slip, load-strain and load-extension relationships are also shown. As previously stated, two identical samples with the same properties were cast and tested, however the results of only one specimen of the two are presented in the charts below. Table 4-4 given at the end of this section shows all the samples results for this group.

Figure 4-44: Twenty four specimens with fcu of 60 MPa

Figure 4-45: Three different EBR materials used

101

0

0

0.005

0.005

0.01

0.01

0.015

0.015

0.02

0.02

0.025

0.025

0

0

10

10

20

20

30

30

40

40

50

50

60

60

Slip (mm)

Slip (mm)

Distance from loaded end (mm)

Distance from loaded end (mm)

0

0

0.5

0.5

1

1

1.5

1.5

2

2

2.5

2.5

0

0

10

10

20

20

30

30

40

40

50

50

60

60

Shear Stress (MPa)

Shear Stress MPa)

Distance from loaded end (mm)

Distance from loaded end (mm)

0

0

0.5

0.5

1

1

1.5

1.5

2

2

2.5

2.5

0

0

0.005

0.005

0.01

0.01

0.015

0.015

0.02

0.02

0.025

0.025

Shear Stress (MPa)

Slip (mm)

Slip (mm)

0

0

100

100

200

200

300

300

400

400

500

500

0

0

10

10

20

20

30

30

40

40

50

50

60

60

Strain (

Strain  $\mu\epsilon\mu\epsilon$ )

Distance from free end (mm)

Distance from free end (mm)

0

0

2000

2000

4000

4000

6000

6000

8000

8000

10000

10000

0

0

200

200

400

400

600

600

800

800

1000

1000

Load (N)

Load N)

Strain (

Strain (μεμε))

SG 1

SG 1

SG 2

SG 2

SG 3

SG 3

0

0

2000

2000

4000

4000

6000

6000  
8000  
8000  
10000  
10000  
0  
0  
0.5  
0.5  
1  
1  
1.5  
1.5  
2  
2  
2.5  
2.5

Load (N)

Extension (mm)

Extension (mm)

(a) Sample failure mode

(b) Bond stress-distance curves

(c) Slip-distance curves

(d) Bond stress-slip curves

(e) Strain gauge-distance curves.

(f) Load-strain curves

(g) Load-extension curve

Figure 4-46: Variation of stress, strain, slip and load of 60-CF-L1 specimen

0

0

0.012

0.012

0.024

0.024

0.036

0.036

0.048

0.048

0.06

0.06

0

0

20

20

40

40

60

60

80

80

100

100

120

120

Slip (mm)

Slip (mm)

Distance from loaded end (mm)

Distance from loaded end (mm)

0

0

0.4

0.4

0.8

0.8

1.2

1.2

1.6

1.6

2

2

0

0

20

20

40

40

60

60

80

80

100

100

120

120

Shear Stress (MPa)

Shear Stress MPa)

Distance from loaded end (mm)

Distance from loaded end (mm)

0

0

0.4

0.4

0.8

0.8

1.2

1.2

1.6

1.6

2

2

0

0

0.012

0.012

0.024

0.024

0.036

0.036

0.048

0.048

0.06

0.06

Shear Stress (MPa)

Slip (mm)

Slip (mm)

0

0

3000

3000

6000

6000

9000

9000

12000

12000

15000

15000

0

0

320

320

640

640

960

960

1280

1280

1600

1600

Load (N)

Load N)

Strain (

Strain ( $\mu\text{m}\epsilon\epsilon$ )

SG 1

SG 1

SG 2

SG 2

SG 3

SG 3

0

0

200

200

400

400

600

600

800

800

1000

1000

0

0

20

20

40

40

60

60

80

80

100

100

120

120

Strain (

Strain  $\mu\epsilon$ )

Distance from free end (mm)

Distance from free end (mm)

0

0

3000

3000

6000

6000

9000

9000

12000

12000

15000

15000

0

0

0.6

0.6

1.2

1.2

1.8

1.8

2.4

2.4

3

3

Load (N)

Extension (mm)

Extension (mm)

(a) Sample failure mode

(b) Bond stress-distance curves

(c) Slip-distance curves

(d) Bond stress-slip curves

(e) Strain gauge-distance curves.

(f) Load-strain curves

(g) Load-extension curve

Figure 4-47: Variation of stress, strain, slip and load of 60-CF-L2 specimen

103

0

0

0.012

0.012

0.024

0.024

0.036

0.036

0.048

0.048

0.06

0.06

0

0

25

25

50

50

75

75

100

100

125

125

150

150

175

175

Slip (mm)

Slip (mm)

Distance from loaded end (mm)

Distance from loaded end (mm)

0

0

0.4

0.4

0.8

0.8

1.2

1.2

1.6

1.6

2

2

0

0

25

25

50

50

75

75

100

100

125

125

150

150

175

175

Shear Stress (MPa)

Shear Stress MPa)

Distance from loaded end (mm)

Distance from loaded end (mm)

0

0

0.4

0.4

0.8

0.8

1.2

1.2

1.6

1.6

2

2

0

0

0.012

0.012

0.024

0.024

0.036

0.036

0.048

0.048

0.06

0.06

Shear Stress (MPa)

Slip (mm)

Slip (mm)

0

0

180

180

360

360

540

540

720

720

900

900

0

0

25

25

50

50

75

75

100

100

125

125

150

150

175

175

Strain (

Strain  $\mu\epsilon\mu\epsilon$ )

Distance from free end(mm)

Distance from free end(mm)

0

0

5000

5000

10000

10000

15000

15000

20000

20000

0

0

300

300

600

600

900

900

1200

1200

1500

1500

Load (N)

Load N)

Strain (

Strain ( $\mu\epsilon\mu\epsilon$ )

SG 1

SG 1

SG 2

SG 2

SG 3

SG 3

SG 4

SG 4

0

0

4000

4000

8000

8000

12000

12000

16000

16000

20000

20000

0

0

1

1

2

2

3

3

4

4

5

5

Load (N)

Extension (mm)

Extension (mm)

(a) Sample failure mode

(b) Bond stress-distance curves

(c) Slip-distance curves

(d) Bond stress-slip curves

(e) Strain gauge-distance curves.

(f) Load-strain curves

(g) Load-extension curve

Figure 4-48: Variation of stress, strain, slip and load of 60-CF-L3 specimen

104

0

0

0.025

0.025

0.05

0.05

0.075

0.075

0.1

0.1

0.125

0.125

0

0

50

50

100

100

150

150

200

200

250

250

Slip (mm)

Slip (mm)

Distance from loaded end (mm)

Distance from loaded end (mm)

0

0

1

1

2

2

3

3

4

4

5

5

0

0

50

50

100

100

150

150

200

200

250

250

Shear Stress (MPa)

Shear Stress MPa)

Distance from loaded end (mm)

Distance from loaded end (mm)

0

0

1

1

2

2

3

3

4

4

5

5

0

0

0.025

0.025

0.05

0.05

0.075

0.075

0.1

0.1

0.125

0.125

Shear Stress (MPa)

Slip (mm)

Slip (mm)

0

0

500

500

1000

1000

1500

1500

2000

2000

2500

2500

0

0

50

50

100

100

150

150

200

200

250

250

Strain (

Strain  $\mu\epsilon\mu\epsilon$ )

Distance from free end (mm)

Distance from free end (mm)

0

0

4000

4000

8000

8000

12000

12000

16000

16000

20000

20000

0

0

500

500

1000

1000

1500

1500

2000

2000

2500

2500

Load (N)

Load N)

Strain (

Strain ( $\mu\mu\epsilon\epsilon$ )

SG 1

SG 1

SG 2

SG 2

SG 3

SG 3

SG 4

SG 4

SG 5

SG 5

0

0

4000

4000

8000

8000

12000

12000

16000

16000

20000

20000

0

0

0.6

0.6

1.2

1.2

1.8

1.8

2.4

2.4

3

3

Load (N)

Extension (mm)

Extension (mm)

(a) Sample failure mode

(b) Bond stress-distance curves

(c) Slip-distance curves

(d) Bond stress-slip curves

(e) Strain gauge-distance curves.

(f) Load-strain curves

(g) Load-extension curve

Figure 4-49: Variation of stress, strain, slip and load of 60-CF-L4 specimen

105

(a) Sample failure mode

(b) Bond stress-distance curves

(c) Slip-distance curves

(d) Bond stress-slip curves

(e) Strain gauge-distance curves.

(f) Load-strain curves

(g) Load-extension curve

0

0

3500

3500

7000

7000

10500

10500

14000

14000

17500

17500

0

0

350

350

700

700

1050

1050

1400

1400

1750

1750

Load (N)

Load (N)

Strain (

Strain ( $\mu\text{m}\epsilon\epsilon$ )

SG 1

SG 1

SG 2

SG 2

SG 3

SG 3

0

0

0.008

0.008

0.016

0.016

0.024

0.024

0.032

0.032

0.04

0.04

0

0

10

10

20

20

30

30

40

40

50

50

60

60

Slip (mm)

Slip mm)

Distance from loaded end (mm)

Distance from loaded end (mm)

0

0

1

1

2

2

3

3

4

4

5

5

0

0

10

10

20

20

30

30

40

40

50

50

60

60

Shear Stress (MPa)

Shear Stress MPa)

Distance from loaded end (mm)

Distance from loaded end (mm)

0

0

1

1

2

2

3

3

4

4

5

5

0

0

0.008

0.008

0.016

0.016

0.024

0.024

0.032

0.032

0.04

0.04

Shear Stress (MPa)

Slip (mm)

Slip (mm)

0

0

250

250

500

500

750

750

1000

1000

1250

1250

0

0

10

10

20

20

30

30

40

40

50

50

60

60

Strain (

Strain  $\mu\epsilon\mu\epsilon$ )

Distance from free end (mm)

Distance from free end (mm)

0

0

3200

3200

6400

6400

9600

9600

12800

12800

16000

16000

0

0

0.8

0.8

1.6

1.6

2.4

2.4

3.2

3.2

4

4

Load (N)

Extension (mm)

Extension (mm)

Figure 4-50: Variation of stress, strain, slip and load of 60-R-L1 specimen

106

0

0

0.015

0.015

0.03

0.03

0.045

0.045

0.06

0.06

0.075

0.075

0

0

20

20

40

40

60

60

80

80

100

100

120

120

Slip (mm)

Slip (mm)

Distance from loaded end (mm)

Distance from loaded end (mm)

0

0

0.8

0.8

1.6

1.6

2.4

2.4

3.2

3.2

4

4

0

0

20

20

40

40

60

60

80

80

100

100

120

120

Shear Stress (MPa)

Shear Stress MPa)

Distance from loaded end (mm)

Distance from loaded end (mm)

0

0

0.8

0.8

1.6

1.6

2.4

2.4

3.2

3.2

4

4

0

0

0.015

0.015

0.03

0.03

0.045

0.045

0.06

0.06

0.075

0.075

Shear Stress (MPa)

Slip (mm)

Slip (mm)

0

0

4000

4000

8000

8000

12000

12000

16000

16000

20000

20000

0

0

0.8

0.8

1.6

1.6

2.4

2.4

3.2

3.2

4

4

Load (N)

Load N)

Extension (mm)

Extension (mm)

0

0

4000

4000

8000

8000

12000

12000

16000

16000

20000

20000

0

0

350

350

700

700

1050

1050

1400

1400

1750

1750

Load (N)

Strain (

Strain ( $\mu\text{m}\epsilon\epsilon$ )

0

0

350

350

700

700

1050

1050

1400

1400

1750

1750

2100

2100

0

0

20

20

40

40

60

60

80

80

100

100

120

120

Strain (

Strain  $\mu\epsilon\mu\epsilon$ )

Distance from free end (mm)

Distance from free end (mm)

(a) Sample failure mode

(b) Bond stress-distance curves

- (c) Slip-distance curves
- (d) Bond stress-slip curves
- (e) Strain gauge-distance curves.
- (f) Load-strain curves
- (g) Load-extension curve

Figure 4-51: Variation of stress, strain, slip and load of 60-R-L2 specimen

107

0

0

0.6

0.6

1.2

1.2

1.8

1.8

2.4

2.4

3

3

0

0

25

25

50

50

75

75

100

100

125

125

150

150

175

175

Shear Stress (MPa)

Shear Stress (MPa)

Distance from loaded end (mm)

Distance from loaded end (mm)

0

0

0.02

0.02

0.04

0.04

0.06

0.06

0.08

0.08

0.1

0.1

0

0

25

25

50

50

75

75

100

100

125

125

150

150

175

175

Slip (mm)

Slip mm)

Distance from loaded end (mm)

Distance from loaded end (mm)

0

0

0.6

0.6

1.2

1.2

1.8

1.8

2.4

2.4

3

3

0

0

0.02

0.02

0.04

0.04

0.06

0.06

0.08

0.08

0.1

0.1

Shear Stress (MPa)

Slip (mm)

Slip (mm)

0

0

300

300

600

600

900

900

1200

1200

1500

1500

0

0

25

25

50

50

75

75

100

100

125

125

150

150

175

175

Strain (

Strain  $\mu\mu\epsilon$ )

Distance from free end (mm)

Distance from free end (mm)

0

0

4000

4000

8000

8000

12000

12000

16000

16000

20000

20000

0

0

400

400

800

800

1200

1200

1600

1600

2000

2000

Load (N)

Load N)

Strain (

Strain ( $\mu\text{m}\epsilon\epsilon$ )

SG 1

SG 1

SG 2

SG 2

SG 3

SG 3

SG 4

SG 4

0

0

4000

4000

8000

8000

12000

12000

16000

16000

20000

20000

0

0

0.8

0.8

1.6

1.6

2.4

2.4

3.2

3.2

4

4

Load (N)

Extension (mm)

Extension (mm)

(a) Sample failure mode

(b) Bond stress-distance curves

(c) Slip-distance curves

(d) Bond stress-slip curves

(e) Strain gauge-distance curves.

(f) Load-strain curves

(g) Load-extension curve

Figure 4-52: Variation of stress, strain, slip and load of 60-R-L3 specimen

108

0

0

0.02

0.02

0.04

0.04

0.06

0.06

0.08

0.08

0.1

0.1

0

0

50

50

100

100

150

150

200

200

250

250

Slip (mm)

Slip (mm)

Distance from loaded end (mm)

Distance from loaded end (mm)

0

0

0.8

0.8

1.6

1.6

2.4

2.4

3.2

3.2

4

4

0

0

50

50

100

100

150

150

200

200

250

250

Shear Stress (MPa)

Shear Stress MPa)

Distance from loaded end (mm)

Distance from loaded end (mm)

-0.8

-0.8

0

0

0.8

0.8

1.6

1.6

2.4

2.4

3.2

3.2

0

0

0.025

0.025

0.05

0.05

0.075

0.075

0.1

0.1

Shear Stress (MPa)

Slip (mm)

Slip (mm)

0

0

300

300

600

600

900

900

1200

1200

1500

1500

0

0

50

50

100

100

150

150

200

200

250

250

Strain (

Strain  $\mu\epsilon\mu\epsilon$ )

Distance from free end (mm)

Distance from free end (mm)

0

0

4000

4000

8000

8000

12000

12000

16000

16000

20000

20000

0

0

600

600

1200

1200

1800

1800

2400

2400

3000

3000

Load (N)

Load N)

Strain (

Strain ( $\mu\text{m}\epsilon\epsilon$ )

0

0

4000

4000

8000

8000

12000

12000

16000

16000

20000

20000

0

0

0.7

0.7

1.4

1.4

2.1

2.1

2.8

2.8

3.5

3.5

Load (N)

Extension (mm)

Extension (mm)

(a) Sample failure mode

(b) Bond stress-distance curves

(c) Slip-distance curves

(d) Bond stress-slip curves

(e) Strain gauge-distance curves.

(f) Load-strain curves

(g) Load-extension curve

Figure 4-53: Variation of stress, strain, slip and load of 60-R-L4 specimen

109

0

0

0.0008

0.0008

0.0016

0.0016

0.0024

0.0024

0.0032

0.0032

0.004

0.004

0

0

10

10

20

20

30

30

40

40

50

50

60

60

Slip (mm)

Slip (mm)

Distance from loaded end (mm)

Distance from loaded end (mm)

0

0

0.05

0.05

0.1

0.1

0.15

0.15

0.2

0.2

0.25

0.25

0

0

10

10

20

20

30

30

40

40

50

50

60

60

Shear Stress (MPa)

Shear Stress MPa)

Distance from loaded end (mm)

Distance from loaded end (mm)

0

0

0.05

0.05

0.1

0.1

0.15

0.15

0.2

0.2

0.25

0.25

0

0

0.0008

0.0008

0.0016

0.0016

0.0024

0.0024

0.0032

0.0032

0.004

0.004

Shear Stress (MPa)

Slip (mm)

Slip (mm)

0

0

5

5

10

10

15

15

20

20

25

25

0

0

10

10

20

20

30

30

40

40

50

50

60

60

Strain (

Strain  $\mu\epsilon\mu\epsilon$ )

Distance from free end (mm)

Distance from free end (mm)

0

0

500

500

1000

1000

1500

1500

2000

2000

2500

2500

0

0

35

35

70

70

105

105

140

140

Load (N)

Load N)

Strain (

Strain ( $\mu\text{m}\epsilon\epsilon$ )

SG 1

SG 1

SG 2

SG 2

SG 3

SG 3

0

0

500

500

1000

1000

1500

1500

2000

2000

2500

2500

0

0

0.6

0.6

1.2

1.2

1.8

1.8

2.4

2.4

3

3

Load (N)

Extension (mm)

Extension (mm)

- (a) Sample failure mode
- (b) Bond stress-distance curves
- (c) Slip-distance curves
- (d) Bond stress-slip curves
- (e) Strain gauge-distance curves.
- (f) Load-strain curves
- (g) Load-extension curve

Figure 4-54: Variation of stress, strain, slip and load of 60-P-L1 specimen

110

0

0

0.15

0.15

0.3

0.3

0

0

0.0025

0.0025

0.005

0.005

0.0075

0.0075

0.01

0.01

0.0125

0.0125

Shear Stress (MPa)

Shear Stress (MPa)

Slip (mm)

Slip (mm)

0

0

1000

1000

2000

2000

3000

3000

4000

4000

5000

5000

0

0

0.25

0.25

0.5

0.5

0.75

0.75

1

1

1.25

1.25

Load (N)

Load N)

Extension (mm)

Extension (mm)

0

0

0.0025

0.0025

0.005

0.005

0.0075

0.0075

0.01

0.01

0.0125

0.0125

0

0

20

20

40

40

60

60

80

80

100

100

120

120

Slip (mm)

Slip mm)

Distance from loaded end (mm)

Distance from loaded end (mm)

0

0

0.15

0.15

0.3

0.3

0.45

0.45

0.6

0.6

0.75

0.75

0

0

20

20

40

40

60

60

80

80

100

100

120

120

Shear Stress (MPa)

Distance from loaded end (mm)

Distance from loaded end (mm)

0

0

30

30

60

60

90

90

120

120

150

150

0

0

20

20

40

40

60

60

80

80

100

100

120

120

Strain (

Strain  $\mu\epsilon$ )

Distance from free end (mm)

Distance from free end (mm)

0

0

1000

1000

2000

2000

3000

3000

4000

4000

5000

5000

0

0

80

80

160

160

240

240

320

320

400

400

Load (N)

Strain (

Strain ( $\mu\text{m}$ )m)

SG 1

SG 1

SG 2

SG 2

SG 3

SG 3

(a) Sample failure mode

(b) Bond stress-distance curves

(c) Slip-distance curves

(d) Bond stress-slip curves

(e) Strain gauge-distance curves.

(f) Load-strain curves

(g) Load-extension curve

Figure 4-55: Variation of stress, strain, slip and load of 60-P-L2 specimen

111

0

0

0.006

0.006

0.012

0.012

0.018

0.018

0.024

0.024

0.03

0.03

0

0

25

25

50

50

75

75

100

100

125

125

150

150

175

175

Slip (mm)

Slip (mm)

Distance from loaded end (mm)

Distance from loaded end (mm)

0

0

0.2

0.2

0.4

0.4

0.6

0.6

0.8

0.8

1

1

0

0

25

25

50

50

75

75

100

100

125

125

150

150

175

175

Shear Stress (MPa)

Shear Stress MPa)

Distance from loaded end (mm)

Distance from loaded end (mm)

0

0

0.2

0.2

0.4

0.4

0.6

0.6

0.8

0.8

1

1

0

0

0.006

0.006

0.012

0.012

0.018

0.018

0.024

0.024

0.03

0.03

Shear Stress (MPa)

Slip (mm)

Slip (mm)

0

0

100

100

200

200

300

300

400

400

500

500

0

0

25

25

50

50

75

75

100

100

125

125

150

150

175

175

Strain (

Strain  $\mu\epsilon\mu\epsilon$ )

Distance from free end (mm)

Distance from free end (mm)

0

0

1200

1200

2400

2400

3600

3600

4800

4800

6000

6000

0

0

100

100

200

200

300

300

400

400

500

500

Load (N)

Load N)

Strain (

Strain ( $\mu\mu\epsilon\epsilon$ )

SG 1

SG 1

SG 2

SG 2

SG 3

SG 3

SG 4

SG 4

0

0

1200

1200

2400

2400

3600

3600

4800

4800

6000

6000

0

0

0.4

0.4

0.8

0.8

1.2

1.2

1.6

1.6

2

2

Load (N)

Extension (mm)

Extension (mm)

(a) Sample failure mode

- (b) Bond stress-distance curves
- (c) Slip-distance curves
- (d) Bond stress-slip curves
- (e) Strain gauge-distance curves.
- (f) Load-strain curves
- (g) Load-extension curve

Figure 4-56: Variation of stress, strain, slip and load of 60-P-L3 specimen

112

0

0

0.012

0.012

0.024

0.024

0.036

0.036

0.048

0.048

0.06

0.06

0

0

50

50

100

100

150

150

200

200

250

250

Slip (mm)

Slip (mm)

Distance from loaded end (mm)

Distance from loaded end (mm)

0

0

0.25

0.25

0.5

0.5

0.75

0.75

1

1

1.25

1.25

0

0

50

50

100

100

150

150

200

200

250

250

Shear Stress (MPa)

Shear Stress MPa)

Distance from loaded end (mm)

Distance from loaded end (mm)

0

0

0.25

0.25

0.5

0.5

0.75

0.75

1

1

1.25

1.25

0

0

0.012

0.012

0.024

0.024

0.036

0.036

0.048

0.048

0.06

0.06

Shear Stress (MPa)

Slip (mm)

Slip (mm)

0

0

120

120

240

240

360

360

480

480

600

600

0

0

50

50

100

100

150

150

200

200

250

250

Strain (

Strain  $\mu\epsilon$ )

Distance from free end (mm)

Distance from free end (mm)

0

0

1800

1800

3600

3600

5400

5400

7200

7200

9000

9000

0

0

140

140

280

280

420

420

560

560

700

700

Load (N)

Load N)

Strain (

Strain ( $\mu\mu\epsilon\epsilon$ )

0

0

1600

1600

3200

3200

4800

4800

6400

6400

8000

8000

0

0

0.4

0.4

0.8

0.8

1.2

1.2

1.6

1.6

2

2

Load (N)

Extension (mm)

Extension (mm)

- (a) Sample failure mode
- (b) Bond stress-distance curves
- (c) Slip-distance curves
- (d) Bond stress-slip curves
- (e) Strain gauge-distance curves.
- (f) Load-strain curves
- (g) Load-extension curve

Figure 4-57: Variation of stress, strain, slip and load of 60-P-L4 specimen

113

Table 4-4: Summary of results for specimens with  $f_c'$  of 60 MPa

Specimen Identification

AA/CFRP Plate

Cube compressive strength (MPa)

Failure Load (KN)

\*Failure

mode

Plate type

Width (mm)

Thickness (mm)

Bonded length (mm)

60-CF-L1

CFRP

50

1.4

50

60

7.77

DA+DB-P

60-CF-L1

CFRP

50

1.4

50

60

5.03

DB-P

60-CF-L2

CFRP

50

1.4

100

60

12.52

DB-C+CS+FR

60-CF-L2

CFRP

50

1.4

100

60

11.96

DB-C+DA

60-CF-L3

CFRP

50

1.4

150

60

14.36

DB-C+CS

60-CF-L3

CFRP

50

1.4

150

60

16.33

DB-C+CS

60-CF-L4

CFRP

50

1.4

200

60

15.54

DB-C+DB-P

60-CF-L4

CFRP

50

1.4

200

60

10.21

DB-P+FR

60-R-L1

AA-R

50

3.0

50

60

6.80

DA

60-R-L1

AA-R

50

3.0

50

60

14.09

DA+CS

60-R-L2

AA-R

50

3.0

100

60

16.83

DB-C+CS

60-R-L2

AA-R

50

3.0

100

60

14.29

DB-C+CS

60-R-L3

AA-R

50

3.0

150

60

16.82

DB-C+CS

60-R-L3

AA-R

50

3.0

150

60

14.75

DB-C+CS

60-R-L4

AA-R

50

3.0

200

60

16.94

DB-C

60-R-L4

AA-R

50

3.0

200

60

13.89

DB-C+CS

60-P-L1

AA-P

50

3.0

50

60

0.50

DB-P

60-P-L1

AA-P

50

3.0

50

60

2.19

DB-P

60-P-L2

AA-P

50

3.0

100

60

3.92

DB-P

60-P-L2

AA-P

50

3.0

100

60

0.35

DB-P

60-P-L3

AA-P

50

3.0

150

60

5.10

DB-P

60-P-L3

AA-P

50

3.0

150

60

2.24

DB-P

60-P-L4

AA-P

50

3.0

200

60

7.10

DB-P

60-P-L4

AA-P

50

3.0

200

60

7.07

DB-P

\*Failure mode: DB-C: Debonding in concrete, DB-P: Plate Debonding (Plate/adhesive interface separation), CS: Concrete spalling, DA: Adhesive debonding (Adhesive/concrete interface separation), FR: Fiber rupture.

4.4.1 CFRP plate failure. The failure mode for specimens with CFRP plates mainly takes place in the concrete adhesive interface accompanied by concrete spalling in some cases. 4.4.2 AA scratched plate failure. The failure mode for this type of plate is similar to

that of the CFRP. However, the concrete spalling in this case takes place in all the

specimens due to scratched AA plate rough surface which causes concentration of

stresses in the vicinity of the loaded end. 4.4.3 AA plain plate failure. The failure mode for AA plain plates in all specimens takes place in the plate adhesive interface due to the weak bond between the plate plain

surface and the adhesive. There is no concrete spalling in this case due to relatively

high concrete strength of this group.

114

#### 4.5 Results Discussion

In this section, the results obtained from the experimental program were summarized. Based on the factors considered in this research, i.e., concrete strength, bond length, and surface roughness of the AA plates, the results have been categorized into the following groups:

4.5.1 Concrete strength - prisms with CFRP plates. Figure 4-58 illustrates the load extension curves for prisms strengthened with CFRP plates. Constant bond length with different concrete strength results were plotted. It is observed that higher loads were obtained with the increase in concrete strength for all bonded lengths.

Figure 4-58: Effect of BL and  $f_{cu}$  on load-extension relationship for CFRP

0

0

3000

3000

6000

6000

9000

9000

12000

12000

15000

15000

0

0

1.2

1.2

2.4

2.4

3.6

3.6

4.8

4.8

Load (N)

Load (N)

Extension (mm)

Extension (mm)

CFRP (

CFRP (BL of 100mmBL of 100mm))

20 MPa

20 MPa

30 MPa

30 MPa

40 MPa

40 MPa

60 MPa

60 MPa

0

0

4000

4000

8000

8000

12000

12000

16000

16000

20000

20000

0

0

0.8

0.8

1.6

1.6

2.4

2.4

3.2

3.2

Load (N)

Extension (mm)

Extension (mm)

CFRP (BL

CFRP (BL of of 5050mmmm))

20 MPa

20 MPa

30 MPa

30 MPa

40 MPa

40 MPa

60 MPa

60 MPa

0

0

4000

4000

8000

8000

12000

12000

16000

16000

20000

20000

0

0

1.2

1.2

2.4

2.4

3.6

3.6

4.8

4.8

Load (N)

Extension (mm)

Extension (mm)

CFRP (BL

CFRP (BL of 150mm of 150mm))

20 MPa

20 MPa

30 MPa

30 MPa

40 MPa

40 MPa

60 MPa

60 MPa

0

0

4000

4000

8000

8000

12000

12000

16000

16000

20000

20000

0

0

0.8

0.8

1.6

1.6

2.4

2.4

3.2

3.2

Load (N)

Extension (mm)

Extension (mm)

CFRP (BL

CFRP (BL of of 200200mmmm))

20 MPa

20 MPa

30 MPa

30 MPa

40 MPa

40 MPa

60 MPa

60 MPa

115

Figure 4-59 shows the variation of failure load, maximum bond stress, maximum slip and ultimate slip with concrete compressive strength for four different sets of bonded lengths. It is observed that each of these factors increases with the increase in concrete compressive strength for constant bond lengths. In addition, failure load, maximum slip and ultimate slip also increase with the increase in bond length. It

has also been observed that the bonded length has no effect on the maximum bond stress of the plate-concrete interface.

0.0

0.0

0.5

0.5

1.0

1.0

1.5

1.5

2.0

2.0

2.5

2.5

3.0

3.0

3.5

3.5

4.0

4.0

4.5

4.5

L1 = 50 mm

L1 = 50 mm

L2 = 100 mm

L2 = 100 mm

L3 = 150 mm

L3 = 150 mm

L4 = 200 mm

L4 = 200 mm

Max bond stress (

Max bond stress ((MPa)MPa)

CFRP plates

CFRP plates

fcu = 20 MPa

fcu = 20 MPa

fcu = 30 MPa

fcu = 30 MPa

fcu = 40 MPa

fcu = 40 MPa

fcu = 60 MPa

fcu = 60 MPa

0

0

2

2

4

4

6

6

8

8

10

10

12

12

14

14

16

16

18

18

L1 = 50 mm

L1 = 50 mm

L2 = 100 mm

L2 = 100 mm

L3 = 150 mm

L3 = 150 mm

L4 = 200 mm

L4 = 200 mm

Failure load (KN)

Failure load (KN)

CFRP plates

CFRP plates

$f_{cu} = 20 \text{ MPa}$

$f_{cu} = 20 \text{ MPa}$

$f_{cu} = 30 \text{ MPa}$

$f_{cu} = 30 \text{ MPa}$

$f_{cu} = 40 \text{ MPa}$

$f_{cu} = 40 \text{ MPa}$

$f_{cu} = 60 \text{ MPa}$

$f_{cu} = 60 \text{ MPa}$

0.00

0.00

0.01

0.01

0.02

0.02

0.03

0.03

0.04

0.04

0.05

0.05

0.06

0.06

0.07

0.07

L1 = 50 mm

L1 = 50 mm

L2 = 100 mm

L2 = 100 mm

L3 = 150 mm

L3 = 150 mm

L4 = 200 mm

L4 = 200 mm

Max slip (

slip CFRP plates

CFRP plates

fcu = 20 MPa

fcu = 20 MPa

fcu = 30 MPa

fcu = 30 MPa

fcu = 40 MPa

fcu = 40 MPa

fcu = 60 MPa

$f_{cu} = 60 \text{ MPa}$

0.00

0.00

0.01

0.01

0.02

0.02

0.03

0.03

0.04

0.04

0.05

0.05

0.06

0.06

0.07

0.07

0.08

0.08

0.09

0.09

0.10

0.10

L1 = 50 mm

L1 = 50 mm

L2 = 100 mm

L2 = 100 mm

L3 = 150 mm

L3 = 150 mm

L4 = 200 mm

L4 = 200 mm

Ultimate slip (

Ultimate mmmm))

CFRP plates

CFRP plates

fcu = 20 MPa

fcu = 20 MPa

fcu = 30 MPa

fcu = 30 MPa

fcu = 40 MPa

fcu = 40 MPa

fcu = 60 MPa

fcu = 60 MPa

Figure 4-59: Variation of load, bond stress and slip with BL and fcu for CFRP

(a) Failure load variation with concrete strength

(b) Bond stress variation with concrete strength

(c) Max. slip variation with concrete strength

(d) Ult. slip variation with concrete strength

116

4.5.2 Bond length- prisms with CFRP plates. Figure 4-60 Shows the load extension curves for prisms strengthened with CFRP plates. Constant concrete strength with different bond length results were plotted. It is observed that higher loads are obtained with increased bond length up to 150 mm. this indicates that the effective bond length falls in the range of (120-170) mm for the CFRP plates.

Figure 4-60: Effect of BL and fcu on load-extension relationship for CFRP

0

0

3000

3000

6000

6000

9000

9000

12000

12000

15000

15000

0

0

1.2

1.2

2.4

2.4

3.6

3.6

4.8

4.8

Load (N)

Load (N)

Extension (mm)

Extension (mm)

CFRP (40 MPA)

CFRP (40 MPA)

50mm

50mm

100mm

100mm

150mm

150mm

200mm

200mm

0

0

4000

4000

8000

8000

12000

12000

16000

16000

20000

20000

0

0

1

1

2

2

3

3

4

4

Load (N)

Extension (mm)

Extension (mm)

CFRP (60 MPA)

CFRP (60 MPA)

50mm

50mm

100mm

100mm

150mm

150mm

200mm

200mm

0

0

4000

4000

8000

8000

12000

12000

16000

16000

20000

20000

0

0

1.2

1.2

2.4

2.4

3.6

3.6

4.8

4.8

Load (N)

Extension (mm)

Extension (mm)

CFRP (30 MPA)

CFRP (30 MPA)

50mm

50mm

100mm

100mm

150mm

150mm

200mm

200mm

0

0

2000

2000

4000

4000

6000

6000

8000

8000

10000

10000

0

0

0.6

0.6  
 1.2  
 1.2  
 1.8  
 1.8  
 2.4  
 2.4  
 Load (N)  
 Extension (mm)  
 Extension (mm)  
 CFRP (20 MPA)  
 CFRP (20 MPA)  
 50mm  
 50mm  
 100mm  
 100mm  
 150mm  
 150mm  
 200mm  
 200mm  
 117

Figure 4-61 shows the variation of failure load, maximum bond stress, maximum slip and ultimate slip with the plate bonded length for four different sets of concrete strength. It is observed that the failure load increases with the increase in bond length up to 150 mm bond length. Hence, the effective bond length of CFRP plates lies between (120-170) mm. In addition, failure load, maximum bond stress, maximum slip and ultimate slip also increase with the increase in concrete compressive strength. It has also been observed that the bonded length has no effect on the maximum bond stress of the plate-concrete interface.

Figure 4-61: Variation of load, bond stress and slip with BL and fcu for CFRP

0  
0

2

2

4

4

6

6

8

8

10

10

12

12

14

14

16

16

18

18

fcu = 20 MPa

fcu = 20 MPa

fcu = 30 MPa

fcu = 30 MPa

fcu = 40 MPa

fcu = 40 MPa

fcu = 60 MPa

fcu = 60 MPa

Failure load (KN)

Failure load (KN)

CFRP plates

CFRP plates

L1 = 50 mm

L1 = 50 mm

L2 = 100 mm

L2 = 100 mm

L3 = 150 mm

L3 = 150 mm

L4 = 200 mm

L4 = 200 mm

0.00

0.00

0.01

0.01

0.02

0.02

0.03

0.03

0.04

0.04

0.05

0.05

0.06

0.06

0.07

0.07

$f_{cu} = 20 \text{ MPa}$

$f_{cu} = 20 \text{ MPa}$

$f_{cu} = 30 \text{ MPa}$

$f_{cu} = 30 \text{ MPa}$

$f_{cu} = 40 \text{ MPa}$

$f_{cu} = 40 \text{ MPa}$

$f_{cu} = 60 \text{ MPa}$

$f_{cu} = 60 \text{ MPa}$

Max slip (

Max slip CFRP plates

CFRP plates

L1 = 50 mm

L1 = 50 mm

L2 = 100 mm

L2 = 100 mm

L3 = 150 mm

L3 = 150 mm

L4 = 200 mm

L4 = 200 mm

0.00

0.00

0.02

0.02

0.04

0.04

0.06

0.06

0.08

0.08

0.10

0.10

0.12

0.12

fcu = 20 MPa

fcu = 20 MPa

fcu = 30 MPa

fcu = 30 MPa

fcu = 40 MPa

fcu = 40 MPa

fcu = 60 MPa

fcu = 60 MPa

Ultimate slip (

Ultimate mmmm))

CFRP plates

CFRP plates

L1 = 50 mm

L1 = 50 mm

L2 = 100 mm

L2 = 100 mm

L3 = 150 mm

L3 = 150 mm

L4 = 200 mm

L4 = 200 mm

0.0

0.0

0.5

0.5

1.0

1.0

1.5

1.5

2.0

2.0

2.5

2.5

3.0

3.0

3.5

3.5

4.0

4.0

fcu = 20 MPa

fcu = 20 MPa

fcu = 30 MPa

fcu = 30 MPa

fcu = 40 MPa

fcu = 40 MPa

fcu = 60 MPa

fcu = 60 MPa

Max. bond stress (MPa)

Max. bond stress MPa)

CFRP plates

CFRP plates

L1 = 50 mm

L1 = 50 mm

L2 = 100 mm

L2 = 100 mm

L3 = 150 mm

L3 = 150 mm

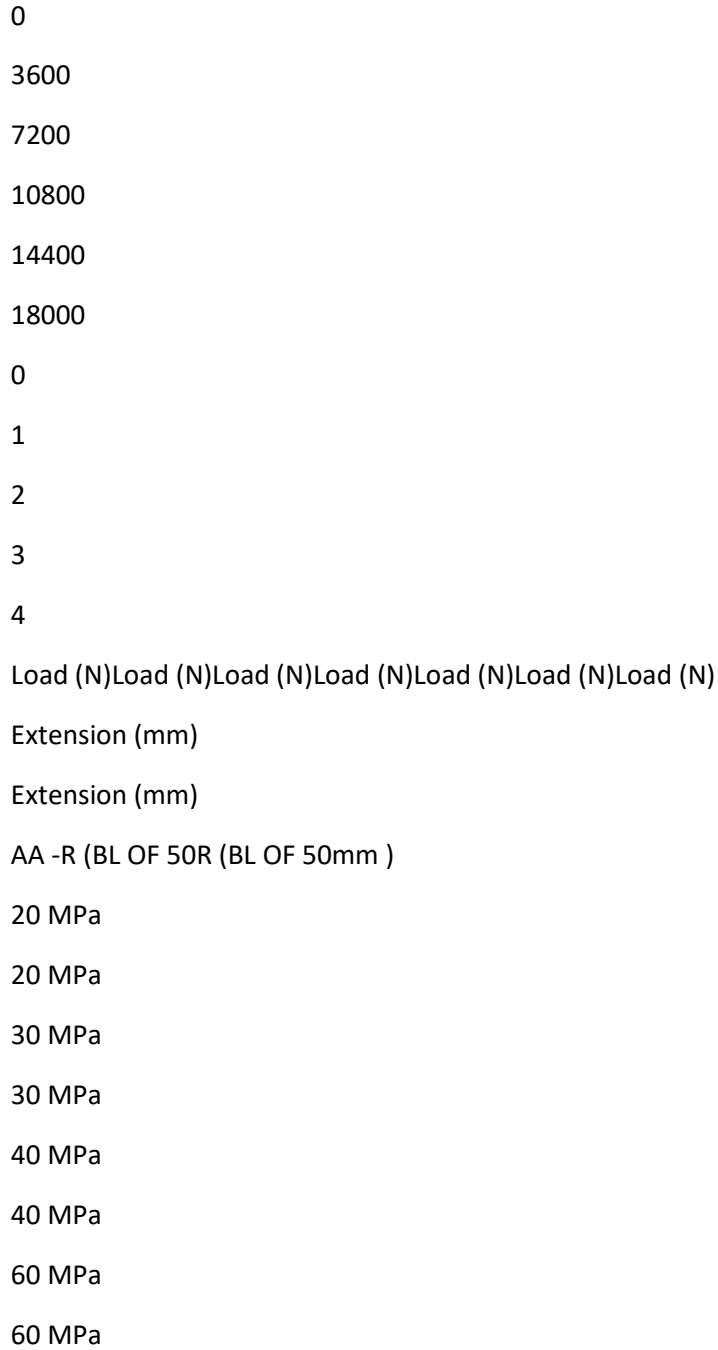
L4 = 200 mm

L4 = 200 mm

- (a) Failure load variation with concrete strength
- (b) Bond stress variation with concrete strength
- (c) Max. slip variation with concrete strength
- (d) Ult. slip variation with concrete strength

118

Figure 4-62: Effect of BL and fcu on load-extension relationship for AA-R



0

4000

8000

12000

16000

20000

0

1

2

3

4

Load (N)Load (N)Load (N)Load (N)Load (N)Load (N)Load (N)

Extension (mm)

Extension (mm)

AA -R (BL OF 100R (BL OF 100mm )

20 MPa

20 MPa

30 MPa

30 MPa

40 MPa

40 MPa

60 MPa

60 MPa

0

5000

10000

15000

20000

25000

0

1.2

2.4

3.6

4.8

Load (N)Load (N)Load (N)Load (N)Load (N)Load (N)Load (N)

Extension (mm)

Extension (mm)

AA -R (BL R (BL of 200 mm )

20 MPa

20 MPa

30 MPa

30 MPa

40 MPa

40 MPa

60 MPa

60 MPa

0

5000

10000

15000

20000

25000

0

1.2

2.4

3.6

4.8

Load (N)Load (N)Load (N)Load (N)Load (N)Load (N)Load (N)

Extension (mm)

Extension (mm)

AA -R (BL R (BL of 150 mm )

20 MPa

20 MPa

30 MPa

30 MPa

40 MPa

40 MPa

60 MPa

60 MPa

4.5.3 Concrete strength - prisms with AA scratched plates. The load extension curves for prisms strengthened with AA scratched plates are displayed in Figure 4-62. Constant bond length with different concrete strength results were plotted. It is observed

from Figure 4-62 that higher loads were obtained with increased concrete strength.

119

Figure 4-63 shows the variation of failure load, maximum bond stress, maximum slip and ultimate slip with concrete compressive strength for four different sets of bonded lengths. It is observed that each of these factors increases with the increase in concrete compressive strength for constant bond lengths. In addition, failure load, maximum slip and ultimate slip also increase with the increase in bond length. It is also observed that the bonded length has no effect on the maximum bond stress of the plate-concrete interface.

Figure 4-63: Variation of load, bond stress and slip with BL and fcu for AA-R

0

0

2

2

4

4

6

6

8

8

10

10

12

12

14

14

16

16

18

18

L1 = 50 mm

L1 = 50 mm

L2 = 100 mm

L2 = 100 mm

L3 = 150 mm

L3 = 150 mm

L4 = 200 mm

L4 = 200 mm

Failure load (KN)

Failure load (KN)

AA scratched plates

AA scratched plates

$f_{cu} = 20 \text{ MPa}$

$f_{cu} = 20 \text{ MPa}$

$f_{cu} = 30 \text{ MPa}$

$f_{cu} = 30 \text{ MPa}$

$f_{cu} = 40 \text{ MPa}$

$f_{cu} = 40 \text{ MPa}$

$f_{cu} = 60 \text{ MPa}$

$f_{cu} = 60 \text{ MPa}$

0.0

0.0

0.5

0.5

1.0

1.0

1.5

1.5

2.0

2.0

2.5

2.5

3.0

3.0

3.5

3.5

4.0

4.0

$L1 = 50 \text{ mm}$

$L1 = 50 \text{ mm}$

$L2 = 100 \text{ mm}$

$L2 = 100 \text{ mm}$

$L3 = 150 \text{ mm}$

$L3 = 150 \text{ mm}$

$L4 = 200 \text{ mm}$

$L4 = 200 \text{ mm}$

Max. bond stress (MPa)

Max. bond stress MPa)

AA scratched plates

AA scratched plates

fcu = 20 MPa

fcu = 20 MPa

fcu = 30 MPa

fcu = 30 MPa

fcu = 40 MPa

fcu = 40 MPa

fcu = 60 MPa

fcu = 60 MPa

0.000

0.000

0.005

0.005

0.010

0.010

0.015

0.015

0.020

0.020

0.025

0.025

0.030

0.030

0.035

0.035

0.040

0.040

0.045

0.045

L1 = 50 mm

L1 = 50 mm

L2 = 100 mm

L2 = 100 mm

L3 = 150 mm

L3 = 150 mm

L4 = 200 mm

L4 = 200 mm

Max slip (mm)

Max slip mm)

AA scratched plates

AA scratched plates

fcu = 20 MPa

fcu = 20 MPa

fcu = 30 MPa

fcu = 30 MPa

fcu = 40 MPa

fcu = 40 MPa

fcu = 60 MPa

fcu = 60 MPa

0.00

0.00

0.01

0.01

0.02

0.02

0.03

0.03

0.04

0.04

0.05

0.05

0.06

0.06

0.07

0.07

0.08

0.08

0.09

0.09

L1 = 50 mm

L1 = 50 mm

L2 = 100 mm

L2 = 100 mm

L3 = 150 mm

L3 = 150 mm

L4 = 200 mm

L4 = 200 mm

L<sub>ultimate slip</sub> (mm)

L<sub>ultimate AA scratched plates</sub>

AA scratched plates

f<sub>cu</sub> = 20 MPa

f<sub>cu</sub> = 20 MPa

f<sub>cu</sub> = 30 MPa

f<sub>cu</sub> = 30 MPa

fcu = 40 MPa

fcu = 40 MPa

fcu = 60 MPa

fcu = 60 MPa

(a) Failure load variation with concrete strength

(b) Bond stress variation with concrete strength

(c) Max. slip variation with concrete strength

(d) Ult. slip variation with concrete strength

120

4.5.4 Bond length- prisms with AA scratched plates. The load extension curves for prisms strengthened with AA scratched plates are shown in Figure 4-64. Constant concrete strength with different bond length results were plotted. It is observed that in general higher loads are obtained with increased bond length up to 150 mm, i.e., the effective bond length lies between (120-180) mm. This indicates that the effective bond length is affected by the surface roughness of the AA plates. Different AA surface roughness will result in changing the effective bond length.

Figure 4-64: Effect of BL and fcu on load-extension relationship for AA-R

0

0

5000

5000

10000

10000

15000

15000

20000

20000

25000

25000

0

0

1.2

1.2

2.4

2.4

3.6

3.6

4.8

4.8

Load (N)

Load (N)

Extension (mm)

Extension (mm)

AA

AA--R (40 MPA)R (40 MPA)

50mm

50mm

100mm

100mm

150mm

150mm

200mm

200mm

0

0

4000

4000

8000

8000

12000

12000

16000

16000

20000

20000

0

0

1

1

2

2

3

3

4

4

Load (N)

Extension (mm)

Extension (mm)

AA

AA--R (60 MPA)R (60 MPA)

50mm

50mm

100mm

100mm

150mm

150mm

200mm

200mm

0

0

5000

5000

10000

10000

15000

15000

20000

20000

25000

25000

0

0

1.5

1.5

3

3

4.5

4.5

6

6

Load (N)

Extension (mm)

Extension (mm)

AA

AA--R (30 MPA)R (30 MPA)

50mm

50mm

100mm

100mm

150mm

150mm

200mm

200mm

0

0

2500

2500

5000

5000

7500

7500

10000

10000

12500

12500

0

0

0.7

0.7

1.4

1.4

2.1

2.1

2.8

2.8

Load (N)

Extension (mm)

Extension (mm)

AA

AA--R (20 MPA)R (20 MPA)

50mm

50mm

100mm

100mm

150mm

150mm

200mm

200mm

121

Figure 4-65 shows the variation of failure load, maximum bond stress, maximum slip and ultimate slip with the plate bonded length for four different sets of concrete strength. It is observed that the failure load increases with the increase in bond length up to (150-200) mm bond length. Hence, the effective bond length of AA scratched plates lies between (120-180) mm. In addition, failure load, maximum bond stress, maximum slip and ultimate slip also increase with the increase in concrete compressive strength. It has also been observed that the bonded length has no effect on the maximum bond stress of the plate-concrete interface.

Figure 4-65: Variation of load, bond stress and slip with BL and fcu for AA-R

0.0

0.0

0.5

0.5

1.0

1.0

1.5

1.5

2.0

2.0

2.5

2.5

3.0

3.0

3.5

3.5

4.0

4.0

fcu = 20 MPa

fcu = 20 MPa

fcu = 30 MPa

fcu = 30 MPa

fcu = 40 MPa

fcu = 40 MPa

fcu = 60 MPa

fcu = 60 MPa

Max. bond stress (Mpa)

Max. bond stress (Mpa)

AA scratched plates

AA scratched plates

L1 = 50 mm

L1 = 50 mm

L2 = 100 mm

L2 = 100 mm

L3 = 150 mm

L3 = 150 mm

L4 = 200 mm

L4 = 200 mm

0

0

2

2

4

4

6

6

8

8

10

10

12

12

14

14

16

16

18

18

fcu = 20 MPa

fcu = 20 MPa

fcu = 30 MPa

fcu = 30 MPa

fcu = 40 MPa

fcu = 40 MPa

fcu = 60 MPa

fcu = 60 MPa

Failure load (KN)

Failure load KN)

AA scratched plates

AA scratched plates

L1 = 50 mm

L1 = 50 mm

L2 = 100 mm

L2 = 100 mm

L3 = 150 mm

L3 = 150 mm

L4 = 200 mm

L4 = 200 mm

0.00

0.00

0.01

0.01

0.02

0.02

0.03

0.03

0.04

0.04

0.05

0.05

0.06

0.06

0.07

0.07

0.08

0.08

0.09

0.09

fcu = 20 MPa

fcu = 20 MPa

fcu = 30 MPa

fcu = 30 MPa

fcu = 40 MPa

fcu = 40 MPa

fcu = 60 MPa

fcu = 60 MPa

Ltimate slip (mm)

Ltimate slip mm)

AA scratched plates

AA scratched plates

L1 = 50 mm

L1 = 50 mm

L2 = 100 mm

L2 = 100 mm

L3 = 150 mm

L3 = 150 mm

L4 = 200 mm

L4 = 200 mm

0.000

0.000

0.005

0.005

0.010

0.010

0.015

0.015

0.020

0.020

0.025

0.025

0.030

0.030

0.035

0.035

0.040

0.040

0.045

0.045

fcu = 20 MPa

fcu = 20 MPa

fcu = 30 MPa

fcu = 30 MPa

fcu = 40 MPa

fcu = 40 MPa

fcu = 60 MPa

fcu = 60 MPa

Max slip (

Max mmmm))

AA scratched plates

AA scratched plates

L1 = 50 mm

L1 = 50 mm

L2 = 100 mm

L2 = 100 mm

L3 = 150 mm

L3 = 150 mm

L4 = 200 mm

L4 = 200 mm

(a) Failure load variation with concrete strength

(b) Bond stress variation with concrete strength

(c) Max. slip variation with concrete strength

(d) Ult. slip variation with concrete strength

122

4.5.5 Comparison between AA scratched and CFRP plates. A comparison is made between the AA scratched and CFRP plates based on the average value of the results. Namely, failure load, maximum bond stress, maximum slip and ultimate slip average results were used in the comparison.

0

2

4

6

8

10

12

14

16

L1 = 50 mm

L1 = 50 mm

L2 = 100 mm

L2 = 100 mm

L3 = 150 mm

L3 = 150 mm

L4 = 200 mm

L4 = 200 mm

Failure load (KN) Failure load (KN) Failure load (KN) Failure load (KN) Failure load (KN) Failure load (KN) Failure load (KN) Failure load (KN)

AA scratched plates

AA scratched plates

CFRP plates

CFRP plates

0.0

0.5

1.0

1.5

2.0

2.5

3.0

L1 = 50 mm

L1 = 50 mm

L2 = 100 mm

L2 = 100 mm

L3 = 150 mm

L3 = 150 mm

L4 = 200 mm

L4 = 200 mm

Max. bond stress (MPa)Max. bond stress (MPa)Max. bond stress (MPa)Max. bond stress (MPa)Max.  
bond stress (MPa)Max. bond stress (MPa)Max. bond stress (MPa)Max. bond stress (MPa)Max. bond  
stress (MPa)Max. bond stress (MPa)Max. bond stress (MPa)Max. bond stress (MPa)

AA scratched plates

AA scratched plates

CFRP plates

CFRP plates

0.00

0.01

0.01

0.02

0.02

0.03

0.03

0.04

L1 = 50 mm

L1 = 50 mm

L2 = 100 mm

L2 = 100 mm

L3 = 150 mm

L3 = 150 mm

L4 = 200 mm

L4 = 200 mm

Max slip (mm)Max slip (mm)Max slip (mm)Max slip (mm)Max slip (mm)Max slip (mm)Max slip (mm)

AA scratched plates

AA scratched plates

CFRP plates

CFRP plates

0.00

0.01

0.02

0.03

0.04

0.05

0.06

0.07

0.08

L1 = 50 mm

L1 = 50 mm

L2 = 100 mm

L2 = 100 mm

L3 = 150 mm

L3 = 150 mm

L4 = 200 mm

L4 = 200 mm

L<sub>ultimate slip</sub> (mm) L<sub>ultimate slip</sub> (mm) L<sub>ultimate slip</sub> (mm) L<sub>ultimate slip</sub> (mm) L<sub>ultimate slip</sub> (mm) L<sub>ultimate slip</sub> (mm)  
(mm) L<sub>ultimate slip</sub> (mm) L<sub>ultimate slip</sub> (mm)

AA scratched plates

AA scratched plates

CFRP plates

CFRP plates

(a) Failure load variation with concrete strength

(b) Bond stress variation with concrete strength

(c) Max. slip variation with concrete strength

(d) Ult. slip variation with concrete strength

Figure 4-66: Variation of bond slip parameters with BL for CFRP and AA-R 4.5.5.1 Average concrete strength. Average concrete strength results were plotted with for sets of bond length. As shown in Figure 4-66 it can be clearly seen that all parameters except for the maximum bond stress increase with the increase in bond length. Moreover, higher results for the increasing parameters were observed in the AA scratched plates compared to the CFRP plates.

123

Table 4-5, Table 4-6 and Table 4-7 illustrate the performance of AA plates compared to the CFRP plates using average concrete strength with constant bond length. As shown, AA scratched plates exhibits higher results than CFRP plates.

Table 4-5: Variation of failure load and bond slip parameters with BL

Bonded Length (mm)

Plate Type

AA Scratched Plates (Avg.)

CFRP Plates (Avg.)

CFRP/ CFRP<sub>L1</sub> ratio

*P<sub>ult</sub>*

$\tau_{max}$

$S_{max}$

$S_{ult}$

$P_{ult}$

$\tau_{max}$

$S_{max}$

$S_{ult}$

$P_{ult}$

$\tau_{max}$

$S_{max}$

$S_{ult}$

L1=50

6.623

1.970

0.010

0.018

6.270

2.178

0.005

0.017

1.0

1.0

1.0

1.0

L2=100

10.729

1.865

0.019

0.043

9.921

1.894

0.016

0.041

1.582

0.87

3.032

2.397

L3=150

13.691

1.994

0.026

0.065

10.801

1.895

0.024

0.060

1.723

0.87

4.691

3.493

L4=200

14.316

2.441

0.032

0.071

11.684

2.217

0.030

0.062

1.863

1.018

5.748

3.639

Table 4-6: Variation of failure load and bond slip parameters with BL

Bonded Length (mm)

Plate Type

AA Scratched Plates (Avg.)

CFRP Plates (Avg.)

AA/AAL1 ratio

*Pult*

*$\tau_{max}$*

*Smax*

*Sult*

*Pult*

*$\tau_{max}$*

*Smax*

*Sult*

*Pult*

*$\tau_{max}$*

*Smax*

*Sult*

L1 =50

6.623

1.970

0.010

0.018

6.270

2.178

0.005

0.017

1.0

1.0

1.0

1.0

L2=100

10.729

1.865

0.019

0.043

9.921

1.894

0.016

0.041

1.620

0.947

1.919

2.331

L3=150

13.691

1.994

0.026

0.065

10.801

1.895

0.024

0.060

2.067

1.012

2.568

3.548

L4=200

14.316

2.441

0.032

0.071

11.684

2.217

0.030

0.062

2.162

1.239

3.179

3.858

Table 4-7: Variation of failure load and bond slip parameters with BL

Bonded Length (mm)

Plate Type

AA Scratched Plates (Avg.)

CFRP Plates (Avg.)

AA/CFRP ratio

*Pult*

$\tau_{max}$

*Smax*

*Sult*

*Pult*

$\tau_{max}$

*Smax*

*Sult*

*Pult*

$\tau_{max}$

*Smax*

*Sult*

L1 =50

6.623

1.970

0.010

0.018

6.270

2.178

0.005

0.017

1.056

0.904

1.960

1.069

L2=100

10.729

1.865

0.019

0.043

9.921

1.894

0.016

0.041

1.081

0.984

1.241

1.040

L3=150

13.691

1.994

0.026

0.065

10.801

1.895

0.024

0.060

1.268

1.052

1.073

1.086

L4=200

14.316

2.441

0.032

0.071

11.684

2.217

0.030

0.062

1.225

1.101

1.084

1.133

4.5.5.2 Average bond length. Average bond length results were plotted with four sets of concrete compressive strength. As shown in Figure 4-67 it can be clearly seen that all parameters increase with the increase in the concrete compressive strength. Moreover, higher results were observed in the AA scratched plates compared to the CFRP plates.

Figure 4-67: Variation of bond slip parameters with bond length

0

0

2

2

4

4

6

6

8

8

10

10

12

12

14

14

16

16

fcu = 20 MPa

fcu = 20 MPa

fcu = 30 MPa

fcu = 30 MPa

fcu = 40 MPa

fcu = 40 MPa

fcu = 60 MPa

fcu = 60 MPa

Failure load (KN)

Failure load (KN)

AA scratched plates

CFRP plates

CFRP plates

0.0

0.0

0.5

0.5

1.0

1.0

1.5

1.5

2.0

2.0

2.5

2.5

3.0

3.0

3.5

3.5

fcu = 20 MPa

fcu = 20 MPa

fcu = 30 MPa

fcu = 30 MPa

fcu = 40 MPa

fcu = 40 MPa

fcu = 60 MPa

fcu = 60 MPa

Max. bond stress (MPa)

Max. bond stress MPa)

AA scratched plates

CFRP plates

CFRP plates

0.000

0.000

0.005

0.005

0.010

0.010

0.015

0.015

0.020

0.020

0.025

0.025

0.030

0.030

0.035

0.035

0.040

0.040

fcu = 20 MPa

fcu = 20 MPa

fcu = 30 MPa

fcu = 30 MPa

fcu = 40 MPa

fcu = 40 MPa

fcu = 60 MPa

fcu = 60 MPa

Max slip (mm)

Max slip mm)

AA scratched plates

AA scratched plates

CFRP plates

CFRP plates

0.00

0.00

0.01

0.01

0.02

0.02

0.03

0.03

0.04

0.04

0.05

0.05

0.06

0.06

0.07

0.07

fcu = 20 MPa

fcu = 20 MPa

fcu = 30 MPa

$f_{cu} = 30 \text{ MPa}$

$f_{cu} = 40 \text{ MPa}$

$f_{cu} = 40 \text{ MPa}$

$f_{cu} = 60 \text{ MPa}$

$f_{cu} = 60 \text{ MPa}$

Ltimate slip (mm)

Ltimate AA scratched plates

AA scratched plates

CFRP plates

CFRP plates

(a) Failure load variation with concrete strength

(b) Bond stress variation with concrete strength

(c) Max. slip variation with concrete strength

(d) Ult. slip variation with concrete strength

125

Table 4-8, Table 4-9 and Table 4-10 illustrate the performance of AA plates compared to the CFRP plates using average bond length with constant concrete compressive strength. As shown, AA scratched plates exhibits higher results than CFRP plates.

Table 4-8: Variation of failure load and bond slip parameters with  $f_{cu}$

Concrete Strength

(MPa)

Plate Type

AA Scratched Plates (Avg.)

CFRP Plates (Avg.)

CFRP/CFRPL1 ratio

$P_{ult}$

$\tau_{max}$

$S_{max}$

$S_{ult}$

$P_{ult}$

$\tau_{max}$

$S_{max}$

$S_{ult}$

$P_{ult}$

$\tau_{max}$

$S_{max}$

$S_{ult}$

$f_{cu} = 20$

6.745

1.085

0.0125

0.032

6.674

1.041

0.0117

0.030

1.0

1.0

1.0

1.0

$f_{cu} = 30$

11.36

2.055

0.0188

0.046

10.068

1.886

0.0154

0.046

1.509

1.812

1.316

1.533

*fcu*= 40

12.365

2.634

0.0240

0.053

10.57

2.232

0.0156

0.044

1.584

2.144

1.333

1.467

*fcu*= 60

14.303

2.914

0.0341

0.064

12.058

2.873

0.0308

0.059

1.807

2.76

2.632

1.967

Table 4-9: Variation of failure load and bond slip parameters with  $f_{cu}$

Concrete Strength

(MPa)

Plate Type

AA Scratched Plates (Avg.)

CFRP Plates (Avg.)

AA/AAL1 ratio

$P_{ult}$

$\tau_{max}$

$S_{max}$

$S_{ult}$

$P_{ult}$

$\tau_{max}$

$S_{max}$

$S_{ult}$

$P_{ult}$

$\tau_{max}$

$S_{max}$

$S_{ult}$

$f_{cu} = 20$

6.745

1.085

0.0125

0.032

6.674

1.041

0.0117

0.030

1.0

1.0

1.0

1.0

*fcu*= 30

11.36

2.055

0.0188

0.046

10.068

1.886

0.0154

0.046

1.684

1.894

1.504

1.438

*fcu*= 40

12.365

2.634

0.0240

0.053

10.57

2.232

0.0156

0.044

1.833

2.428

1.92

1.656

$f_{cu} = 60$

14.303

2.914

0.0341

0.064

12.058

2.873

0.0308

0.059

2.121

2.686

2.728

2.0

Table 4-10: Variation of failure load and bond slip parameters with  $f_{cu}$

Concrete Strength

(MPa)

Plate Type

AA Scratched Plates (Avg.)

CFRP Plates (Avg.)

AA/CFRP ratio

$P_{ult}$

$\tau_{max}$

$S_{max}$

$S_{ult}$

$P_{ult}$

$\tau_{max}$

$S_{max}$

$S_{ult}$

*Pult*

*τmax*

*Smax*

*Sult*

*f<sub>cu</sub>*= 20

6.745

1.085

0.0125

0.032

6.674

1.041

0.0117

0.030

1.011

1.042

1.068

1.067

*f<sub>cu</sub>*= 30

11.36

2.055

0.0188

0.046

10.068

1.886

0.0154

0.046

1.128

1.09

1.221

1.0

*f<sub>cu</sub>*= 40

12.365

2.634

0.0240

0.053

10.57

2.232

0.0156

0.044

1.17

1.18

1.538

1.205

*f<sub>cu</sub>*= 60

14.303

2.914

0.0341

0.064

12.058

2.873

0.0308

0.059

1.186

1.014

1.107

1.085

126

4.5.6 Concrete strength - prisms with AA natural plates. Figure 4-68 shows the load extension curves for prisms strengthened with AA natural plates. Constant bond length with different concrete strength results was plotted. It is observed that higher loads are not proportional to the increase in concrete strength due to the fact that for all prisms with natural AA surface the debonding takes place in the plate adhesive interface rather than the adhesive concrete interface. In other words the concrete strength does not contribute directly to the increase in the loads because the concrete didn't experience any failure. The failure takes place only in the plate adhesive interface.

Figure 4-68: Effect of BL and fcu on load-extension relationship for AA-P

0  
0  
2000  
2000  
4000  
4000  
6000  
6000  
8000  
8000  
10000  
10000  
0  
0  
0.7  
0.7  
1.4  
1.4  
2.1  
2.1  
2.8  
2.8  
Load (N)

Load (N)

Extension (mm)

Extension (mm)

AA

AA--P (BL P (BL of of 150 150 mmmm))

20 MPa

20 MPa

30 MPa

30 MPa

40 MPa

40 MPa

60 MPa

60 MPa

0

0

1500

1500

3000

3000

4500

4500

6000

6000

7500

7500

9000

9000

0

0

0.5

0.5

1

1

1.5

1.5

2

2

Load (N)

Extension (mm)

Extension (mm)

AA

AA--P (BL P (BL ofof200 200 mmmm))

20 MPa

20 MPa

30 MPa

30 MPa

40 MPa

40 MPa

60 MPa

60 MPa

0

0

1000

1000

2000

2000

3000

3000

4000

4000

5000

5000

6000

6000

0

0

0.8

0.8

1.6

1.6

2.4

2.4

3.2

3.2

Load (N)

Extension (mm)

Extension (mm)

AA

AA--P (BL P (BL ofof50 50 mmmm))

20 MPa

20 MPa

30 MPa

30 MPa

40 MPa

40 MPa

60 MPa

60 MPa

0

0

2000

2000

4000

4000

6000

6000

8000

8000

10000

10000

0

0

0.8

0.8

1.6

1.6

2.4

2.4

3.2

3.2

Load (N)

Extension (mm)

Extension (mm)

AA

AA--P (BL P (BL ofof100 100 mmmm))

20 MPa

20 MPa

30 MPa

30 MPa

40 MPa

40 MPa

60 MPa

60 MPa

127

4.5.7 Bond length- prisms with AA natural plates. Figure 4-69 illustrates the load extension curves for prisms strengthened with AA natural plates. Constant concrete strength with different bond length results was plotted. It is observed that higher loads are obtained with increased bond length up to 150 mm. This indicates that the effective bond length falls in the range between 120mm-170 mm for AA natural surface plates.

Figure 4-69: Effect of BL and fcu on load-extension relationship for AA-P

0

0

1000

1000

2000

2000

3000

3000

4000

4000

5000

5000

6000

6000

0

0

0.4

0.4

0.8

0.8

1.2

1.2

1.6

1.6

Load (N)

Load (N)

Extension (mm)

Extension (mm)

AA

AA--P (30 MPA)P (30 MPA)

50mm

50mm

100mm

100mm

150mm

150mm

200mm

200mm

0

0

2000

2000

4000

4000

6000

6000

8000

8000

10000

10000

0

0

0.8

0.8

1.6

1.6

2.4

2.4

3.2

3.2

Load (N)

Extension (mm)

Extension (mm)

AA

AA--P (20 MPA)P (20 MPA)

50mm

50mm

100mm

100mm

150mm

150mm

200mm

200mm

0

0

2000

2000

4000

4000

6000

6000

8000

8000

10000

10000

0

0

0.6

0.6

1.2

1.2

1.8

1.8

2.4

2.4

Load (N)

Extension (mm)

Extension (mm)

AA

AA--P (40 MPA)P (40 MPA)

50mm

50mm

100mm

100mm

150mm

150mm

200mm

200mm

0

0

1500

1500

3000

3000

4500

4500

6000

6000

7500

7500

9000

9000

0

0

0.8

0.8

1.6

1.6

2.4

2.4

3.2

3.2

Load (N)

Extension (mm)

Extension (mm)

AA

AA--P (60 MPA)P (60 MPA)

50mm

50mm

100mm

100mm

150mm

150mm

200mm

200mm

128

## 5 Chapter 5: Development of Aluminum Alloys and CFRP Plate Models

In this chapter the behavior of CFRP and AA-R plates is evaluated, and the models of AA-R and CFRP plates were developed. The development of these models is based on previous models from the literature. Mainly Popovic equation was used as a benchmark for developing the models presented in this study.

### 5.1 Fitting for Popovic's Equation

One of the main objectives of this research is to develop models that capture the relationship between the local bond stress and bond slip. The Popovic's equation [55] is adopted in this research to fit the bond stress-slip curve. The following expression was adopted by several previous studies for developing bond stress-slip relationships for CFRP [20, 21, 56, 57]. In this study this expression is adopted for AA-R plates

$$\tau_{max} = SS_{max} \cdot n(n-1) + (SS_{max})n$$

(3)

Where:  $\tau_{max}$  = Maximum local bond stress.  $S_{max}$  = Slip at maximum load stress.  $n$  = Constant governing the softening branch.

It can be deduced from Equation (3) above, the local bond stress-slip curve has three key parameters which include the ultimate bond stress  $\tau_{max}$ , the slip corresponding to the ultimate bond stress  $S_{max}$  and the constant governing the softening branch  $n$ . The values of these key points for each specimen are listed in section 5.3 for both CFRP and AA-R plates. Bond shear stress-slip results along with the failure energy are used to evaluate the three unknown parameters in Equation (3), i.e.  $\tau_{max}$ ,  $S_{max}$

and  $n$ . Least square minimization between experimental and theoretical shear is carried out using the fracture energy as a constrain in the minimization process, i.e.

$$\min_{\tau_{max}, S_{max}, n} \sum_{i=1}^n (\tau_i - \tau_{exp,i})^2$$

(4)

Subjected to the following constraint  $g(n) \tau_{max} S_{max} = F_{max,exp} \sqrt{2 E_p t_p b_p}$

129

Figure 5-1 shows the Popovic fitting for specimen 30-R-L4 using equations (3-5) above.

Figure 5-1: Fitting results by Popovic's equation

## 5.2 Analysis of Factors Affecting the Bond Stress–Slip Model

As previously stated in the literature, many factors have effect on the bond stress-slip relation. four of these factors has been adopted in this study that include the concrete strength, bond length, plate type and surface preparation. The following section illustrates the effect of these factors on the bond stress-slip relationship.

5.2.1 Bond length. As observed from experimental results and previously stated in chapter 4, the bond length has no effect on the maximum bond stress for CFRP and AA-R plates.

5.2.2 Concrete Strength. The relationship between the maximum bond stress and the concrete compressive strength is obtained using the experimental results. Max bond stress for CFRP and AA-R is plotted against the concrete compressive strength as shown in Figure 5-2 and Figure 5-3 respectively. A wide range of values starting from low strength concrete of 20 MPa and ending at a relatively high strength concrete of 60 MPa is shown.

0

0

1

1

2

2

3

3

4

4

5

5

6

6

7

7

0

0

0.05

0.05

0.1

0.1

0.15

0.15

0.2

0.2

Stress (Mpa)

Stress (Mpa)

Slip (mm)

Slip (mm)

Popovic's Fitting

Popovic's Fitting

30-R-L4

30-R-L4

Popovic's fitting

Popovic's fitting

130

The results of a regression analysis using linear regression are given in Equations (5-8) for both CFRP and AA-R plates. Whereby Equations (6) and (8) are modifications of Equations (5) and (7) assuming that, theoretically the bond stress must be zero for a zero concrete strength.

For CFRP plates

$$\tau_{max}=f_{cu}=0 \text{ (not included)} \quad \tau_{max}=0.0461f_{cu}+0.317$$

(5)

$$\tau_{max}=f_{cu}=0 \text{ (included)} \quad \tau_{max}=0.0509f_{cu}+0.111$$

(6)

For scratched AA plates

$$\tau_{max}=f_{cu}=0 \text{ (not included)} \quad \tau_{max}=0.0423+0.35$$

(7)

$$\tau_{max}=f_{cu}=0 \text{ (included)} \quad \tau_{max}=0.0476f_{cu}+0.115$$

(8)

Figure 5-2: Linear relation between max bond stress and concrete strength

$$y = 0.0509x + 0.1108$$

$$y = 0.0509x + 0.1108R^2 = 0.7247R^2 = 0.7247$$

$$y = 0.0461x + 0.3167$$

$$y = 0.0461x + 0.3167R^2 = 0.4907R^2 = 0.4907$$

0

0.5

1

1.5

2

2.5

3

3.5

4

4.5

5

0

10

20

30

40

50

60

70

Bons Stress (MPa) Bons Stress (MPa) Bons Stress (MPa) Bons Stress (MPa) Bons Stress (MPa) Bons Stress (MPa) Bons Stress (MPa) Bons Stress (MPa)

Concrete strength  $f_{cu}$  (MPa)

Concrete strength  $f_{cu}$  (MPa)

CFRP Plates

CFRP Plates

$f_{cu} = 20$  MPa

$f_{cu} = 20$  MPa

$f_{cu} = 30$  Mpa

$f_{cu} = 30$  Mpa

$f_{cu} = 40$  Mpa

$f_{cu} = 40$  Mpa

$f_{cu} = 60$  Mpa

$f_{cu} = 60$  Mpa

It is clearly observed that the bond stress increases with the increase in the concrete compressive strength and also there is a minimal difference in the slope of both lines for both CFRP and scratched AA-R plates as shown in Figure 5-2 and Figure 5-3 respectively.

131

Figure 5-3: Linear regression between max bond stress and concrete strength

It is clearly observed that the accuracy of fit (*R value*) for the above linear regressions is low due to the way that the data points are scattered. A new regression analysis is adopted based on the average value of the bond stress for each compressive strength as shown in Equations (9) to (12) for CFRP and AA-R plates. Taking the average is a very effective way considering that there is no direct relation between the bond length and the bond stress. Polynomial and power functions are used which results in a very high (*R value*) for the bond stress relation with the concrete compressive strength. The average max bond stress value based on the cylindrical compressive strength is also obtained by using a factor of 0.8. i.e.  $f_c' = 0.8 f_{cu}$ . Figure 5-4 shows the regression analysis based on the average value of the maximum bond stress.

For CFRP plates

$$\tau_{max}=f_{cu}=0 \text{ (included)} \quad \tau_{max}=0.0003f_{cu}^2+0.0672+0.0256$$

(9)

$$\tau_{max}=f_{cu}=0 \text{ (not included)} \quad \tau_{max}=0.076f_{cu}^{0.912}$$

(10)

For scratched AA plates

$$\tau_{max}=f_{cu}=0 \text{ (included)} \quad \tau_{max}=0.0003f_{cu}^2+0.0674+0.0488$$

(11)

$$\tau_{max}=f_{cu}=0 \text{ (not included)} \quad \tau_{max}=0.072f_{cu}^{0.91}$$

(12)

$$y = 0.0476x + 0.1148$$

$$y = 0.0476x + 0.1148 \quad R^2 = 0.6261 \quad R^2 = 0.6261$$

$$y = 0.0423x + 0.3495$$

$$y = 0.0423x + 0.3495 \quad R^2 = 0.3582 \quad R^2 = 0.3582$$

0

0

0.5

0.5

1

1

1.5

1.5

2

2

2.5

2.5

3

3

3.5

3.5

4

4

4.5

4.5

5

5

0

0

10

10

20

20

30

30

40

40

50

50

60

60

70

70

Bond Stress (MPa)

Bond Stress (MPa)

Concrete strength  $f_{cu}$  (MPa)

Concrete strength  $f_{cu}$  (MPa)

AA scratched Plates

AA scratched Plates

$f_{cu} = 20 \text{ Mpa}$

fcu= 20 Mpa

fcu= 30 Mpa

fcu= 30 Mpa

fcu= 40 Mpa

fcu= 40 Mpa

fcu= 60 Mpa

fcu= 60 Mpa

132

Figure 5-4: Average max bond stress based on fcu and fc'

The bond stress-concrete strength relations in Equations (10) and (12) were used to develop the bond-slip models for the CFRP and AA-R plates respectively.

$$y = 0.0757x$$

$$y = 0.0757x^{0.9115} \quad R^2 = 0.9578$$

$$y =$$

$$y = -0.0003x^{0.0003x^2} + 0.0672x + 0.0672x \quad R^2 = 0.9914$$

0

0

0.5

0.5

1

1

1.5

1.5

2

2

2.5

2.5

3

3

3.5

3.5

0

0

20

20

40

40

60

60

80

80

Avg. max. bond stress (MPa)

Avg. max. bond stress (MPa)

Concrete compressive strength fcu (MPa)

Concrete compressive strength fcu (MPa)

*G2F*

*G1F*

*G3F*

*G4F*

$$y = 0.0719x$$

$$y = 0.0719x \quad 0.9099 \quad 0.9099R^2 = 0.9602 \quad R^2 = 0.9602$$

$$y =$$

$$y = -0.0003x^2 + 0.0674x - 0.0488 \quad -0.0488 \quad 0.0488R^2 = 0.9886 \quad R^2 = 0.9886$$

0

0

0.5

0.5

1

1

1.5

1.5

2

2

2.5

2.5

3

3

3.5

3.5

0

0

20

20

40

40

60

60

80

80

Avg. max. bond stress (MPa)

Concrete compressive strength  $f_{cu}$  (MPa)

Concrete compressive strength  $f_{cu}$  (MPa)

*G1R*

*G2R*

*G3R*

*G4R*

$y = 0.0928x$

$$y = 0.0928x + 0.91150.9115R^2 = 0.9578R^2 = 0.9578$$

y =

$$y = -0.0004x^2 + 0.0841x + 0.0841x - 0.02560.0256R^2 = 0.9914R^2 = 0.9914$$

0

0

0.5

0.5

1

1

1.5

1.5

2

2

2.5

2.5

3

3

3.5

3.5

0

0

15

15

30

30

45

45

60

60

Avg. max bond stress (MPa)

max Concrete compressive strength f

Concrete compressive strength fcc' (MPa)(MPa)

*G2F*

*G1F*

*G3F*

*G4F*

$$y = 0.0881x$$

$$y = 0.0881x \quad 0.9099 \quad 0.9099R^2 = 0.9602R^2 = 0.9602$$

$$y =$$

$$y = -0.0005x^2 + 0.0842x + 0.0842x - 0.0488 \quad 0.0488R^2 = 0.9886R^2 = 0.9886$$

0

0

0.5

0.5

1

1

1.5

1.5

2

2

2.5

2.5

3

3

3.5

3.5

0

0

15

15

30

30

45

45

60

60

Avg. max bond stress (MPa)

Concrete compressive strength  $f_c$

Concrete compressive strength  $f_{cc}$  (MPa) (MPa)

*G1R*

*G2R*

*G3R*

*G4R*

(a) CFRP plates

(b) AA scratched plates

(a) CFRP plates

(b) AA scratched plates

133

### 5.3 Development of Bond-Slip Models

The bond slip models for CFRP and AA-R plates were developed. As previously

Table 5-1: Bond- Slip parameters for CFRP plates.

(CFRP plates)

Concrete Compressive Strength  $f_{cu}$  (MPa)

20

30

40

60

20

30

40

60

20

30

40

60

n value

Smax value (mm)

Sult value (mm)

3.148

2.379

2.786

2.005

0.008

0.004

0.006

0.008

0.018

0.014

0.014

0.023

1.797

2.812

2.983

2.518

0.001

0.006

0.003

0.005

0.004

0.020

0.027

0.017

1.924

1.921

2.124

2.000

0.008

0.009

0.019

0.026

0.026

0.037

0.051

0.045

1.989

1.953

1.984

2.003

0.004

0.024

0.015

0.021

0.022

0.059

0.037

0.052

2.291

2.412

2.917

4.072

0.020

0.032

0.007

0.048

0.045

0.060

0.038

0.086

2.180

2.824

3.051

2.744

0.020

0.019

0.027

0.022

0.040

0.077

0.078

0.056

3.187

2.169

3.003

6.534

0.015

0.038

0.021

0.061

0.043

0.070

0.055

0.106

4.554

1.812

4.046

6.435

0.018

0.005

0.024

0.057

0.048

0.037

0.052

0.089

2.634

2.285

2.862

3.539

0.012

0.017

0.015

0.031

0.031

0.047

0.044

0.059

Avg. (n) = 2.83

Avg. Smax = 0.019

Avg. Sult = 0.045 mentioned the development of these models depends directly on the fitting of experimental results using Popovic's formula. In addition, the bond stress expression illustrated in Equations (10) and (12) is also used in identifying the models for CFRP and AA-R plates, respectively. The important parameters needed for CFRP and AA-R

models for each compressive strength are shown in Table 5-1 and Table 5-2, respectively. The average values of these parameters along with the bond stress

expression illustrated in Equations (10) and (12) were used for the development of the models. The CFRP and AA-R plates models for four different compressive strengths

are shown in Figure 5-5 and 5-6 respectively. The effect of concrete compressive strength is evident in the developed models. As shown in Figure 5-7 the bond stress increases with the increase in the concrete compressive strength.

134

Figure 5-5: Bond-slip curves for CFRP for different concrete strength

Table 5-2: Bond-Slip parameters for AA scratched plates

(AA scratched plates)

Concrete Compressive Strength  $f_{cu}$  (MPa)

20

30

40

60

20

30

40

60

20

30

40

60

n value

Smax value (mm)

Sult value (mm)

1.894

4.405

3.708

5.769

0.017

0.002

0.000

0.005

0.020

0.004

0.000

0.016

2.268

2.515

3.526

2.012

0.000

0.009

0.007

0.016

0.001

0.011

0.016

0.036

1.879

1.959

2.052

2.089

0.004

0.015

0.017

0.041

0.011

0.040

0.033

0.070

2.366

1.996

3.208

2.658

0.005

0.003

0.029

0.042

0.009

0.035

0.050

0.061

1.708

3.500

4.304

3.323

0.029

0.033

0.052

0.041

0.053

0.060

0.083

0.080

1.357

2.268

2.316

2.647

0.012

0.005

0.032

0.014

0.022

0.027

0.110

0.044

3.052

3.339

4.018

5.653

0.026

0.099

0.034

0.038

0.087

0.160

0.069

0.084

2.066

2.473

6.762

6.065

0.024

0.032

0.023

0.008

0.051

0.077

0.071

0.034

2.074

2.807

3.737

3.777

0.015

0.025

0.024

0.025

0.032

0.052

0.054

0.053

Avg. (n) = 3.099

Avg. Smax = 0.022

Avg. Sult = 0.048

0

0

0.6

0.6

1.2

1.2

1.8

1.8

2.4

2.4

3

3

0

0

0.03

0.03

0.06

0.06

0.09

0.09

0.12

0.12

0.15

0.15

Bond stress (MPa)

Bond stress (MPa)

Slip (mm)

20 Mpa Exp

20 Mpa Exp

20 Mpa Model

20 Mpa Model

0

0

0.6

0.6

1.2

1.2

1.8

1.8

2.4

2.4

3

3

0

0

0.03

0.03

0.06

0.06

0.09

0.09

0.12

0.12

0.15

0.15

Bond stress (MPa)

Slip (mm)

30 Mpa Exp

30 Mpa Exp

30 Mpa Model

30 Mpa Model

0

0

0.8

0.8

1.6

1.6

2.4

2.4

3.2

3.2

4

4

0

0

0.03

0.03

0.06

0.06

0.09

0.09

0.12

0.12

0.15

0.15

Bond stress (MPa)

Slip (mm)

Slip (mm)

40 Mpa Exp

40 Mpa Exp

40 Mpa Model

40 Mpa Model

0

0

1

1

2

2

3

3

4

4

5

5

0

0

0.03

0.03

0.06

0.06

0.09

0.09

0.12

0.12

0.15

0.15

Bond stress (MPa)

Slip (mm)

Slip (mm)

60 Mpa Exp

60 Mpa Exp

60 Mpa Model

60 Mpa Model

135

Figure 5-6: Bond-slip curves for AA-R plates for different concrete strength

Figure 5-7: Developed bond slip models for AA-R and CFRP plates

0

0

0.7

0.7

1.4

1.4

2.1

2.1

2.8

2.8

3.5

3.5

0

0

0.03

0.03

0.06

0.06

0.09

0.09

0.12

0.12

0.15

0.15

Bond stress (MPa)

Bond stress (MPa)

Slip (mm)

Exp. 20 MPa

Exp. 20 MPa

Series2

Series2

0

0

0.7

0.7

1.4

1.4

2.1

2.1

2.8

2.8

3.5

3.5

0

0

0.05

0.05

0.1

0.1

0.15

0.15

0.2

0.2

0.25

0.25

Bond stress (MPa)

Slip (mm)

Exp. 30 MPa

Exp. 30 MPa

Model 30 MPa

Model 30 MPa

0

0

0.6

0.6

1.2

1.2

1.8

1.8

2.4

2.4

3

3

0

0

0.04

0.04

0.08

0.08

0.12

0.12

0.16

0.16

0.2

0.2

Bond stress (MPa)

Slip (mm)

Slip (mm)

Exp. 40 Mpa

Exp. 40 Mpa

Model 40 MPa

Model 40 MPa

0

0

1

1

2

2

3

3

4

4

5

5

0

0

0.05

0.05

0.1

0.1

0.15

0.15

0.2

0.2

0.25

0.25

Bond stress (Mpa)

Mpa)

Slip (mm)

Slip (mm)

Exp. 60 MPa

Exp. 60 MPa

Series2

Series2

0

0

0.6

0.6

1.2

1.2

1.8

1.8

2.4

2.4

3

3

3.6

3.6

0

0

0.03

0.03

0.06

0.06

0.09

0.09

0.12

0.12

0.15

0.15

Bond Stress (MPa)

Stress Slip (mm)

Slip (mm)

20 Mpa Model

20 Mpa Model

30 Mpa Model

30 Mpa Model

40 Mpa Model

40 Mpa Model

60 Mpa Model

60 Mpa Model

0

0

0.6

0.6

1.2

1.2

1.8

1.8

2.4

2.4

3

3

3.6

3.6

0

0

0.03

0.03

0.06

0.06

0.09

0.09

0.12

0.12

0.15

0.15

Bond Stress (Mpa)

Slip (mm)

Slip (mm)

20 Mpa model

20 Mpa model

30 Mpa model

30 Mpa model

40 Mpa model

40 Mpa model

60 Mpa model

60 Mpa model

AA Scratched plates

CFRP plates

136

### 5.3.1 AA and CFRP model expressions

The equations of the models for AA-R plates and CFRP plates are illustrated in Table 5-3. Five equations for each plate type have been developed. The first four equations were developed based on the average maximum bond stress for each compressive strength whereas the development of the fifth generalized equation is based on the maximum bond stress relation with the concrete compressive strength. The bond slip parameters for each sample are shown in Tables 5-4 and 5-5 for CFRP and AA-R plates, respectively.

Table 5-3: developed CFRP and AA scratched models based on  $f_{cu}$  and  $f_c'$

AA scratched plates

CFRP plates

Compressive Strength (Cube)

20

$$1.5(SS_{max})[ 3.01(2.01)+(SS_{max})3.01]$$

$$1.07(SS_{max})[ 2.83(1.83)+(SS_{max})1.83]$$

30

$$2.12(SS_{max})[ 3.01(2.01)+(SS_{max})3.01]$$

$$1.9(SS_{max})[ 2.83(1.83)+(SS_{max})1.83]$$

40

$$2.29(SS_{max})[ 3.01(2.01)+(SS_{max})3.01]$$

$$2.19(SS_{max})[ 2.83(1.83)+(SS_{max})1.83]$$

60

$$2.76(SS_{max})[ 3.01(2.01)+(SS_{max})3.01]$$

$$3.02(SS_{max})[2.83(1.83)+(SS_{max})1.83]$$

Based on  $f_{cu}$

Generalized

$$\tau_{max}(SS_{max})[3.01(2.01)+(SS_{max})3.01]$$

$$\tau_{max}(SS_{max})[2.83(1.83)+(SS_{max})1.83]$$

$$\tau_{max} = 0.072f_{cu}^{0.91}$$

$$S_{max} = 0.022$$

$$\tau_{max} = 0.076f_{cu}^{0.912}$$

$$S_{max} = 0.019$$

Based on  $f_{c'}$

Generalized

$$\tau_{max}(SS_{max})[3.01(2.01)+(SS_{max})3.01]$$

$$\tau_{max}(SS_{max})[2.83(1.83)+(SS_{max})1.83]$$

$$\tau_{max} = 0.0881f_{c'}^{0.91}$$

$$S_{max} = 0.022$$

$$\tau_{max} = 0.093f_{c'}^{0.912}$$

$$S_{max} = 0.019$$

137

Table 5-4: CFRP bond-slip Parameters for different concrete strength

Specimen Identification

AA/CFRP Plate

Failure Load (KN)

Ultimate bond stress  $\tau_{max}$

(MPa)

Slip at  $\tau_{max}$

$S_{max}$  (mm)

Ultimate slip  $S_{ult}$

(mm)

parameter governing the

softening branch (n)

Plate type

Thickness (mm)

Bonded length (mm)

20-CF-L1

CFRP

1.4

50

4.75

2.283

0.008

0.018

3.148

20-CF-L1

CFRP

1.4

50

6.95

0.335

0.001

0.004

1.797

20-CF-L2

CFRP

1.4

100

8.39

1.259

0.008

0.026

1.924

20-CF-L2

CFRP

1.4

100

6.78

1.141

0.004

0.022

1.989

20-CF-L3

CFRP

1.4

150

8.49

1.074

0.020

0.045

2.291

20-CF-L3

CFRP

1.4

150

7.54

0.8055

0.020

0.040

2.180

20-CF-L4

CFRP

1.4

200

7.89

0.921

0.015

0.043

3.187

20-CF-L4

CFRP

1.4

200

7.36

0.776

0.018

0.048

4.554

30-CF-L1

CFRP

1.4

50

4.36

1.8048

0.004

0.014

2.379

30-CF-L1

CFRP

1.4

50

6.9

2.0527

0.006

0.020

2.812

30-CF-L2

CFRP

1.4

100

9.64

1.8336

0.009

0.037

1.921

30-CF-L2

CFRP

1.4

100

11.77

4.2017

0.024

0.059

1.953

30-CF-L3

CFRP

1.4

150

11.34

2.2865

0.032

0.060

2.412

30-CF-L3

CFRP

1.4

150

15.3

2.6277

0.019

0.077

2.824

30-CF-L4

CFRP

1.4

200

9.89

2.5717

0.038

0.070

2.169

30-CF-L4

CFRP

1.4

200

11.34

1.9602

0.005

0.037

1.812

40-CF-L1

CFRP

1.4

50

4.4

3.683

0.006

0.014

2.786

40-CF-L1

CFRP

1.4

50

10.0

2.61

0.003

0.027

2.983

40-CF-L2

CFRP

1.4

100

12.4

2.678

0.019

0.051

2.124

40-CF-L2

CFRP

1.4

100

10.5

1.606

0.015

0.037

1.984

40-CF-L3

CFRP

1.4

150

7.58

0.997

0.007

0.038

2.917

40-CF-L3

CFRP

1.4

150

11.4

2.981

0.027

0.078

3.051

40-CF-L4

CFRP

1.4

200

12.23

1.645

0.021

0.055

3.003

40-CF-L4

CFRP

1.4

200

9.95

2.008

0.024

0.052

4.046

60-CF-L1

CFRP

1.4

50

7.77

1.991

0.008

0.023

2.005

60-CF-L1

CFRP

1.4

50

5.03

4.184

0.005

0.017

2.518

60-CF-L2

CFRP

1.4

100

12.52

2.475

0.026

0.045

2.000

60-CF-L2

CFRP

1.4

100

11.96

2.356

0.021

0.052

2.003

60-CF-L3

CFRP

1.4

150

14.36

2.889

0.048

0.086

4.072

60-CF-L3

CFRP

1.4

150

16.33

2.417

0.022

0.056

2.744

60-CF-L4

CFRP

1.4

200

15.54

4.519

0.061

0.106

6.534

60-CF-L4

CFRP

1.4

200

10.21

3.334

0.057

0.089

6.435

138

Table 5-5: AA scratched bond-slip Parameters for different concrete strength

Specimen Identification

AA/CFRP Plate

Failure Load (KN)

Ultimate bond stress  $\tau_{max}$

(MPa)

Slip at  $\tau_{max}$

$S_{max}$  (mm)

Ultimate slip  $S_{ult}$

(mm)

parameter governing the

softening branch (n)

Plate type

Thickness (mm)

Bonded length (mm)

20-R-L1

AA-R

3.0

50

2.39

0.241

0.017

0.020

1.894

20-R-L1

AA-R

3.0

50

10.6

4.759

0.000

0.001

2.268

20-R-L2

AA-R

3.0

100

3.95

0.486

0.004

0.011

1.879

20-R-L2

AA-R

3.0

100

3.42

0.459

0.005

0.009

2.366

20-R-L3

AA-R

3.0

150

9.64

1.766

0.029

0.053

1.708

20-R-L3

AA-R

3.0

150

5.45

0.7634

0.012

0.022

1.357

20-R-L4

AA-R

3.0

200

11.0

1.6707

0.026

0.087

3.052

20-R-L4

AA-R

3.0

200

9.29

1.8447

0.024

0.051

2.066

30-R-L1

AA-R

3.0

50

2.65

2.9912

0.002

0.004

4.405

30-R-L1

AA-R

3.0

50

5.85

2.2831

0.009

0.011

2.515

30-R-L2

AA-R

3.0

100

10.64

1.842

0.015

0.040

1.959

30-R-L2

AA-R

3.0

100

12.5

1.6325

0.003

0.035

1.996

30-R-L3

AA-R

3.0

150

13.95

2.6028

0.033

0.060

3.500

30-R-L3

AA-R

3.0

150

8.64

1.415

0.005

0.027

2.268

30-R-L4

AA-R

3.0

200

19.75

5.431

0.099

0.160

3.339

30-R-L4

AA-R

3.0

200

15.67

2.6111

0.032

0.077

2.473

40-R-L1

AA-R

3.0

50

7.8

0.0183

0.001

0.000

3.708

40-R-L1

AA-R

3.0

50

5.0

2.55

0.007

0.016

3.526

40-R-L2

AA-R

3.0

100

14.0

2.573

0.017

0.033

2.052

40-R-L2

AA-R

3.0

100

10.2

1.768

0.029

0.050

3.208

40-R-L3

AA-R

3.0

150

16.45

2.787

0.052

0.083

4.304

40-R-L3

AA-R

3.0

150

20.07

2.776

0.032

0.110

2.316

40-R-L4

AA-R

3.0

200

14.51

2.041

0.034

0.069

4.018

40-R-L4

AA-R

3.0

200

9.59

1.684

0.023

0.071

6.762

60-R-L1

AA-R

3.0

50

6.81

1.461

0.005

0.016

5.769

60-R-L1

AA-R

3.0

50

14.09

4.556

0.016

0.036

2.012

60-R-L2

AA-R

3.0

100

16.83

3.414

0.041

0.070

2.089

60-R-L2

AA-R

3.0

100

14.29

3.641

0.042

0.061

2.658

60-R-L3

AA-R

3.0

150

16.82

2.456

0.041

0.080

3.323

60-R-L3

AA-R

3.0

150

14.75

2.144

0.014

0.044

2.647

60-R-L4

AA-R

3.0

200

16.94

2.7766

0.038

0.084

5.653

60-R-L4

AA-R

3.0

200

13.89

1.602

0.008

0.034

6.065

139

#### 5.4 Analytical Predictions

The performance of the developed models has been statistically evaluated. The sections below provide some statistical measurements that assess the performance of the developed models in predicting the bond stress of the strengthened specimens. Mean Absolute Error (MAE), Mean Absolute Percent Error (MAPE), Mean Square Error (MSE), variance and Normalized Mean Square Error (NMSE) were used to evaluate the models accuracy. The following equations have been used to calculate these statistical measures.

$$MAE = \text{ABS}(\text{Predicted value} - \text{Experimental value})$$

(13)

$$MAPE\% = 100\% \frac{\sum \text{ABS}(\text{Predicted value} - \text{Experimental value})}{\sum \text{Experimental value}} \quad n=1$$

(14)

$$MSE = \text{ABS}[(\text{Predicted value} - \text{Experimental value})]^2$$

(15)

Variance=(Average of exp.values-Exp.value of specified specimen)

(16)

NMSE=(Average MSE/Average variance)

(17)

Correlation coefficient (r)=( $\sum((x_i-\bar{x})(y_i-\bar{y}))$ )/ $\sqrt{\sum((x_i-\bar{x})^2)\sum((y_i-\bar{y})^2)}$

(18)

Where:  $x_i$ ≡Experimental value  $\bar{x}$ ≡Average of Experimental values  $y_i$ ≡Proposed model value  $\bar{y}$ ≡Average of Proposed model value  $n$ ≡Number of data pairs

the statistical measures for the three types of plates with different concrete compressive strength for each plate are shown in the following tables.

140

#### 5.4.1 CFRP statistical measures

Table 5-6: Statistical measures for 20 MPa CFRP plates

Specimen Identification

Slip  $S$  (mm)

Experimental. bond stress

$\tau$ (MPa)

Proposed Model bond stress  $\tau$ (MPa)

MSE

MAE

MAPE%

Variance

Exp.

20-CF-L1

0.01770

1.88020

1.28655

0.3524

0.5937

31.5739

1.5875

0.00794

2.66362

0.63112

4.1310

2.0325

76.3058

4.1754

0

0

0

0

0

-

0.3847

20-CF-L1

0.00425

0.32130

0.33773

0.0003

0.0164

5.1145

0.0894

0.00083

0.33518

0.06967

0.0705

0.2655

79.2134

0.0813

0

0

0

0

0

-

0.3847

20-CF- L2

0.02635

1.25876

1.57842

0.1022

0.3197

25.3946

0.4077

0.00844

0.80392

0.66941

0.0181

0.1345

16.7310

0.0337

0

0

0

0

0

-

0.3847

20-CF- L2

0.01983

1.14112

1.38396

0.0590

0.2428

21.2809

0.2713

0.00290

0.27600

0.22873

0.0022

0.0473

17.1255

0.1185

0

0

0

0

0

-

0.3847

20-CF-L3

0.02133

0.27392

1.44837

1.3793

1.1744

428.7542

0.1199

0.01420

2.35352

1.07987

1.6222

1.2736

54.1166

3.0042

0

0

0

0

0

-

0.3847

20-CF- L3

0.04494

0.15447

1.33642

1.3970

1.1820

765.1579

0.2169

0.02007

0.23550

1.39495

1.3443

1.1595

492.3344

0.1480

0.01760

1.67506

1.27324

0.1615

0.4018

23.9886

1.1126

0

0

0

0

0

-

0.3847

20-CF- L4

0.04813

0.17609

1.25029

1.1539

1.0742

610.0182

0.1973

0.02541

1.15871

1.56575

0.1657

0.4070

35.1289

0.2899

0.01780

1.44079

1.28655

0.0238

0.1542

10.7055

0.6733

0.00267

0.25409

0.20186

0.0027

0.0522

20.5532

0.1341

0

0

0

0

0

-

0.3847

20-CF- L4

0.04307

0.97082

1.39007

0.1758

0.4193

43.1859

0.1229

0.01472

0.23096

1.11188

0.7760

0.8809

381.4254

0.1515

0.00957

0.65118

0.74509

0.0088

0.0939

14.4213

0.0010

0.00273

0.25984

0.21873

0.0017

0.0411

15.8194

0.1299

0

0

0

0

0

-

0.3847

Average

-

0.63845

0.73460

0.4465

0.4126

10.66

0.5564

$NMSE = (\text{Average MSE} \times \text{Average variance}) = 0.4465 \times 0.5564 = 0.8024$

Minimum absolute error value = 0

Maximum absolute error value = 2.0325

r (correlation coefficient) = 0.5336

141

Table 5-7: Statistical measures for 30 MPa CFRP plates

Specimen Identification

Slip  $S$  (mm)

Experimental. bond stress

$\tau$ (MPa)

Proposed Model bond stress  $\tau$ (MPa)

MSE

MAE

MAPE%

Variance

Exp.

30-CF-L1

0.0142

1.6105

1.3740

0.0559

0.2365

14.6862

0.2458

0.0060

1.8048

0.6052

1.4390

1.1996

66.4652

0.4763

0

0

0

0

0

-

1.2425

30-CF-L1

0.0204

1.9417

1.8018

0.0196

0.1399

7.2055

0.6839

0.0063

2.0528

0.6422

1.9897

1.4106

68.7167

0.8800

0

0

0

0

0

-

1.2425

30-CF- L2

0.0337

1.8336

2.0145

0.0327

0.1809

9.8631

0.5169

0.0086

0.8214

0.8617

0.0016

0.0403

4.9115

0.0860

0

0

0

0

0

-

1.2425

30-CF- L2

0.0588

1.7668

1.2407

0.2769

0.5262

29.7805

0.4253

0.0441

4.2017

1.7302

6.1081

2.4715

58.8209

9.5295

0

0

0

0

0

-

1.2425

30-CF- L3

0.0597

1.9321

1.2140

0.5156

0.7181

37.1653

0.6682

0.0315

2.2865

2.0384

0.0615

0.2481

10.8494

1.3732

0.0075

0.7141

0.7540

0.0016

0.0398

5.5756

0.1604

0

0

0

0

0

-

1.2425

30-CF- L3

0.0598

2.6277

1.2110

2.0071

1.4167

53.9134

2.2893

0.0214

1.6043

1.8465

0.0587

0.2422

15.0969

0.2398

0.0046

0.4369

0.4649

0.0008

0.0279

6.3914

0.4593

0

0

0

0

0

-

1.2425

30-CF- L4

0.0701

2.0795

0.9472

1.2822

1.1324

54.4522

0.9309

0.0376

2.5717

1.9287

0.4134

0.6430

25.0016

2.1228

0.0085

0.6007

0.8517

0.0630

0.2510

41.7935

0.2642

0.0022

0.2058

0.2124

0.0000

0.0066

3.2247

0.8261

0

0

0

0

0

-

1.2425

30-CF- L4

0.0367

1.9602

1.9539

0.0000

0.0063

0.3234

0.7149

0.0048

0.1925

0.4800

0.0827

0.2875

149.3508

0.8504

0.0021

0.1285

0.2024

0.0055

0.0739

57.4891

0.9725

0.0007

0.0667

0.0759

0.0001

0.0092

13.8651

1.0983

0

0

0

0

0

-

1.2425

Average

-

1.1147

0.8150

0.4805

0.3769

26.8812

1.1918

$NMSE = (\text{Average MSE} \times \text{Average variance}) = 0.4805 \times 1.1918 = 0.4032$

Minimum absolute error value = 0

Maximum absolute error value = 2.4715

r (correlation coefficient) = 0.8364

142

Table 5-8: Statistical measures for 40 MPa CFRP plates

Specimen Identification

Slip  $S$  (mm)

Experimental. bond stress

$\tau$ (MPa)

Proposed Model bond stress  $\tau$ (MPa)

MSE

MAE

MAPE%

Variance

Exp.

40-CF-L1

0.0136

1.5887

1.5655

0.0005

0.0232

1.4591

0.3135

0.0061

3.6831

0.7180

8.7913

2.9650

80.5043

7.0453

0

0

0

0

0

-

1.0583

40-CF-L1

0.0224

1.2436

2.2485

1.0100

1.0050

80.8154

0.0461

0.0046

2.6101

0.5396

4.2867

2.0704

79.3246

2.5006

0

0

0

0

0

-

1.0583

40-CF- L2

0.0478

2.6487

1.9033

0.5556

0.7454

28.1415

2.6244

0.0219

2.6775

2.2233

0.2063

0.4542

16.9619

2.7184

0.0039

0.7765

0.4799

0.0880

0.2966

38.1956

0.0636

0

0

0

0

0

-

1.0583

40-CF- L2

0.0369

1.6055

2.3108

0.4974

0.7053

43.9276

0.3327

0.0152

1.5173

1.7255

0.0434

0.2082

13.7233

0.2386

0.0050

1.1692

0.5993

0.3248

0.5699

48.7444

0.0197

0

0

0

0

0

-

1.0583

40-CF- L3

0.0317

0.9965

2.4183

2.0216

1.4218

142.6810

0.0010

0.0100

0.3641

1.1810

0.6673

0.8169

224.3237

0.4417

0.0062

0.5923

0.7476

0.0241

0.1553

26.2303

0.1905

0

0

0

0

0

-

1.0583

40-CF- L3

0.0780

0.1738

0.9346

0.5789

0.7608

437.7380

0.7309

0.0433

1.1452

2.0882

0.8894

0.9431

82.3545

0.0136

0.0313

2.9814

2.4201

0.3150

0.5612

18.8247

3.8127

0

0

0

0

0

-

1.0583

40-CF- L4

0.0751

0.7247

1.0004

0.0761

0.2758

38.0562

0.0925

0.0336

0.5769

2.3887

3.2827

1.8118

314.0684

0.2042

0.0224

1.6449

2.2485

0.3643

0.6036

36.6951

0.3797

0.0052

0.4905

0.5993

0.0118

0.1087

22.1680

0.2897

0

0

0

0

0

-

1.0583

40-CF- L4

0.0525

1.9959

1.7088

0.0825

0.2872

14.3888

0.9355

0.0201

1.2389

2.1056

0.7511

0.8667

69.9542

0.0442

0.0050

0.2713

0.5993

0.1076

0.3280

120.8839

0.5737

0.0021

0.2035

0.2522

0.0024

0.0487

23.9148

0.6810

0

0

0

0

0

-

1.0583

Average

-

1.0287

1.0940

0.7806

0.5635

6.3383

1.0238

$NMSE = (\text{Average MSE} \times \text{Average variance}) = 0.7806 \times 1.0238 = 0.7625$

Minimum absolute error value = 0

Maximum absolute error value = 2.965

r (correlation coefficient) = 0.5828

143

Table 5-9: Statistical measures for 60 MPa CFRP plates.

Specimen Identification

Slip  $S$  (mm)

Experimental. bond stress

$\tau$ (MPa)

Proposed Model bond stress  $\tau$ (MPa)

MSE

MAE

MAPE%

Variance

Exp.

60-CF-L1

0.0202

1.8931

2.6996

0.6505

0.8065

42.6042

0.1656

0.0060

1.9910

0.9136

1.1609

1.0774

54.1150

0.2549

0.0000

0.0000

0.0000

0.0000

0.0000

-

2.2086

60-CF-L1

0.0169

3.0569

2.3927

0.4411

0.6642

21.7273

2.4673

0.0153

4.1839

2.2054

3.9146

1.9785

47.2893

7.2778

0.0000

0.0000

0.0000

0.0000

0.0000

-

2.2086

60-CF- L2

0.0454

1.6260

2.5535

0.8602

0.9275

57.0384

0.0196

0.0260

2.4752

3.0237

0.3009

0.5485

22.1617

0.9782

0.0000

0.0000

0.0000

0.0000

0.0000

-

2.2086

60-CF- L2

0.0398

1.4418

2.8262

1.9164

1.3843

96.0112

0.0020

0.0209

1.9914

2.7482

0.5728

0.7568

38.0048

0.2553

0.0000

0.0000

0.0000

0.0000

0.0000

-

2.2086

60-CF- L3

0.0561

2.4165

2.0009

0.1727

0.4156

17.1980

0.8655

0.0217

1.6655

2.8120

1.3143

1.1464

68.8323

0.0322

0.0043

0.4047

0.6486

0.0595

0.2439

60.2591

1.1695

0.0000

0.0000

0.0000

0.0000

0.0000

-

2.2086

60-CF- L3

0.0855

1.9000

1.0092

0.7936

0.8908

46.8861

0.1713

0.0475

2.8894

2.4349

0.2065

0.4545

15.7289

1.9690

0.0171

1.6291

2.3927

0.5831

0.7636

46.8746

0.0204

0.0000

0.0000

0.0000

0.0000

0.0000

-

2.2086

60-CF- L4

0.1056

3.2947

0.6798

6.8378

2.6149

79.3670

3.2710

0.0606

4.5189

1.8170

7.3005

2.7019

59.7921

9.1976

0.0107

0.7863

1.6087

0.6763

0.8224

104.5811

0.4897

0.0024

0.2323

0.3819

0.0224

0.1496

64.4234

1.5722

0.0000

0.0000

0.0000

0.0000

0.0000

-

2.2086

60-CF- L4

0.0855

0.8417

1.0092

0.0280

0.1674

19.8914

0.4153

0.0570

3.3337

1.9534

1.9051

1.3802

41.4033

3.4133

0.0211

1.9284

2.7582

0.6885

0.8298

43.0274

0.1956

0.0009

0.0839

0.1446

0.0037

0.0607

72.3120

1.9663

0.0000

0.0000

0.0000

0.0000

0.0000

-

2.2086

Average

-

1.4861

1.3671

1.0136

0.6929

8.0087

1.7946

$NMSE = (Average\ MSE \cdot Average\ variance) = 1.0136 \cdot 1.7946 = 0.5648$

Minimum absolute error value = 0

Maximum absolute error value = 2.702

r (correlation coefficient) = 0.6834

## 5.4.2 AA scratched statistical measures

Table 5-10: Statistical measures for 20 MPa AA scratched plates.

Specimen Identification

Slip  $S$  (mm)

Experimental. bond stress

$\tau$ (MPa)

Proposed Model bond stress  $\tau$ (MPa)

MSE

MAE

MAPE%

Variance

Exp.

20-R-L1

0.0198

2.8061

1.4374

1.8735

1.3688

48.7772

4.2285

0.0166

4.7592

1.2724

12.1580

3.4868

73.2648

16.0753

0

0

0

0

0

-

0.5622

20-R-L1

0.0004

0.1296

0.0314

0.0097

0.0983

75.8118

0.3846

0.0009

0.2406

0.0713

0.0287

0.1693

70.3547

0.2593

0

0

0

0

0

-

0.5622

20-R- L2

0.0107

0.4864

0.2761

0.0442

0.2103

43.2383

0.0694

0.0043

0.3745

0.3509

0.0006

0.0236

6.2920

0.1409

0

0

0

0

0

-

0.5622

20-R- L2

0.0085

0.3272

0.6771

0.1224

0.3499

106.9191

0.1786

0.0052

0.4592

0.4306

0.0008

0.0286

6.2327

0.0845

0

0

0

0

0

-

0.5622

20-R- L3

0.0457

1.3729

1.3258

0.0022

0.0471

3.4300

0.3883

0.0253

1.7658

1.6347

0.0172

0.1311

7.4232

1.0323

0.0052

0.4518

0.4306

0.0004

0.0212

4.6954

0.0888

0

0

0

0

0

-

0.5622

20-R- L3

0.0183

0.6110

1.3593

0.5600

0.7483

122.4849

0.0193

0.0101

0.7635

0.8011

0.0014

0.0376

4.9256

0.0002

0.0014

0.1248

0.1113

0.0002

0.0135

10.8405

0.3906

0

0

0

0

0

-

0.5622

20-R- L4

0.0870

0.4638

0.4316

0.0010

0.0323

6.9542

0.0818

0.0467

1.2276

1.2927

0.0042

0.0651

5.3020

0.2283

0.0259

1.6707

1.6452

0.0006

0.0254

1.5218

0.8480

0.0068

0.5946

0.5494

0.0020

0.0452

7.6027

0.0241

0

0

0

0

0

-

0.5622

20-R- L4

0.0502

1.8448

1.1780

0.4446

0.6668

36.1453

1.1990

0.0235

1.7358

1.5802

0.0242

0.1556

8.9656

0.9721

0.0032

0.2485

0.2711

0.0005

0.0227

9.1313

0.2514

0.0004

0.0360

0.0314

0.0000

0.0046

12.8246

0.5096

0

0

0

0

0

-

0.5622

Average

-

0.7498

0.5730

0.5099

0.2584

23.5832

1.0651

$NMSE = (\text{Average MSE} \times \text{Average variance}) = 0.5099 \times 1.0651 = 0.5428$

Minimum absolute error value = 0

Maximum absolute error value = 3.4868

r (correlation coefficient) = 0.7657

145

Table 5-11: Statistical measures for 30 MPa AA scratched plates.

Specimen Identification

Slip  $S$  (mm)

Experimental. bond stress

$\tau$ (MPa)

Proposed Model bond stress  $\tau$ (MPa)

MSE

MAE

MAPE%

Variance

Exp.

30-R-L1

0.0110

1.5713

1.0532

0.2685

0.5181

32.9753

0.1192

0.0085

2.2831

0.8206

2.1387

1.4624

64.0555

1.1172

0

0

0

0

0

-

1.5033

30-R-L1

0.0040

2.8014

0.3884

5.8226

2.4130

86.1369

2.4815

0.0033

2.9912

0.3399

7.0294

2.6513

88.6375

3.1155

0

0

0

0

0

-

1.5033

30-R- L2

0.0396

1.8420

1.8555

0.0002

0.0134

0.7288

0.3794

0.0118

1.0374

1.1185

0.0066

0.0811

7.8200

0.0356

0

0

0

0

0

-

1.5033

30-R- L2

0.0348

1.6325

1.9867

0.1255

0.3543

21.7006

0.1651

0.0072

0.5694

0.6978

0.0165

0.1284

22.5496

0.4312

0.0031

0.7364

0.2914

0.1981

0.4450

60.4343

0.2398

0

0

0

0

0

-

1.5033

30-R- L3

0.0604

2.1581

1.0737

1.1760

1.0844

50.2498

0.8686

0.0333

2.6028

2.0163

0.3440

0.5865

22.5336

1.8952

0.0036

0.3185

0.3414

0.0005

0.0229

7.1900

0.8238

0

0

0

0

0

-

1.5033

30-R- L3

0.0266

1.4150

2.0215

0.3678

0.6065

42.8579

0.0357

0.0020

0.0632

0.1113

0.0023

0.0481

76.2239

1.3524

0.0013

0.1153

0.1257

0.0001

0.0104

9.0113

1.2338

0

0

0

0

0

-

1.5033

30-R- L4

0.1600

2.6412

0.1312

6.2998

2.5099

95.0315

2.0024

0.0994

5.4314

0.3897

25.4188

5.0417

92.8257

17.6843

0.0296

1.9134

2.0461

0.0176

0.1328

6.9400

0.4723

0.0078

0.6814

0.7532

0.0052

0.0718

10.5403

0.2967

0

0

0

0

0

-

1.5033

30-R- L4

0.0768

2.6111

0.6854

3.7083

1.9257

73.7499

1.9183

0.0322

1.9469

2.0365

0.0080

0.0896

4.5996

0.5196

0.0074

0.4187

0.7256

0.0942

0.3069

73.2951

0.6519

0.0026

0.2275

0.2428

0.0002

0.0154

6.7566

0.9973

0

0

0

0

0

-

1.5033

Average

-

1.2261

0.6856

1.7113

0.6619

44.0861

1.6408

$NMSE = (\text{Average MSE} \times \text{Average variance}) = 1.7113 \times 1.6408 = 1.043$

Minimum absolute error value = 0

Maximum absolute error value = 5.042

r (correlation coefficient) = 0.6022

146

Table 5-12: Statistical measures for 40 MPa AA scratched plates.

Specimen Identification

Slip  $S$  (mm)

Experimental. bond stress

$\tau$ (MPa)

Proposed Model bond stress  $\tau$ (MPa)

MSE

MAE

MAPE%

Variance

Exp.

40-R-L1

0.0001

0.0073

0.0089

0.0000

0.0016

22.2143

1.1424

0.0001

0.0183

0.0056

0.0002

0.0127

69.4464

1.1192

0

0

0

0

0

-

1.1581

40-R-L1

0.0142

1.2866

1.5318

0.0601

0.2452

19.0561

0.0443

0.0059

2.5495

0.6679

3.5407

1.8817

73.8047

2.1708

0

0

0

0

0

-

1.1581

40-R- L2

0.0326

1.5449

2.3316

0.6189

0.7867

50.9254

0.2197

0.0166

1.7684

1.7511

0.0003

0.0173

0.9790

0.4792

0.0037

1.0539

0.4202

0.4016

0.6337

60.1304

0.0005

0

0

0

0

0

-

1.1581

40-R- L2

0.0496

1.0768

1.6606

0.3409

0.5839

54.2269

0.0000

0.0290

2.3269

2.3468

0.0004

0.0199

0.8547

1.5643

0.0120

2.5733

1.3127

1.5891

1.2606

48.9886

2.2413

0

0

0

0

0

-

1.1581

40-R- L3

0.0833

1.2505

0.6554

0.3542

0.5951

47.5886

0.0304

0.0515

2.7871

1.5936

1.4244

1.1935

42.8220

2.9274

0.0197

1.7234

1.9776

0.0646

0.2542

14.7519

0.4189

0

0

0

0

0

-

1.1581

40-R- L3

0.1098

1.6471

0.1113

2.3587

1.5358

93.2422

0.3260

0.0528

1.8502

0.1257

2.9738

1.7245

93.2059

0.5991

0.0317

2.7761

2.3432

0.1874

0.4329

15.5939

2.8897

0

0

0

0

0

-

1.1581

40-R- L4

0.0714

0.0163

0.9018

0.7840

0.8855

5417.0191

1.1232

0.0433

1.3752

1.9587

0.3405

0.5835

42.4320

0.0894

0.0234

1.6838

2.2087

0.2755

0.5249

31.1720

0.3693

0.0042

0.3681

0.4659

0.0096

0.0977

26.5526

0.5013

0

0

0

0

0

-

1.1581

40-R- L4

0.0688

1.9761

0.9669

1.0185

1.0092

51.0703

0.8100

0.0337

2.0405

2.3148

0.0753

0.2743

13.4438

0.9300

0.0084

0.5598

0.9422

0.1462

0.3824

68.3088

0.2666

0.0020

0.1767

0.2230

0.0021

0.0463

26.2336

0.8090

0

0

0

0

0

-

1.1581

Average

-

1.0761

0.9008

0.5177

0.4682

16.2931

0.9480

$NMSE = (\text{Average MSE} \text{Average variance}) = 0.5177 \cdot 0.948 = 0.5461$

Minimum absolute error value = 0

Maximum absolute error value = 1.882

r (correlation coefficient) = 0.7213

147

Table 5-13: Statistical measures for 60 MPa AA scratched plates.

Specimen Identification

Slip  $S$  (mm)

Experimental. bond stress

$\tau$ (MPa)

Proposed Model bond stress  $\tau$ (MPa)

MSE

MAE

MAPE%

Variance

Exp.

60-R-L1

0.0162

1.4613

2.0620

0.3608

0.6007

41.1063

0.0169

0.0048

1.3274

0.6392

0.4737

0.6882

51.8456

0.0000

0

0

0

0

0

-

1.7723

60-R-L1

0.0355

3.5990

2.7547

0.7129

0.8443

23.4598

5.1425

0.0156

4.5558

2.0075

6.4941

2.5483

55.9362

10.3977

0

0

0

0

0

-

1.7723

60-R- L2

0.0643

2.4305

1.3539

1.1590

1.0765

44.2935

1.2083

0.0390

3.4138

2.6117

0.6434

0.8021

23.4964

4.3368

0

0

0

0

0

-

1.7723

60-R- L2

0.0612

2.1059

1.4760

0.3968

0.6299

29.9109

0.6001

0.0416

3.6411

2.4871

1.3317

1.1540

31.6940

5.3353

0

0

0

0

0

-

1.7723

60-R- L3

0.0795

2.0169

0.8829

1.2861

1.1340

56.2262

0.4702

0.0408

2.4556

2.5130

0.0033

0.0575

2.3403

1.2641

0.0128

1.1219

1.7174

0.3547

0.5956

53.0869

0.0438

0

0

0

0

0

-

1.7723

60-R- L3

0.0469

2.1438

2.1843

0.0016

0.0404

1.8868

0.6603

0.0117

0.7668

1.5521

0.6168

0.7854

102.4283

0.3187

0.0030

0.2613

0.4064

0.0211

0.1451

55.5415

1.1449

0

0

0

0

0

-

1.7723

60-R- L4

0.0842

3.1979

0.7862

5.8161

2.4117

75.4149

3.4842

0.0380

2.7766

2.6570

0.0143

0.1196

4.3085

2.0891

0.0049

0.3178

0.6767

0.1288

0.3589

112.9610

1.0272

0.0013

0.1153

0.2032

0.0077

0.0879

76.2478

1.4786

0

0

0

0

0

-

1.7723

60-R- L4

0.0343

1.6024

2.7860

1.4010

1.1836

73.8650

0.0735

0.0076

0.4689

1.0120

0.2950

0.5432

115.8433

0.7437

0.0018

0.1178

0.2432

0.0157

0.1254

106.4793

1.4725

0.0005

0.0402

0.0622

0.0005

0.0220

54.6842

1.6668

0

0

0

0

0

-

1.7723

Average

-

1.3313

1.1025

0.7178

0.5318

17.1844

1.9051

$$NMSE = (\text{Average MSE} / \text{Average variance}) = 0.71781 / 1.9051 = 0.3768$$

Minimum absolute error value = 0

Maximum absolute error value = 2.702

r (correlation coefficient) = 0.8097

148

#### 5.4.3 Summary and discussion of the predicted results

Table 5-14 shows the results of the statistical measurements for CFRP and AA-R plates with different concrete strength. As observed, the AA-R plates model exhibits more accurate and close prediction for the bond-slip with respect to the experimental data for all concrete compressive strength except the concrete strength of 30 MPa. The models with the highest accuracy for CFRP and AA-R plates are 30-CFRP and 60-AA-R with a correlation coefficient of 0.8364 and 0.81 respectively. In addition, the NMSE for both of the models is relatively lower with 0.4032 for 30-CFRP and 0.3767 for 60-AA-R. The lower the NMSE values the better which indicate higher accuracy.

Table 5-14: Summary of the statistical measures for CFRP and AA-R plates

Normalized means square Error (NMSE)

Minimum absolute error (MAE)

Maximum absolute error (MAE)

MAPE %

r

20-CFRP

0.8024

0

2.033

10.66

0.5336

30-CFRP

0.4032

0

2.472

26.881

0.8364

40-CFRP

0.7625

0

2.965

6.338

0.583

60-CFRP

0.565

0

2.702

8.009

0.6834

20-AA-R

0.4787

0

3.4868

23.583

0.766

30-AA-R

1.043

0

5.042

44.086

0.602

40-AA-R

0.546

0

1.882

16.293

0.7213

60-AA-R

0.3768

0

2.702

17.184

0.8097

149

## 6 Chapter 6: Finite Element Model Development

In this chapter, the use of finite element modeling (FEM) is presented to analyze the behavior of a number of tested samples discussed in chapter 5. FEM is a great tool in predicting and validating the performance of the proposed AA plates as an EBR material. The multipurpose software ANSYS [58] was used in developing FE models for four tested specimens. Particularly ANSYS workbench 17.0 [58] was used for creating and analyzing the developed models. A detailed description of the FE model is provided herein, including geometry, element types, constitutive material properties, loading and boundary conditions used.

### 6.1 Geometry

The effect of different bond lengths of AA plates, taken as 50mm, 100mm, 150mm, and 200mm has been studied. The developed FE models is taken to have the same dimensions of the tested samples as shown in Table 6-1. Only AA scratched plate type with different concrete strength was considered for the model development.

Table 6-1: four specimens considered for the FE simulation

Specimen

Exp. bonded & free lengths (mm)

FEM bonded & free lengths (mm)

AA scratched plate length (mm)

60-R-L1

210

40-R-L2

260

30-R-L3

310

30-R-L4

360

100

160

160

200

50

160

150

160

100

160

50

160

160

200

160

200

150

The geometry of the developed four 3D FE models is illustrated in Figure 6-1. All FE models have the same geometry with different bonded length. The FE concrete prisms have a length of 250 mm and equal width and depth of 75 mm. All of the AA scratched plates have an unbonded length, width and thickness of 160mm, 50mm and 3mm respectively. Four bonded lengths of 50mm, 100mm, 150mm, 200mm were considered to study the effect of different AA bond length on the bond slip behavior. Zero thickness contact and target elements were used to model the adhesive layer. Hence, no physical thickness is given for the adhesive material.

(a) 60-R-L1

(b) 40-R-L2

(c) 40-R-L3

(d) 30-R-L4

75 mm

250 mm

50 mm

160 mm

50 mm

75 mm

250 mm

100 mm

160 mm

50 mm

75 mm

250 mm

200 mm

160 mm

50 mm

75 mm

250 mm

150 mm

160 mm

50 mm

75 mm

75 mm

75 mm

75 mm

Figure 6-1: FE models

Concrete Prism

AAR Plate

Concrete Prism

AAR Plate

Concrete Prism

AAR Plate

Concrete Prism

AAR Plate

151

## 6.2 Element Types and Material Models

In this section, the different material models and element types used to model concrete, AA plates and epoxy adhesive are described.

6.2.1 Concrete. SOLID65 [58] element was used to model the concrete prisms. This element is used particularly to model reinforced concrete members with or without rebars. As shown in Figure 6-2, The brick element has eight nodes with three degrees of freedom per node. The element has the ability to crack in tension and crush in compression. The materials properties assigned to concrete were obtained from the experimental tests, presented in chapter five. The materials properties assigned for concrete were linearly isotropic with an elastic modulus, compressive strength and Poisson's ratio values provided in Table 6-2. The nonlinear behavior of concrete in compression and tension is captured by using some mathematical models. William and Warnke model [59] was used to define the concrete failure criteria. Concrete failure is mainly governed by two parameters, namely the concrete ultimate compressive strength and ultimate tensile strength. The first parameter is associated with concrete crushing, whereas the latter is related to cracking of concrete. Cracking and crushing of concrete will take place once the principle compressive stress or principle tensile stress in any direction exceeds the ultimate compressive or ultimate tensile stress of concrete. SOLID65 has the ability to neutralize cracked or crushed elements for further analysis when cracking or crushing occurs. The elastic modulus of the cracked or crushed elements is set to zero by the software in order for the elements to be deactivated. It's worth mentioning that no concrete crushing was encountered experimentally. Hence, crushing was deactivated to reduce the run time by assigning a value of -1 for concrete compressive strength.

Table 6-2: Properties assigned to concrete.

Compressive strength  $f_{cu}$  (MPa)

Elasticity modulus (GPa)

Poisson's Ratio

Tensile strength (MPa)

30

25

0.2

3.396

40

26

0.22

3.921

60

29

0.23

4.802

Figure 6-2: ANSYS SOLID65 reinforced concrete element [58]

152

As mentioned above, the tensile strength of concrete is obtained using Equation (19). According to William and Warnke, the concrete tensile behavior is represented by linear elastic response up to a maximum tensile strength (concrete rupture) corresponding to a strain of  $\epsilon_t$  obtained by equation (20). Subsequently, the concrete elements start to crack resulting in a sudden stress drop of  $0.6f_t$ , followed by linear reduction of tensile stress reaching a value of zero at  $6\epsilon_t$ .

$$f_t = 0.62\sqrt{f_c'}$$

(19)

$$\epsilon_t = \frac{f_t}{E}$$

(20)

Where:  $f_t$ =concrete tensile strength (MPa)  $f_c'$ =concrete compressive strength (MPa)  $\epsilon_t$ = concrete strain corresponding to  $f_t$   $E$ = elastic modulus of concrete (MPa)

A shear transfer coefficient value ranging between 0 and 1 is required for SOLID65 element, with 0 for a smooth crack (complete loss of shear transfer), and 1 for a rough crack (full shear transfer). Two coefficients values are required, one for open shear  $\beta_t$  and another for close shear  $\beta_c$ , the close shear coefficient  $\beta_c$  should be greater than the open shear coefficient  $\beta_t$ . The value of  $\beta_t$  used in several studies [60-62] varied between 0.05 and 0.25. As reported by a number of studies, an open shear transfers coefficient values less than 0.2 resulted in a solution convergence problem. Hence, in this research an open shear transfer coefficient of 0.2 and closed shear transfer coefficient of 0.25 were used.

153

6.2.2 AA plates. SOLID185 [58] element was used for modeling the AA plate. SOLID185 is used for 3-D modeling of solid structures. As shown in Figure 6-3, similar to SOLID65, it is defined by eight nodes having three degrees of freedom at each node: translations in the nodal x, y, and z directions. The element has plasticity, hyperelasticity, stress stiffening, creep, large deflection, and large strain capabilities. It also has mixed formulation capability for simulating deformations of nearly incompressible elastoplastic materials, and fully incompressible hyperelastic materials. The mechanical

properties of the AA plates were measured experimentally as stated in the fifth chapter of this research. Table 6-3 shows the mechanical properties assigned to the AA plate.

Experimentally, the yield stress of the bonded AA plates was not reached. Additionally, the CFRP also did not reach their rupture stress. The major mode of failure in the experimental was observed to be debonding. Hence, no plastic properties were assigned to the AA scratched plates. The AA scratched plates were treated as linear elastic and isotropic material, which results in a simpler model reducing the run time and convergence problems. The dimensions used in the FE model for the AA plates were the same as those of the experimentally tested AA plates.

Table 6-3: Properties assigned to AA plate

Aluminum Alloy

Elasticity modulus (GPa)

Poisson's Ratio

5083-H111

70.3

0.33

Figure 6-3: ANSYS SOLID185 3D structural element [58]

154

6.2.3 AA- concrete interface element. The epoxy adhesive which represents the interface between the AA plate and concrete can be modeled using either the cohesive zone model CZM or the virtual crack closure technique VCCT. Both methods require the use of special elements. Essentially, elements that define the interface of separation. Particularly, contact elements pair i.e. CONTA174 and TARGE170 or interface elements viz. INTER205 could be used [58]. In this research, CZM was conducted to simulate the interface debonding. Two main features are available through CZM to simulate debonding, namely The debonding using contact elements can be simulated through one of the two following material models i.e. (i) bilinear material behavior with traction and separation distance, and (ii) bilinear material behavior with tractions and critical fracture energies. On the other hand, interface elements can also be used to simulate debonding using either exponential material behavior for interface delamination or bilinear material behavior for interface delamination. In this study the bilinear material behavior with traction and separation distance was used to simulate interface debonding. Six parameters are required for using this model. Maximum normal contact stress ( $\sigma_{max}$ ), contact gap at the completion of debonding ( $\delta_{nc}$ ), Maximum equivalent tangential contact stress ( $T_{max}$ ), Tangential slip at the completion of debonding ( $\delta_{tc}$ ), Artificial damping coefficient ( $\eta$ ) and Flag for tangential slip under compressive normal contact stress ( $\beta$ ). According to H.L. Ewalds [63], three debonding failure modes could be encountered as shown in Figure 6-4. In this study, the cause of debonding is tangential shear failure (mode II), then the normal stress is neglected and only shear failure stress is considered. Therefore, Maximum normal contact stress ( $\sigma_{max}$ ) and contact gap at the completion of debonding ( $\delta_{nc}$ ) were ignored. Figure 6-5 shows the bilinear model with traction and separation distance.

Mode (I): Tensile opening

Mode (II): in-plane shear

Mode (III): anti-plane shear Figure 6-4: Three modes of shear crack [63]

155

Generally, convergence problems may occur when using Newton-Raphson solution, thus an artificial damping coefficient is used for stabilizing the numerical solution. According to ANSYS manual [58] the artificial damping coefficient value ranges from 0.01 to 0.1. Hence, a value of 0.1 was used for the artificial damping coefficient. The CZM properties used for traction and separation of the modeled specimens are illustrated in Table 6-4. These values were obtained directly from the experimental results presented in chapter five.

Table 6-4: CZM parameters for the modeled specimens

Specimen

$T_{max}$  (MPa)

$\delta t_c$  (mm)

$\eta$

60-R-L1

4.63

0.035

0.1

40-R-L2

1.79

0.033

0.1

30-R-L3

2.61

0.06

0.1

30-R-L4

5.43

0.13

0.1

Contact elements were used to model the interface (epoxy) layer between the AA

Where:  $T_t$  = Maximum equivalent tangential contact stress  $\delta t_c$  = Tangential slip at the completion of debonding  $\delta t^*$  = Tangential slip at max contact stress  $T_t \eta$  = artificial damping coefficient

Figure 6-5: Bilinear model for

traction and separation [58]

plate and concrete. These elements consist of the contact pair CONTA174 and

TARGE170. CONTA174 is used to represent contact and sliding between 3-D target

surfaces and a deformable surface defined by this element. TARGE170 is used to represent various 3-D "target" surfaces for the associated contact elements. The contact elements themselves overlay the solid elements describing the boundary of a deformable body and are potentially in contact with the target surface, defined by TARGE170 [58]. Figure 6-6 shows the contact and target elements used in the model.

The contact and target surfaces are illustrated in Figure 6-7.

156

Five default (Program controlled) key options for the contact region were changed to simulate debonding correctly. Namely, the contact type which was set to "bonded", the formulation which was set to "Pure penalty", the detection method which was set to "on gauss points", the contact stiffness which was set to "manual", and the stiffness update which was set to "each iteration". The pure penalty formulation introduces a force at the contact detection points that has penetrated across the target surface to eliminate penetration. This method uses the following simple formula

$$F_{Tangential} = K T_{angential} * x_{sliding}$$

(21)

$T_{angential}$ ,  $K T_{angential}$  and  $x_{sliding}$  represents the applied tangential force on the plate free end, contact tangential stiffness and contact slip respectively.

Figure 6-7: Contact and target bodies and surfaces

Contact Body

(AAR Plate)

Contact Surface

Target Surface

Target Body

Concrete Prism

(AAR Plate)

Concrete Prism Figure 6-6: ANSYS CONTA174 and TARGE170 [58]

where  $F$

157

6.2.4 Boundary conditions and mesh generation. A mesh with an element size of 5 mm has been used through the whole geometry. The element mid-side nodes were set to “dropped” in order to convert the element type from the default 20 nodes SOLID186 to the 8 nodes SOLID185. A command block has been used for the concrete prism to force the use of the SOLID65 element instead of the SOLID185 element. The support conditions were set as fixed support on two faces. A tensile load is applied normal to the free end face of the plate in the form of a force. Figure 6-8 shows the meshing, boundary conditions and the load application on the plate’s free end.

Figure 6-8: Generated mesh, loading and boundary conditions

(c) Boundary conditions (fixed supports).

(a) Meshing

(b) Loading

F

158

Table 6-5: Strain gauge locations for the Exp. samples Modeled

Bonded & free lengths (mm)

Strain gauges locations from free end (mm)

AA/CFRP plate length (mm)

S.G 20, 50, 110

210

S.G 50, 100, 160

260

S.G 50, 100, 150, 210

310

S.G 50, 100, 150, 200, 260

360

160

200

160

100

50

160

160

150

Figure 6-9: Path generation for different bonded lengths

(a) Path of 200 mm

(b) Path of 150 mm

(c) Path of 100 mm

(d) Path of 50 mm

6.2.5 Construction geometry and path generation. To validate the AA-concrete interface finite element results with the experiment ones, a path is generated in order to map the strain gauge results. The path method is very useful specially for mapping results at different load levels. The strains developed in the AA plate at different locations as

shown in table Table 6-5 were compared to the mapped strain simulation results

using the generated paths. Figure 6-9 shows the paths generated for different lengths.

159

6.2.6 Analysis settings and nonlinear solution. The load was applied in a series of load steps. The load step will automatically be divided into smaller load steps called sub-steps based on the structural model behavior in the former step. ANSYS employs Newton-Raphson method in solving nonlinear Models. The Newton-Raphson method along with the Load steps and sub-steps are displayed in Figure 6-10. According to this method the difference between the applied loads and the model loads corresponding to the elements stresses is calculated before each iteration. After that, ANSYS checks for convergence by performing a linear solution. If convergence is not reached, the load vector is recalculated in a new attempt to reach convergence and the stiffness matrix is updated. This procedure is repeated until a converged solution is achieved. In order to obtain convergence in highly nonlinear problems, a number of analysis settings could be applied to help with convergence in ANSYS workbench. First of all, the load needs to be applied in a very small amount. Moreover, the following analysis settings could be activated to obtain convergence in workbench. Under analysis settings the following key options could be activated. Namely, stabilization, large deflections, weak springs, line search, force and moment convergence could be activated and adjusted. For the single shear FE models, failure was recognized when a solution for a 0.0001 KN load increment fails to converge.

Figure 6-10: Solution process

(b) Load steps and sub-steps

(a) Newton Raphson method

160

between the developed FE models and the corresponding experimental results. A contact tool is inserted in the solution branch containing contact frictional stress and sliding distance, these were compared to the experimental bond stress and slip results respectively. In addition, the stress strain results and the strain gauges' readings at different load levels were also compared with the experimental results. Figure 6-11: Contact Bond stress along the bonded length

0123456050100150200250Bond Stress (

MPa)Distance from loaded end (mm)1.0P Exp1.0P FEMP: Failure Load  $L_e = 135\text{mm}$  6.3 FE Modeling Results of AA Plate-Concrete Interface To validate the FEM results of AA plate-concrete interface, a comparison is made

FE model validation. The FE predicted and measured bond stress results along the bonded length of specimen 30-R-L4 at failure are displayed in Figure 6-11. As shown, the FE model contact frictional stress effectively simulates the experimental

### 6.3.1

bond stress.

161

Figure 6-12 shows the FE predicted and measured slip results along the bonded length at failure for 30-R-L4 sample. As displayed, the FE model contact sliding distance distribution along the bonded length effectively simulates the experimental slip for 30-R-L4 specimen.

Figure 6-12: Contact sliding distance along the bonded length

0

0

0.03

0.03

0.06

0.06

0.09

0.09

0.12

0.12

0.15

0.15

0.18

0.18

0

0

50

50

100

100

150

150

200

200

250

250

Slip (mm)

Slip (mm)

Distance from loaded end (mm)

Distance from loaded end (mm)

1.0P FEM

1.0P FEM

1.0P Exp

1.0P Exp

P: Failure Load

162

Figure 6-13: Stress strain curve for 30-R-L4 specimen

Figure 6-14: Strain gauge readings along the bonded length

0

25

50

75

100

125

150

0

0.0005

0.001

0.0015

0.002

0.0025

Stress (MPa)Stress (MPa)Stress (MPa)Stress (MPa)

Strain (

Strain ( $\epsilon$ )

Exp.

Exp.

FEM

FEM

P:FailureFailureLoadLoad

0

400

800

1200

1600

2000

2400

0

40

80

120

160

200

240

Strain (Strain (Strain (Strain (Strain ( $\mu\epsilon$ )

Distance from free end (mm)

Distance from free end (mm)

Exp. 0.2P

Exp. 0.2P

Exp. 0.4P

Exp. 0.4P

Exp. 0.6P

Exp. 0.6P

Exp. 0.8P

Exp. 0.8P

Exp. 1.0P

Exp. 1.0P

FE 0.2P

FE 0.2P

FE 0.4P

FE 0.4P

FE 0.6P

FE 0.6P

FE 0.8P

FE 0.8P

FE 1.0P

FE 1.0P

P:FailureFailureLoadLoad

Figure 6-13 and Figure 6-14 illustrate the stress strain curve and strain gauge readings along the bonded length at different applied loading steps. It can be clearly seen from these figures that the FE model results are in a good agreement with the obtained experimental results at all loading stages.

predicts the bond stress effectively specially at the strain gauge locations.

Figure 6-15: Contact Bond stress along the bonded length

0

0.5

1

1.5

2

2.5

3

0

25

50

75

100

125

150

175

Bond stress (MPa) Bond stress (MPa) Bond stress (MPa) Bond stress (MPa) Bond stress (MPa) Bond stress (MPa) Bond stress (MPa)

Distance from loaded end (mm)

Distance from loaded end (mm)

FE 1.0P

FE 1.0P

Exp. 1.0P

Exp. 1.0P

P: Failure Load

The FE predicted and measured bond stress results along the bonded length of specimen 40-R-L3 at failure are displayed in Figure 6-15. as shown, the FE model

Figure 6-16 illustrates FE predicted and measured slip results along the bonded length at failure for 40-R-L3 sample. As displayed, the FE model contact sliding distance distribution along the bonded length effectively simulates the experimental slip for 40-R-L3 specimen.

Figure 6-16: Contact sliding distance along the bonded length

0  
0  
0.018  
0.018  
0.036  
0.036  
0.054  
0.054  
0.072  
0.072  
0.09  
0.09  
0  
0  
25  
25  
50  
50  
75  
75  
100  
100  
125  
125

150

150

175

175

Slip (mm)

Slip (mm)

Distance from loaded end (mm)

Distance from loaded end (mm)

FE 1.0P

FE 1.0P

Exp. 1.0P

Exp. 1.0P

P: Failure Load

165

Figure 6-17: Stress strain curve for 40-R-L3 specimen

Figure 6-18: Strain gauge readings along the bonded length

0

300

600

900

1200

1500

1800

0

25

50

75

100

125

150

175

Strain (Strain (Strain (Strain (Strain ( $\mu\epsilon$ )

Distance from free end (mm)

Distance from free end (mm)

Exp. 0.2P

Exp. 0.2P

Exp. 0.4P

Exp. 0.4P

Exp. 0.6P

Exp. 0.6P

Exp. 0.8P

Exp. 0.8P

Exp. 1.0P

Exp. 1.0P

FE 0.2P

FE 0.2P

FE 0.4P

FE 0.4P

FE 0.6P

FE 0.6P

FE 0.8P

FE 0.8P

FE 1.0P

FE 1.0P

P:FailureFailureLoadLoad

0

20

40

60

80

100

120

0

0.0004

0.0008

0.0012

0.0016

0.002

Stress (MPa)Stress (MPa)Stress (MPa)Stress (MPa)

Strain (

Strain ( $\epsilon$ )

Exp.

FE

Figure 6-17 and Figure 6-18 illustrate the stress strain curve and the strain gauge

readings along the bonded length at different applied loading steps. it can be clearly seen that the FE model results are in a good agreement with the obtained experimental results at all stages of loading.

166

The FE predicted and measured bond stress results along the bonded length at failure for 40-R-L2 sample are shown in Figure 6-19. As displayed, the FE model contact frictional stress distribution along the bonded length effectively simulates the experimental bond stress for 40-R-L2 specimen.

Figure 6-19: Contact bond stress along the bonded length

0

0.35

0.7

1.05

1.4

1.75

2.1

0

20

40

60

80

100

120

Bond Stress (MPa) Bond Stress (MPa) Bond Stress (MPa) Bond Stress (MPa) Bond Stress (MPa) Bond Stress (MPa) Bond Stress (MPa) Bond Stress (MPa) Bond Stress (MPa) Bond Stress (MPa)

Distance from loaded end (mm)

Distance from loaded end (mm)

Exp. 1.0P

Exp. 1.0P

P: Failure Load

FE 1.0P

167

Figure 6-20 illustrates the FE predicted and measured slip results along the bonded length at failure for 40-R-L2 sample. As displayed, the FE model contact sliding distance distribution along the bonded length effectively simulates the experimental slip for 40-R-L2 specimen.

Figure 6-20: Contact sliding distance along the bonded length

0

0

0.006

0.006

0.012

0.012

0.018

0.018

0.024

0.024

0.03

0.03

0.036

0.036

0

0

20

20

40

40

60

60

80

80

100

100

120

120

Slip (mm)

Slip (mm)

Distance from loaded end (mm)

Distance from loaded end (mm)

Exp. 1.0P

Exp. 1.0P

FE 1.0P

FE 1.0P

P: Failure Load

168

Figure 6-21 and Figure 6-22 illustrate the stress strain curve and the strain gauge readings along the bonded length at different applied loading steps. It can be clearly seen that the FE model results are in a good agreement with the obtained experimental results at all stages of loading for 40-R-L2 specimen.

0

0

160

160

320

320

480

480

640

640

800

800

960

960

0

0

20

20

40

40

60

60

80

80

100

100

120

120

Strain ( $\mu\epsilon$ )

Strain ( $\mu\epsilon$ )

Distance from free end (mm)

Distance from free end (mm)

Exp. 0.2P

Exp. 0.2P

Exp. 0.4P

Exp. 0.4P

Exp. 0.6P

Exp. 0.6P

Exp. 0.8P

Exp. 0.8P

Exp. 1.0P

Exp. 1.0P

FE 0.2P

FE 0.2P

FE 0.4P

FE 0.4P

FE 0.6P

FE 0.6P

FE 0.8P

FE 0.8P

FE 1.0P

FE 1.0P

P

P::FailureFailureLoadLoad

0

0

12

12

24

24

36

36

48

48

60

60

72

72

0

0

0.00025

0.00025

0.0005

0.0005

0.00075

0.00075

0.001

0.001

0.00125

0.00125

Stress (MPa)

Stress MPa)

Strain (

Strain ( $\epsilon\epsilon$ )

Exp

Exp

FE

FE

Figure 6-21: Stress strain curve for 40-R-L2 specimen

Figure 6-22: Strain gauges readings along the bonded length

169

The FE predicted versus the measured bond stress results along the bonded length of specimen 60-R-L1 are shown in Figure 6-23. as shown, the FE model fairly predicts the bond stress for 60-R-L1 sample. It can be observed that there is a difference between the FE and the experimental bond stress at the free end of the plate at 50mm. This is due to the fact that the bond length is very short causing bond stresses concentration at the plate edges as displayed

0

0

0.8

0.8

1.6

1.6

2.4

2.4

3.2

3.2

4

4

4.8

4.8

0

0

10

10

20

20

30

30

40

40

50

50

60

60

Bond stress (MPa)

Bond stress (MPa)

Distance from loaded end (mm)

Distance from loaded end (mm)

Exp. 1.0P

Exp. 1.0P

FE 1.0P

FE 1.0P

Figure 6-23: Contact bond stress along the bonded length

P: Failure Load

170

Figure 6-24 illustrates the FE predicted and measured slip results along the bonded length at failure for 60-R-L1 sample. As displayed, the FE model contact sliding distance distribution along the bonded length effectively simulates the experimental slip at failure for 60-R-L1 specimen.

Figure 6-24: Contact sliding distance along the bonded length

0

0.007

0.014

0.021

0.028

0.028

0.035

0.042

0

10

20

30

40

50

60

Slip (mm)Slip (mm)Slip (mm)Slip (mm)Slip (mm)

Distance from loaded end (mm)

Distance from loaded end (mm)

Exp. 1.0P

FE 1.0P

P: Failure Load

171

Figure 6-25 and Figure 6-26 illustrate the stress strain curve and the strain gauge readings along the bonded length at different applied loading steps. It can be clearly seen that the FE model results are in a good agreement with the obtained experimental results at all stages of loading for 60-R-L1 specimen.

Figure 6-25: Stress strain curve for 60-R-L1 specimen

Figure 6-26: Strain gauges readings along the bonded length

0

0

20

20

40

40

60

60

80

80

100

100

0

0

0.0003

0.0003

0.0006

0.0006

0.0009

0.0009

0.0012

0.0012

0.0015

0.0015

Stress (Mpa)

Stress (Mpa)

Strain (

Strain ( $\mu\mu\epsilon\epsilon$ )

Exp.

Exp.

FE

FE

0

0

300

300

600

600

900

900

1200

1200

1500

1500

0

0

10

10

20

20

30

30

40

40

50

50

60

60

AXIS TITLE

AXIS TITLE

AXIS TITLE

AXIS TITLE

Exp. 0.2P

Exp. 0.2P

Exp. 0.4P

Exp. 0.4P

Exp. 0.6P

Exp. 0.6P

Exp. 0.8P

Exp. 0.8P

Exp. 1.0P

Exp. 1.0P

FE 0.2P

FE 0.2P

FE 0.4P

FE 0.4P

FE 0.6P

FE 0.6P

FE 0.8P

FE 0.8P

FE 1.0P

FE 1.0P

P

P::FailureFailureLoadLoad

172

### 6.3.2 3D failure modes

The failure modes of the four tested samples are illustrated in Figure 6-27. The failure mode is maximized for the first two bonded lengths, i.e., 50mm and 100mm to show the separation in a clear way. A true scale failure mode is displayed for the bond length of 150mm and 200mm.

(c) 40-R-L3

(d) 30-R-L4

(b) 40-R-L2

(a) 60-R-L1

## Chapter 7: Summary and Conclusion

Several materials have been used globally in the field of strengthening and repairing in order to increase the carrying capacities of the deteriorated and damaged reinforced concrete structures. In this research, a new material has been proposed as an externally bonded reinforcement EBR for reinforced concrete structures. A total of ninety-six concrete prisms strengthened with the newly innovated aluminum alloys plates (5083-111) were experimentally tested to investigate the performance of the aluminum alloys as an EBR materials. Three parameters were considered in this study, namely, concrete strength, bond length and the type of the plate used. The bond strength of AA-concrete interface has been evaluated and proved to be effective and adequate for strengthening of RC members. A 3D Finite element model is also presented in this study to evaluate and predict the bond slip behavior of AA-concrete interface. Four FE models were developed and the generated results were validated by comparing the predicted FE results to the corresponding ones in the experimental program. Based on the experimental results presented the following observations and conclusions can be drawn: □ The bond stress has a direct relationship with the concrete compressive strength for the CFRP and AA plates with scratched surface, in other words a higher concrete strength will result in a higher bond stress. On the other hand, for the AA plates with plain surface the concrete strength appears to have no direct effect on the bond stress due to the fact that the failure in this case takes place in the plate adhesive interface. □ The loading capacity increases with the increase in the bond length up to a certain length called the effective bond length EBL. The effective bond length of the tested samples differs depending on the type and surface roughness of the EBR plates. Hence, the EBL for AA scratched and CFRP plates ranges between 120mm-180mm. □ The loading capacity, bond stress, slip and modes of failure vary with respect to AA surface roughness. Hence, the AA surface roughness greatly improves

the bond slip behavior of the AA plates. The load capacity and maximum bond stress increased by 254.7% and 253.7%, respectively for randomly grinded AA surface compared with those of normal AA surface indicating that AA plates with scratched surface could be used in practical applications. □ The AA plates with scratched surface resulted in a higher failure load, maximum bond stress, maximum and ultimate slip compared with the CFRP plates using average bond length and compressive strength results. Hence, the load capacity for AA scratched plates increases by 5.6% for the short bonded length up to 22.5% for the long bonded length when compared to the CFRP plates. □ Failure modes varies with the plate type and surface roughness. Hence, the failure mode for all AA plates with plain surface takes place in the plate-adhesive interface due to the weak bond between these two surfaces. Whereas the failure mode for almost all AA plates with scratched surface takes place in the adhesive-concrete interface due to the fact that the bond of the plate-adhesive interface is relatively higher than the adhesive-concrete interface in this case. □ The developed models for CFRP and AA scratched plates are similar in behavior. In addition, these models for these plate types where with a good agreement with previous developed FRP models from literature. □ The predicted frictional stress and slip for the developed FE models along with strain and load responses are with a good agreement with the obtained experimental data. □ The developed FE models in this study could work as a numerical platform instead

of the costly and time consuming experimental testing to investigate the behavior of AA plates as an EBR material. Further investigation should be carried in a future studies and more parameters should be considered. Concrete surface preparation and the AA plate to concrete width ratio represent some of the parameters that should be taken under consideration. The developed FE model could work as an environment for implementing the effect of such parameters on the bond slip performance.

## References

- [1] J. Yao, J. G. Teng, and J. F. Chen, "Experimental Study on FRP-To-Concrete Bonded Joints," *Composites. Part B, Engineering*, vol. 36, no. 2, pp. 99-113, 2005.
- [2] G. J. Plieger, "Reinforced Concrete Strengthened With Externally Bonded Carbon-Fiber Reinforced Polymers," Department of Architecture, building and planing, Eindhoven University of Technology, MSc Thesis, 2011.
- [3] J. G. Teng, *FRP-Strengthened RC Structures*. New York; Chichester, England: Wiley, 2002.
- [4] J. H. Zhu, M. C. Zhu, L. L. Wei, W. W. Li, and F. Xing, "Bond Behavior of Aluminum Laminates in NSM Technique," in *Applied Mechanics and Materials*, 2014, vol. 501-504, pp. 1053-1060.
- [5] M. Naser, R. Hawileh, J. A. Abdalla, and A. Al-Tamimi, "Bond Behavior of CFRP Cured Laminates: Experimental and Numerical Investigation," *Journal of engineering materials and technology*, vol. 134, no. 2, pp. 1-9, 2012.
- [6] X. Z. Lu, J. G. Teng, L. P. Ye, and J. J. Jiang, "Bond–Slip Models for FRP Sheets/Plates Bonded To Concrete," *Engineering Structures*, vol. 27, no. 6, pp. 920-937, 2005.
- [7] J. G. Teng, S. T. Smith, J. Yao, and J. F. Chen, "Intermediate Crack-Induced Debonding in RC Beams and Slabs," *Construction and Building Materials*, vol. 17, no. 6–7, pp. 447-462, 2003.
- [8] J. F. Chen and J. G. Teng, "Anchorage Strength Models for FRP and Steel Plates Bonded to Concrete," *Journal of structural engineering*, vol. 127, no. 7, pp. 784-791, 2001.
- [9] J. Pan and Y.-F. Wu, "Analytical Modeling of Bond Behavior Between FRP Plate And Concrete," *Composites Part B: Engineering*, vol. 61, pp. 17-25, 2014.
- [10] Y. Wu, Z. Zhou, Q. Yang, and W. Chen, "On Shear Bond Strength of FRP-Concrete Structures," *Engineering Structures*, vol. 32, no. 3, pp. 897-905, 2010.
- [11] H. Ko, S. Matthys, A. Palmieri, and Y. Sato, "Development of a Simplified Bond Stress–Slip Model for Bonded FRP–Concrete Interfaces," *Construction and Building Materials*, vol. 68, pp. 142-157, 2014.
- [12] H. Yuan, J. G. Teng, R. Seracino, Z. S. Wu, and J. Yao, "Full-Range Behavior of FRP-to-Concrete Bonded Joints," *Engineering Structures*, vol. 26, no. 5, pp. 553-565, 2004.
- [13] A. Hosseini and D. Mostofinejad, "Effective Bond Length of FRP-to-Concrete Adhesively-Bonded Joints: Experimental Evaluation of Existing Models," *International Journal of Adhesion and Adhesives*, vol. 48, pp. 150-158, 2014.
- [14] H. M. Diab and O. A. Farghal, "Bond Strength and Effective Bond Length of FRP Sheets/Plates Bonded to Concrete Considering the Type of Adhesive Layer," *Composites Part B: Engineering*, vol. 58, pp. 618-624, 2014.
- [15] M. B. Ouezdou, A. Belarbi, and S.-W. Bae, "Effective Bond Length of FRP Sheets Externally Bonded to Concrete," *International Journal of Concrete Structures and Materials*, vol. 3, no. 2, pp. 127-131, 2009.

- [16] ISIS Canada. Strengthening Reinforced Concrete Structures with Externally-Bonded Fibre Reinforced Polymers (Design manual ; no. 4). ISIS Canada, 2001.
- [17] C.S.A. Standard, Design and Construction of Building Components with Fibre-Reinforced Polymers (CSA standard, 0317-5669 ; S806-02; CSA standard 0317-5669 S806-02.). Toronto, Canadian Standards Association, 2002.
- [18] E. Y. Sayed-Ahmed, R. Bakay, and N. G. Shrive, "Bond Strength of FRP Laminates to Concrete: State-of-the-Art Review," *Electronic Journal of Structural Engineering*, vol. 9, pp. 45-61, 2009.
- [19] D. Mostofinejad and A. Moghaddas, "Bond Efficiency of EBR and EBROG Methods in Different Flexural Failure Mechanisms of FRP Strengthened RC Beams," *Construction and Building Materials*, vol. 54, pp. 605-614, 2014.
- [20] K. Nakaba, T. Kanakubo, T. Furuta, and H. Yoshizawa, "Bond Behavior Between Fiber-Reinforced Polymer Laminates and Concrete," *ACI structural journal*, vol. 98, no. 3, pp. 359-367, 01/2001.
- [21] C. Mazzotti, M. Savoia, and B. Ferracuti, "A New Single-Shear Set-Up For Stable Debonding of FRP-Concrete Joints," *Construction and Building Materials*, vol. 23, no. 4, pp. 1529-1537, 2009.
- [22] P. Mukhopadhyaya and N. Swamy, "Interface Shear Stress: A New Design Criterion for Plate Debonding," (in en), *Journal of composites for construction*, vol. 5, no. 1, pp. 35-43, 2001.
- [23] H. Toutanji and G. Ortiz, "The Effect of Surface Preparation on The Bond Interface Between FRP Sheets and Concrete Members," *Composite Structures*, vol. 53, no. 4, pp. 457-462, 2001.
- [24] H. Yoshizawa, T. Myojo, M. Okoshi, M. Mizukoshi, and H. S. Kliger, "Effect of Sheet Bonding Condition on Concrete Members Having Externally Bonded Carbon Fiber Sheet," in *Materials for the New Millennium*, pp. 1608-1616: ASCE, 1996.
- [25] C. Talbot, M. Pigeon, D. Beaupré, and D. Morgan, "Influence of Surface Preparation on Long-Term Bonding of Shotcrete," *Materials Journal*, vol. 91, no. 6, pp. 560-566, 1995.
- [26] E. N. Julio, F. A. Branco, and V. t. D. Silva, "Concrete-to-Concrete Bond Strength. Influence of The Roughness of The Substrate Surface," *Construction and Building Materials*, vol. 18, no. 9, pp. 675-681, 2004.
- [27] M. J. Chajes, W. W. Finch, T. F. Januszka, and T. A. Thomson, "Bond and Force Transfer of Composite Material Plates Bonded to Concrete," *ACI Structural Journal*, vol. 93, no. 2, pp. 208-217, 1996.
- [28] G. Spadea, R. N. Swamy, and F. Bencardino, "Strength and Ductility of RC Beams Repaired with Bonded CFRP Laminates," (in en), *Journal of Bridge Engineering*, vol. 6, no. 5, pp. 349-355, 2001.
- [29] Rahimi, Hamid, and Hutchinson, "Concrete beams strengthened with Externally bonded FRP plates," *Journal of Composite for Structures*, vol. 5, no.1, pp. 44-56, 2001.
- [30] B. E. Parth Athawale "Analysis of Factors Affecting Effective Bond Length for Fiber Reinforced Polymer Composite Laminate Externally Bonded to Concrete Substrate," Texas Tech University, PhD dissertation, 2012.

- [31] F. Della Croce, R. Tadei, and G. Volta, "A Genetic Algorithm for the Job Shop Problem," *Computers and Operations Research*, vol. 22, no. 1, pp. 15-24, 1995.
- [32] M. A. Aiello and M. Leone, "Interface Analysis Between FRP EBR System and Concrete," *Composites Part B: Engineering*, vol. 39, no. 4, pp. 618-626, 2008.
- [33] D. Mostofinejad and S. M. Shameli, "Externally Bonded Reinforcement in Grooves (EBRIG) Technique to Postpone Debonding of FRP Sheets in Strengthened Concrete Beams," *Construction and Building Materials*, vol. 38, pp. 751-758, 2013.
- [34] I. Iovinella, A. Prota, and C. Mazzotti, "Influence of Surface Roughness on the Bond of FRP Laminates to Concrete," *Construction and Building Materials*, vol. 40, pp. 533-542, 2013.
- [35] A. C. I. committee. (2008). *Guide for the Design and Construction of Externally Bonded FRP Systems for Strengthening Concrete Structures (ACI 440.2R-02)* (ASCE).
- [36] Y. Sato, T. Ueda, Y. Kakuta, and T. Tanaka, "Shear Reinforcing Effect of Carbon Fiber Sheet Attached to Side of Reinforced Concrete Beams," In *Proceedings of The 2nd International Conference on Advanced Composite Materials in Bridges and Structures*, AcmbS-li, Montreal, 1996.
- [37] Y. Hiroyuki and Z. Wu, "Analysis of Debonding Fracture Properties of CFS Strengthened Member Subject to Tension," in *Proceedings of 3rd International Symposium on Non-Metallic (FRP) Reinforcement For Concrete Structures*, 1997, vol. 1, pp. 284-94.
- [38] T. Maeda, Y. Asano, Y. Sato, T. Ueda, and Y. Kakuta, "A Study on Bond Mechanism of Carbon Fiber Sheet," in *Non-Metallic (FRP) Reinforcement for Concrete Structures*, *Proceedings of the Third Symposium*, 1997, vol. 1, pp. 279-286.
- [39] M. Blaschko, R. Niedermeier, and K. Zilch, "Bond Failure Modes of Flexural Members Strengthened with FRP," in *Second International Conference on Composites in Infrastructure*, 1998, vol. 1.
- [40] B. Täljsten, "Plate Bonding Strengthening of Existing Concrete Structures with Epoxy Bonded Plates of Steel or Fibre Reinforced Plastics," PhD dissertation 1994.
- [41] H. Yuan and Z. Wu, "Interfacial Fracture Theory in Structures Strengthened with Composite of Continuous Fiber," in *Proceedings of the Symposium of China and Japan, Science and Technology of the 21st Century*, Tokyo, Japan, vol. 1315, p. 142155, 1999.
- [42] U. Neubauer and F. Rostasy, "Design Aspects of Concrete Structures Strengthened with Externally Bonded CFRP-Plates," in *Proceedings of the Seventh International Conference on Structural Faults and Repair*. 8 July 1997, Volume 2: Concrete and Composites.
- [43] D. Van Gemert, "Force Transfer in Epoxy Bonded Steel/Concrete Joints," *International Journal of Adhesion and Adhesives*, vol. 1, no. 2, pp. 67-72, 1980.
- [44] O. Chaallal, M.-J. Nollet, and D. Perraton, "Strengthening of Reinforced Concrete Beams with Externally Bonded Fiber-Reinforced-Plastic Plates: Design Guidelines for Shear and Flexure," *Canadian Journal of Civil Engineering*, vol. 25, no. 4, pp. 692-704, 1998.

- [45] A. Khalifa, W. J. Gold, A. Nanni, and A. A. MI, "Contribution of Externally Bonded FRP to Shear Capacity of RC Flexural Members," *Journal of Composites for Construction*, vol. 2, no. 4, pp. 195-202, 1998.
- [46] K. Izumo, N. Saeki, M. Fukao, and T. Horiguchi, "Bond Behavior and Strength Between Fiber Sheets and Concrete," *Transactions of the Japan Concrete Institute*, vol. 21, pp. 423-430, 2000.
- [47] J. Dai, T. Ueda, and Y. Sato, "Development of the Nonlinear Bond Stress–Slip Model of Fiber Reinforced Plastics Sheet–Concrete Interfaces with A Simple Method," *Journal of Composites for Construction*, vol. 9, no. 1, pp. 52-62, 2005.
- [48] Y. Sato, Y. Asano, And T. Ueda, "Fundamental Study on Bond Mechanism of Carbon Fiber Sheet," *Concrete Library International*, JSCE vol. 37, pp. 97-115, 2001.
- [49] F. M. Mazzolani, and M. Feder, *Aluminium Alloy Structures*, Second Edition. Spon, 1995, p. 693.
- [50] F. M. Mazzolani, "Structural Applications of Aluminium in Civil Engineering," *Structural Engineering International*, vol. 16, no. 4, 2006.
- [51] M. S. Mamlouk and J. P. Zaniwski, *Materials for Civil and Construction Engineers*. Upper Saddle River, N.J: Pearson Prentice Hall, 2006.
- [52] JR. Davis, *Aluminum and Aluminum Alloys*. ASM international; 1993.
- [53] C. Pellegrino, D. Tinazzi, and C. Modena, "Experimental Study on Bond Behavior between Concrete and FRP Reinforcement," vol. 12, no. 2, pp. 180-189, 2008.
- [54] B. Ferracuti, M. Savoia, and C. Mazzotti, "Interface Law for FRP–Concrete Delamination," *Composite Structures*, vol. 80, no. 4, pp. 523-531, 2007.
- [55] S. Popovics, "A Numerical Approach to the Complete Stress-Strain Curve of Concrete," *Cement and Concrete Research*, vol. 3, no. 5, pp. 583-599, 1973.
- [56] H. Ko and Y. Sato, "Bond Stress–Slip Relationship Between FRP Sheet and Concrete Under Cyclic Load," *Journal of Composites for Construction*, vol. 11, no. 4, pp. 419-426, 2007.
- [57] Z. Guo, S. Cao, W. Sun, and X. Lin, "Experimental Study on Bond Stress-Slip Behaviour Between FRP Sheets and Concrete," in *FRP in Construction, Proceedings of the International Symposium on Bond Behaviour of FRP in Structures*, 2005, pp. 77-84.
- [58] "ANSYS<sup>®</sup> Academic Research, Release 17.0. "A Finite Element Computer Software and User Manual for Nonlinear Structural Analysis. inc.," ed. Canonsburg, PA.
- [59] K. Willam and E. Warnke, "Constitutive Model for the Triaxial Behavior of Concrete," in *Proceedings, International Association for Bridge and Structural Engineering*, vol. 19, no. 1, pp. 1-30: ISMES, Bergamo, Italy, 1975.
- [60] M. Bangash, *Concrete and Concrete Structures: Numerical Modelling and Applications*," Elsevier Science Publishers, England, 1989.

- [61] Y. Hemmaty, "Modeling of the Shear Force Transferred Between Cracks in Reinforced and Fiber Reinforced Concrete Structures," in Proceedings of the ANSYS Conference, 1998, vol. 1, no. 1, pp. 201-209.
- [62] L. Huyse, Y. Hemmaty, and L. Vandewalle, "Finite Element Modeling of Fiber Reinforced Concrete Beams," in Proceedings of the ANSYS Conference, 1994, vol. 2.
- [63] H. Ewalds and R. Wanhill, "Fracture Mechanics (2nd edn.)," Taylor & Francis, London, 1984.

180

## Vita

Ahmed Mirghani was born in 1988, in Riyadh, Saudi Arabia. He received a Bachelor of Science in Civil Engineering from the University of Khartoum in Sudan in 2011. He joined the Master's program at AUS in fall 2013, and he is a graduate research assistant at the American University of Sharjah. His research interests include design, construction, analysis and simulation of reinforced concrete and steel structures.